# Cerebral Amyloid Angiopathy: New Insights from Transgenic Mice

## Inauguraldissertation

zur
Erlangung der Würde eines Doktors der Philosophie
vorgelegt der
Philosophisch-Naturwissenschaftlichen Fakultät
der Universität Basel

von

**Martin C. Herzig**

aus Grub (AR)

Institut für Pathologie
Universität Basel
2004

Genehmigt von der Philosophisch-Naturwissenschaftlichen Fakultät
auf Antrag von
Prof. Dr. Heinrich Reichert und Prof. Dr. Mathias Jucker.

Basel, den 6. Juli 2004

Prof. Dr. Marcel Tanner
Dekan

# - Table of Contents -

# Acknowledgments

I would like to acknowledge my supervisor Prof. Dr. Mathias Jucker for giving me the opportunity to carry out my PhD thesis in his research laboratory. He has always had a good nose for initiating scientific projects that were not only fascinating to me, but have also been of a great interest for the research community in general. I'm also grateful to Prof. Dr. Heinrich Reichert for his participation in this dissertation and for academic support.

Sincere thanks to Dr. Matthias Staufenbiel, his research group and co-workers, namely to Doro Abramowski and Karl-Heinz Wiederhold. They were involved in each project presented herein, providing us with mice, materials, and lots of profound scientific knowledge. Many thanks to our collaborator Prof. Dr. Paul Mathews who spared no effort in contributing his scientific ideas to our work, and to Stephen Schmidt for running a vast number of ELISAs. I am also grateful to Dr. Marion Maat-Schieman for providing us with HCHWA-D tissue and for experimental help. Not forgetting Dr. Hans-Ruedi Widmer who invested significant time in cell cultures experiments.

Many people working at the Institute of Pathology contributed to this work. Namely the director of the institute Prof. Dr. Michael Mihatsch, the neuropathologists Prof. Dr. Alphonse Probst and Prof. Dr. Markus Tolnay, and the members of their team, particularly Claudia Mistl, Sabine Ipsen, and Edith Hui Bon Hoa. People from the photography unit Thomas Schürch, Jan Schwegler, and Hans-Ruedi Zysset. Thanks to Mark Wirdnam for computer support and Oskar Herrera for providing us with laboratory essentials. I'm also grateful to people of the animal research facilities from the Department of Research and the Biocenter for their competent work.

Especially I would like to thank my colleagues, previous and present, for their team spirit during all the ups and downs. Thanks to Patrick Burgermeister for generating the APPDutch mice, to Esther Kohler for error-free mouse genotyping and performing ELISAs, to Michelle Pfeifer for teaching me "biochemistry for housewives", to Dr. Luca Bondolfi, Stephan Käser, Dr. Melanie Meyer-Lühmann, and Dr. Anne Stalder for having both, encouraging scientific, as well as other earth-shattering discussions, to Tristan Bolmont, Dr. Sonia Boncristiano, Florence Clavaguera, Janaky Coomaraswamy, Florian Ermini, Dr. Lukas Jann, Irene Neudorfer, Dr. Amie Phinney, Claudia Schäfer, Dr. Martina Stalder, and Dr. David Winkler, for sharing day-to-day life and research activities. A thousand pardons for this formal stereotyped thinking ;-)

I am looking forward to future collaboration and an inspiring teamwork!!!

# Summary

Cerebral amyloid angiopathy (CAA) is characterized by the deposition of congophilic material within the walls of small to medium-sized blood vessels of the brain and leptomeninges. The incidence of CAA increases with aging, and in its most severe stages, the vascular amyloid causes a breakdown of the blood vessel wall which results in spontaneous, often recurrent, lobar intracerebral hemorrhage. CAA is estimated to account for four to twenty percent of all nontraumatic intracerebral hemorrhages. Besides this major complication, extensive CAA has been associated with ischemic white matter damage with progressive dementia, perivascular inflammation, and secondary vasculitis. CAA occurs as a sporadic disorder in the elderly and in association with Alzheimer's disease (AD) with virtually all AD patients showing some degree of vascular amyloid in addition to parenchymal plaques. There are also familial forms of CAA such as hereditary cerebral hemorrhage with amyloidosis-Dutch type (HCHWA-D). The vascular amyloid in these disorders mainly consists of β-amyloid peptide (Aβ) that is produced by proteolytic cleavage from its precursor, which is the β-amyloid precursor protein (APP). The major Aβ species that is deposited in the vasculature is Aβ40, while parenchymal amyloid is mainly composed of Aβ42. One major difficulty in studying CAA is that it can be definitely diagnosed only postmortem. Moreover, spontaneous CAA occurs only in old primates and dogs, both of which are not practical models to study the pathogenesis and therapy of CAA. Rodents do not spontaneously develop CAA.

The purpose of this thesis was to provide useful model systems to study the pathomechanism of vascular amyloid formation and associated pathology. To this end we generated and used mice that are transgenic for human genes bearing mutations that are well known to cause either hereditary Aβ-CAA or classical familial AD. In a first study we analyzed CAA and CAA-associated pathological changes in APP23 transgenic mice. These mice overexpress human APP bearing the Swedish K670N/M671L double mutation, a typical early-onset AD-causing mutation, under the control of the neuron-specific Thy-1 promoter. In addition to parenchymal amyloid plaques, APP23 mice show consistent amyloid within leptomeningeal, neocortical, hippocampal, and thalamic vessel walls. Both CAA frequency and severity significantly increase with aging, demonstrating that not only more vessels are affected, but also that the amyloid burden of individual vessels increases with the progression of amyloid deposition. Cerebrovascular amyloid causes degeneration of vascular smooth muscle cells (SMCs). In severely affected vessels, SMCs are completely replaced by the amyloid. Similar to humans, amyloid depositing APP23 mice develop spontaneous hemorrhages, some of them being recurrent. The bleedings are associated with amyloid-laden vessels and therefore, their anatomical distribution appears very similar to

that of CAA. In aged mice, a quantitative analysis revealed a positive correlation between hemorrhages and CAA. Interestingly, no significant relationship between hemorrhages and total amyloid load was observed. Occasionally, CAA-associated vasculitis is seen in animals with extensive vascular amyloid.

In a second study, we generated transgenic mice that express human APP E693Q under the control of the same neuron-specific Thy-1 promoter (APPDutch mice) that has been used in APP23 mice. In HCHWA-D patients, the APP E693Q Dutch mutation causes severe CAA with recurrent cerebral hemorrhagic strokes often leading to death early in their fifties, or to dementia in patients that survive the strokes. In contrast to AD patients that show parenchymal amyloid plaques, HCHWA-D patients exhibit few parenchymal amyloid deposits. Similar to HCHWA-D, aged APPDutch mice show extensive Aβ deposits mainly within the walls of leptomeningeal vessels followed by cortical vessels. Parenchymal Aβ deposits are mostly absent. In severely affected vessels, the SMCs are completely displaced by the amyloid. In regions with CAA, fresh and old hemorrhages are observed, and activated perivascular microglia and reactive astrocytes are found. To examine the mechanism that leads to the almost exclusive vascular amyloid formation in APPDutch mice, we compared the mice with transgenic mice overexpressing wild-type (wt) human APP using the same neuronal promoter (APPwt mice). As they age, APPwt mice develop parenchymal plaques with limited vascular amyloid deposits. A biochemical analysis of Aβ40 and Aβ42 levels revealed significant higher Aβ40:42 ratios in amyloid depositing and pre-depositing APPDutch mice compared to APPwt mice. To demonstrate that the high Aβ40:42 ratio in APPDutch mice is linked to the almost exclusive vascular amyloid deposition, we crossed APPDutch mice with mice that overexpress human presenilin-1 bearing the G384A mutation (PS45 mice) that is known to dramatically increase the production of Aβ42. Strikingly, young APPDutch/PS45 double-transgenic mice develop massive diffuse and compact parenchymal amyloid with only very little CAA. Thus, shifting the Aβ40:42 ratio towards Aβ42 is sufficient to redistribute the amyloid pathology from the vasculature to the parenchyma.

A third series of experiments using neurografting techniques was performed to investigate the mechanisms involved in the initiation of cerebral amyloidosis *in vivo*. Cell suspensions of transgenic APP23 and wild-type B6 embryonic brain tissue were injected into the neocortex and hippocampus of both APP23 and B6 mice, respectively. In wild-type hosts, APP23 grafts did not show amyloid deposits up to 20 months after grafting. Interestingly, transgenic and wild-type grafts in young APP23 hosts develop amyloid plaques as early as three months after grafting. Although the majority of the amyloid is of the diffuse type, some compact and congophilic amyloid plaques are observed in the wild-type grafts. These congophilic amyloid lesions are

surrounded by neuritic changes and gliosis, comparable to the amyloid-associated pathology that has previously been described in APP23 mice. These results support the importance of neuronally secreted Aβ for the development of cerebral amyloidosis which can be initiated distant from the site of Aβ production, a finding that supports the observation of the above mentioned APPDutch mouse model.

In summary, we demonstrate that APP23 and APPDutch mice recapitulate CAA and CAA-associated pathology observed in humans and thus are valuable models for studying the human disease. Our results stress the importance of neuronally secreted Aβ for the development of CAA and emphasize the Aβ40:42 ratio as an important factor in determining parenchymal versus vascular amyloid deposition. The understanding that different Aβ species can drive amyloid pathology in different cerebral compartments not only provides insights into the pathomechanism of sporadic and familial CAA but also has implications for current anti-amyloid therapeutic strategies.

# Introduction

# 1. Cerebral Aβ-Amyloidosis

## 1.1. Alzheimer's Disease - The Most Common Form of Cerebral Aβ-Amyloidosis

Traditionally, amyloidoses have been defined as diseases in which normally soluble proteins accumulate in the extracellular space of various tissues as insoluble deposits of 10 nm fibrils that are rich in β-sheet structure and have characteristic dye-binding properties such as birefringent labeling by Congo red [41,42]. Many secreted, circulating and highly soluble proteins are known that can be transformed to highly stable extracellular fibrils under abnormal conditions [99,133]. One of these proteins is a small soluble protein of unknown function, the β-amyloid peptide (Aβ). In Alzheimer's disease (AD) patients, by definition, Aβ is deposited extracellularly in the brain as diffuse or compact neuritic plaques (Fig. 1A). In addition and at least to some degree, almost all AD brains show cerebrovascular Aβ deposits termed as cerebral amyloid angiopathy (CAA) (Fig. 1B). The other pathological hallmark defining AD is the intracellular accumulation of hyperphosphorylated microtubule-associated protein tau in neurons called neurofibrillary tangles (NFTs) (Fig 1C). There has been a great deal of discussion which of these proteins takes priority over the other in the pathogenic mechanism of AD. The fact that in hereditary forms of early-onset AD the production of Aβ, and therewith amyloid deposition, is increased points out the importance of the amyloid. Further, mutations within the tau protein do not cause AD but produce frontotemporal dementia with parkinsonism, a less common but equally severe disease in which tau-containing neurofibrillary tangles accumulate in the absence of extracellular amyloid [61].

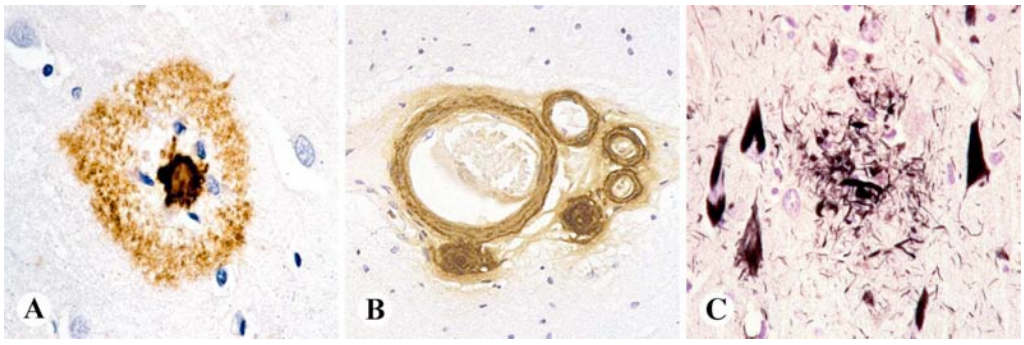


**Figure 1.** The pathological hallmarks of AD. Amyloid plaque (**A**) and neurofibrillary tangles (surrounding a neuritic plaque) (**C**) in an AD brain. These two lesions are the hallmarks for a definite diagnosis of AD. Additionally, virtually all AD patients show some degree of cerebrovascular amyloid (**B**).

## 1.2. The Role of Secretases in APP Processing and Aβ Formation

### 1.2.1. Aβ is Produced by β- and γ-Secretase Cleavage

Aβ is a small hydrophobic peptide that mainly occurs in two lengths, Aβ1-40 (Aβ40) and Aβ1-42 (Aβ42) (Fig. 2), the latter being highly amyloidogenic [44,65,91]. Besides these two major forms, truncated Aβ peptides with N- and C-terminal heterogeneity exist. Aβ is proteolytically cleaved form the β-amyloid precursor protein (APP) [71], a large type 1 membrane glycoprotein the function of which has not been identified yet (Fig. 2). In a first step APP is cleaved by β-secretase (BACE-1, β-site APP-cleaving enzyme) producing APPsβ and C99 (Fig. 3, lower part) [141,160,161]. In a second step C99 undergoes γ-secretase-mediated cleavage yielding Aβ40 or Aβ42 [132]. The Aβ monomers either aggregate to form amyloid fibrils or they are degraded or cleared. γ-secretase has been shown to be a multiprotein high molecular weight complex composed of presenilin-1 and presenilin-2 (PS1 and PS2), Nct (nicastrin), APH-2 (anterior pharynx-defective phenotype) and PEN-2 (PS-enhancer) all of which are essential for its proper function [20,29,45,136,193]. Aβ was originally thought to be produced only under pathological conditions. However, this concept was disproved when mammalian cells have been shown to constitutively release and secrete Aβ throughout lifetime and when Aβ was found in plasma and cerebrospinal fluid (CSF) [56,135,140]. Based on these findings, many detailed studies focusing on the effect of AD-causing genetic mutations on Aβ production have been performed, not only in cell culture experiments but also in transgenic animals.

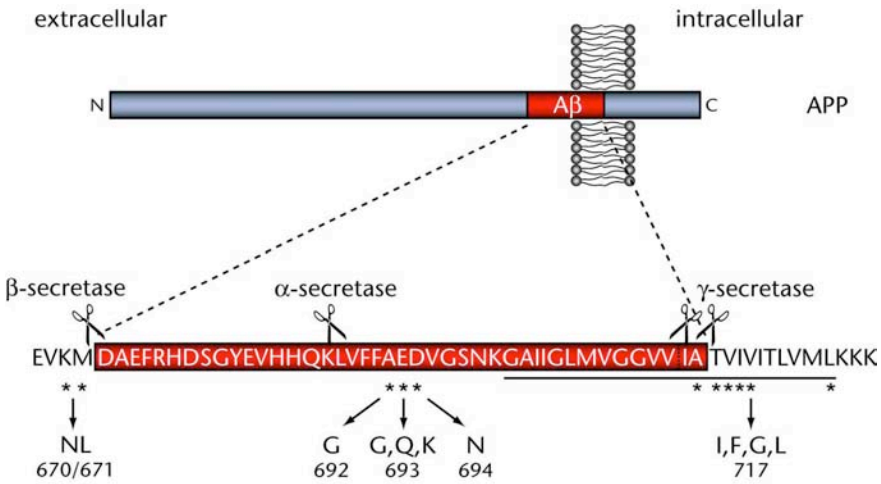


**Figure 2.** Structure of APP, the secretase cleavage sites, and the location of APP mutations causing familial AD and/or CAA. APP is shown in blue, the amino acid sequences of Aβ42 (boxed) and Aβ40 (dashed line) are shown in red, and the predicted transmembrane domain of APP is underscored. The major cleavage sites for α-, β-, and γ-secretases are indicated by the scissors. The location of all known APP mutations causing either familial AD and/or CAA are marked by asterisks and the most important amino acid substitutions are indicated.

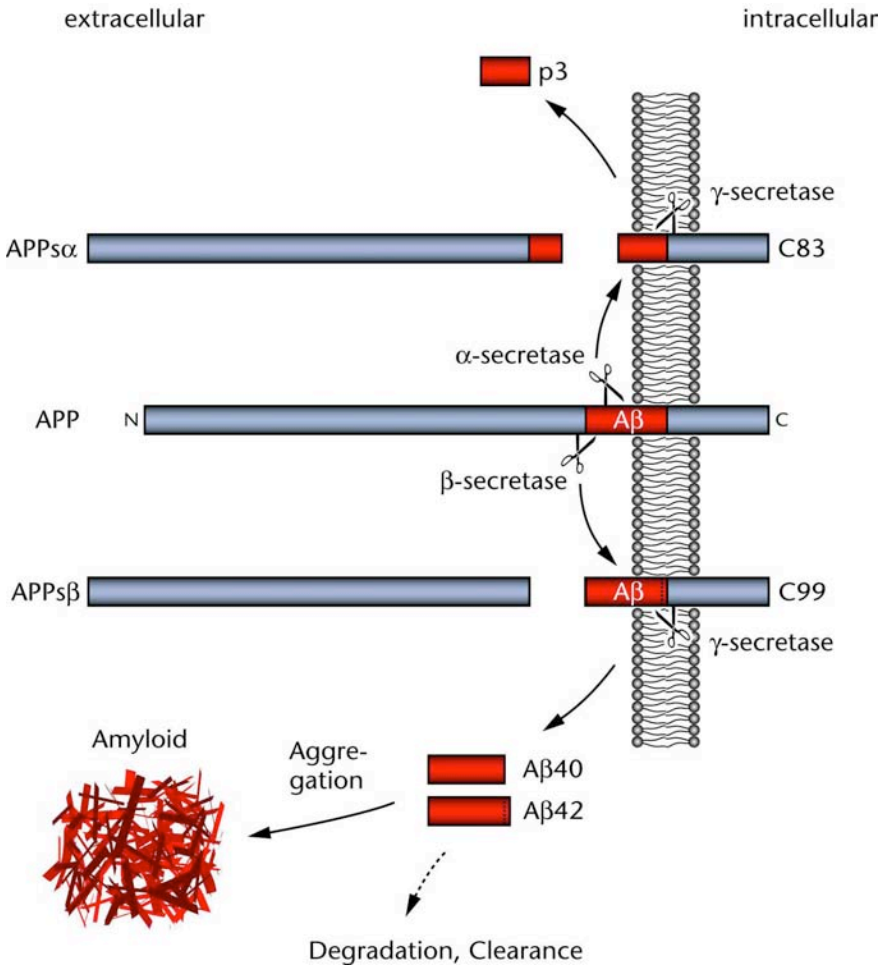


**Figure 3.** APP processing by α-, β-, and γ-secretase. In a non-amyloidogenic pathway (upper part) APP undergoes cleavage by α-secretase which results in release of APPsα and retention of the 83-residue C-terminal fragment (C83) in the membrane. The subsequent cleavage of C83 by γ-secretase liberates the non-amyloidogenic p3 which begins at position 17 of Aβ. In an alternative amyloidogenic pathway (lower part), APP is cleaved by β-secretase resulting in release of APPsβ and retention of the 99-residue C-terminal fragment (C99). γ-secretase cleaves C99 and produces either Aβ40 or Aβ42, respectively. Aβ aggregates and elongates to form oligomers, protofibrils, and fibrils that are deposited as insoluble amyloid. Alternatively, Aβ can be degraded or cleared.

### 1.2.3. α -Secretase Cleavage Prevents Aβ Generation

The above mentioned amyloidogenic pathway of APP cleavage results in Aβ production. The main pathway that occurs, however, does not lead to Aβ generation (Fig. 3, upper part). In this non-amyloidogenic pathway, APP is processed by α-secretase (ADAM: a disintegrin and metalloproteinase, TACE: tumor necrosis factor-α convertase) which cleaves near the middle of the Aβ region to produce a large soluble ectodomain (APPsα) which is released from the cell and a 83-residue C-terminal fragment (C83) that remains membrane-bound [25,116,142]. Then γ-

secretase cleaves C83 yielding the small p3 peptide. Most activity of the α-secretase on APP takes place at the cell surface, but some processing also occurs intracellularly in secretory compartments. Within the cell β- and γ-secretase seem to be localized in the early, recycling endosomes [76,112]. Like the function of APP itself remains unclear the role of the proteolytically produced fragments are not known. APP intracellular domain (AICD) which is released to the nucleus from APP after α- and γ-secretase cleavage may be involved in transcriptional signaling [74,76,130].

# 2. Cerebral Amyloid Angiopathies

## 2.1. General Features

Cerebral amyloid angiopathy (CAA) is the term used to define the deposition of amyloid within the vessel walls of small- and medium-sized leptomeningeal and cortical arteries, arterioles, and less often, of capillaries and veins [37,85,124]. The amyloid is visualized by the positive staining with the Congo red dye with an apple-green color in polarized light and with the fluorescence of thioflavin S or T since both methods are dependent on the presence of β-pleated secondary structure characteristic of amyloid. CAA has first been described as "drusige Entartung der Hirnarterien und -capillaren" in 1938 [131]. It occurs as sporadic or familial forms with many different amyloid proteins being involved (Table 1, Fig. 4) [120,123,124]. Usually, amyloid proteins are cleaved from a larger precursor protein before they are deposited. In hereditary conditions, mutations lead to amino acid substitutions or elongation of the precursor proteins. These changes in amino acids can be located either within the sequence of the amyloid protein, resulting in a mutated amyloid protein with different aggregation properties, or they can affect flanking regions, increasing proteolytic cleavage of the amyloid protein from its precursor. Actually, the secretases that are involved in this cleavage are known to contain a lot of different mutations too, all increasing amyloid production.

| | Sporadic CAAs | | Hereditary CAAs | | | | | | | |
|---|---|---|---|---|---|---|---|---|---|---|
| **Disease** | **SCAA** | **SAD** | **HCHWA-D** | **FAD** | **HCHWA-I** | **FBD** | **FDD** | **PrP-CAA** | **FAP/MVA** | **FAF** |
| **Gene** | *APP* | *APP* | *APP* | *APP, PS1, PS2* | *CYST C* | *BRI2* | *BRI2* | *PRNP* | *TTR* | *GEL* |
| **Precursor Protein** | Amyloid Precursor Protein (APP) | Amyloid Precursor Protein (APP) | Amyloid Precursor Protein (APP) | Amyloid Precursor Protein (APP) | Cystatin C (Cyst C) | ABri Precursor Protein (ABriPP) | ABri Precursor Protein (ABriPP) | Prion Protein (PrP) | Transthyretin (TTR) | Gelsolin (GEL) |
| **Amyloid Protein** | Aβ | Aβ | Aβ | Aβ | ACys | ABri | ADan | APrP | ATTR | AGel |

**Table 1.** Sporadic and hereditary cerebral amyloid angiopathies (CAAs). SCAA = Sporadic cerebral amyloid angiopathy; SAD = Sporadic Alzheimer's disease; HCHWA-D = Hereditary cerebral hemorrhage with amyloidosis-Dutch type; FAD = familial Alzheimer's disease; HCHWA-I = Hereditary cerebral hemorrhage with amyloidosis-Icelandic type; FBD = Familial British dementia; FDD = Familial Danish dementia; PrP-CAA = Prion disease with cerebral amyloid angiopathy; FAP/MVA = Familial amyloid polyneuropathy/meningo-vascular amyloidoses; FAF = Familial amyloidoses Finnish type; APP = Amyloid precursor protein gene; PS1 = presenilin-1 gene; PS2 = presenilin-2 gene; CYST C = Cystatin C gene; BRI2 = BRI2 gene; PRNP= Prion protein gene; TTR = Transthyretin gene; GEL = Gelsolin gene; Aβ = Amyloid-β protein; ACys = Amyloid-cystatin C; ABri = Amyloid-Bri; ADan = Amyloid-Dan; APrP = Amyloid-Prion protein; ATTR = Amyloid-transthyretin; AGel = Amyloid-gelsolin.

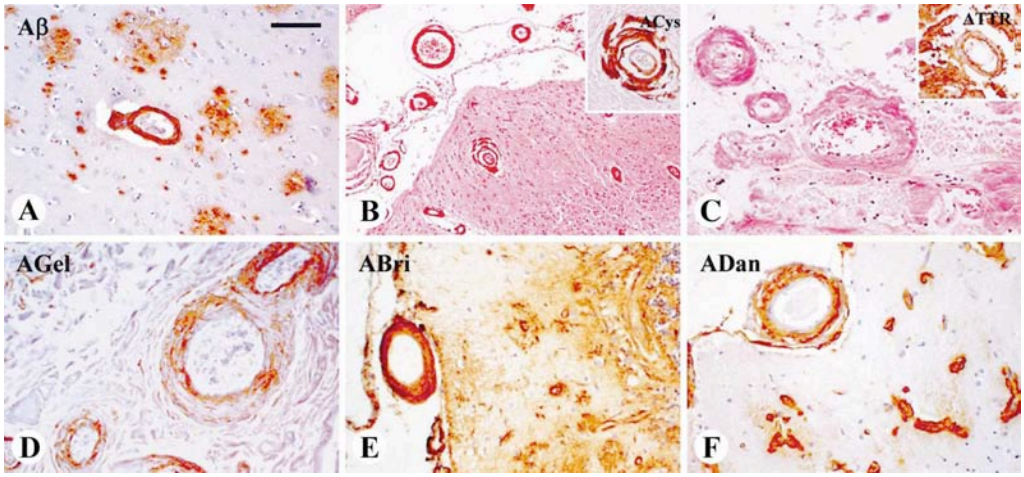


**Figure 4.** Familial forms of CAAs. Deposition of Aβ in parenchymal vessels and diffuse plaques in HCHWA-D (**A**) (Aβ immunohistochemistry). Severe CAA due to deposition ACys (inset) in HCHWA-I (**B**) (hematoxylin and eosin, inset ACys immunohistochemistry). Deposition of variant ATTR in blood vessel wall and leptomeninges in the Hungarian (D18G) form of meningovascular amyloidosis (**C**) (Hematoxylin and eosin; inset: TTR immunohistochemistry). Gelsolin deposition in skin blood vessels in familial amyloidosis-Finnish type (**D**) (Gelsolin immunohistochemistry). Extensive deposition of ABri in cerebellar blood vessels and parenchyma in familial British dementia (**E**) (ABri immunohistochemistry). In familial Danish dementia deposition of ADan takes place mainly in blood vessels in the cerebellum (**F**) (ADan immunohistochemistry). Scale bar in panel A represents 70 μm in A, C, D, E, F and inset of B; 200 μm in panel B and inset in C. (modified from Revesz et al., 2003).

The most common type of CAA is caused by Aβ and thus termed as CAA of the Aβ type (Aβ-CAA). Aβ-CAA is particularly associated with sporadic and familial AD, or occurs as hereditary cerebral hemorrhage with amyloidosis-Dutch type (HCHWA-D) and similar familial disorders, or with normal aging in the elderly (Table 1). Biochemical and immunohistochemical analyses of vascular amyloid deposits of patients showing severe Aβ-CAA revealed Aβ40 as the predominant form of Aβ peptides deposited in CAA [1,12,69,87,95,117].

## 2.2. Morphological Aspects

The cortex, in particular the occipital lobe, is the brain region that is most frequently and severely affected by Aβ-CAA [151,153,168,190]. Hippocampus, cerebellum and basal ganglia are less affected while deep central grey matter, subcortical white matter and brain stem usually show no vascular amyloid. Leptomeningeal and cortical small to medium-sized arteries and arterioles are most frequently affected, veins and capillaries tend to be less frequently affected by vascular Aβ deposits [180]. Light microscopically, amyloid-laden blood vessels show an acellular thickening of the wall (Fig. 5A, B) and they are stained with both Congo red (Fig. 5C) and thioflavin S or T, respectively [123,124].

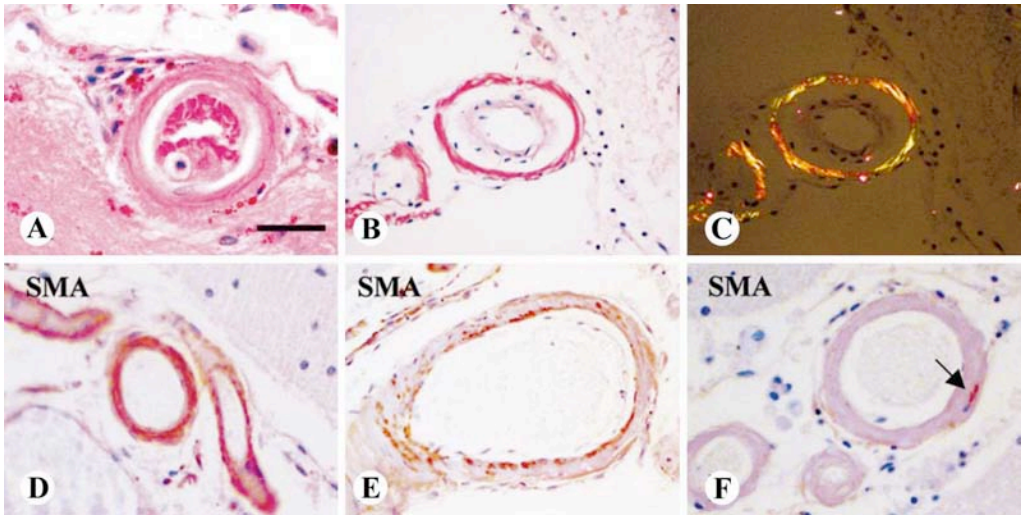


**Figure 5.** Cerebral blood vessels with mural amyloid deposition (**A**) and double barreling (**B**, **C**) in a case of sporadic CAA with multiple cerebral hemorrhages (Fig. 6A, B) (A: Hematoxylin and eosin; B, C: Congo red). In the same case, increasing amyloid deposition is demonstrated to be associated with progressive smooth muscle cell loss (**D**–**F**) (arrow pointing to a preserved smooth muscle cell on F) (D–F: smooth muscle actin immunohistochemistry, SMA). Scale bar in panel A represents 20 μm in A, D–F; and 70 μm in B and C. (from Revesz *et al.*, 2003).

To quantify CAA, a simple neuropathological three-tiered grading system has been proposed that distinguishes between "mild", "moderate", and "severe" involvement [170,172]. In "mild" CAA, vascular amyloid is restricted to a congophilic rim in the media around smooth muscle cells (SMCs) of otherwise normal vessels. Initially, amyloid deposition occurs in the outer portion of the media and its accumulation correlates with the loss of SMC nuclei (Fig. 5D-F). In "moderate" CAA, the SMCs are mainly lost since the media is replaced by amyloid. No evidence of recent or old blood leakage is found. In "severe" CAA, the vascular architecture is severely disrupted by amyloid showing focal fragmentation of vessel walls. CAA-associated perivascular leakage of blood, fibrinoid necrosis, aneurysm formation, or microangiopathies may be seen [85,123].

Ultrastructurally, vascular amyloid consists of randomly orientated 8 to 10 nm filaments that are short and arranged in a disorderly way [123]. At an early stage, amyloid fibrils are found in the outermost portion of the basement membrane at the media-adventitia border in arteries and in smaller vessels mostly in the outer part of the basement membrane around intact SMCs. At later stages, amyloid deposits are seen at the abluminal part of the basement membrane and neighboring SMCs may show signs of degeneration [191]. The wall of severely affected vessels is completely occupied by amyloid that causes loss of SMCs [72,183]. In affected capillaries or small arteries, amyloid fibrils have a tendency to radiate in the surrounding neuropil (dyshoric amyloid) [104]. Even at highly advanced stages of CAA, however, the endothelial cells seem not to be affected by the amyloid.

## 2.3. Hereditary Aβ-CAA Caused by APP and Presenilin Mutations

### 2.3.1. HCHWA-D Occurs Due to a Mutation within the Aβ Sequence of APP

In 1990, the first mutation occurring in APP was discovered in two families originating from the Dutch villages Katwijk and Scheveningen [79]. In both pedigrees, a familial occurrence of cerebral hemorrhage has been described already in 1964 [82] and in the early eighties, severe CAA has been found to be the pathological cause of this disease (Fig. 4A) [176]. The point mutation causing this autosomal dominant disorder, meanwhile termed hereditary cerebral hemorrhage with amyloidosis-Dutch type (HCHWA-D), is located at codon 693 of the APP gene that corresponds to amino acid 22 of Aβ (Fig. 2) [79]. The first nucleotide of this triplet is mutated, cytosine (C) instead of guanine (G), changing the original codon GAA to CAA, and resulting in an amino acid substitution, glutamine for glutamic acid, in APP. Patients are heterozygous for this so called APP E693Q Dutch mutation since the non-mutated wild-type APP allele is also present. The mutated AβDutch peptide shows an altered fibrillogenesis [31,100,143] and toxicity towards vascular cells

[17,22,98,100,162,175] in various experimental *in vitro* systems. Besides the occurrence of large lobar intracerebral hemorrhage, HCHWA-D patients may show cognitive deterioration, often associated with white matter abnormalities on MRI scan and small ischemic infarctions and hemorrhages on pathologic examination [7,177]. In spite of the extensive vascular amyloid observed, congophilic parenchymal amyloid plaques, however, are nearly absent in HCHWA-D patients.

### 2.3.2. Other Aβ Mutations Leading to CAA

In addition to the APP E693Q Dutch mutation, four other mutations occurring within Aβ have been described. They are located at amino acids 21 to 23 of Aβ (Fig. 2). Typically, all these mutations cause severe CAA and additionally, some of them produce AD. The APP A692G Flemish mutation located at residue 21 of Aβ [57] is not only associated with severe CAA and, in most cases, cerebral hemorrhage, but also with AD showing large core plaques that are associated with, or enclose vessels. The dementia in patients is compatible with AD both, clinically and neuropathologically [14,77,127]. HCHWA-Italian type is caused by the APP E693K Italian mutation, a substitution of glutamic acid by lysine at residue 22 of Aβ [8,149]. In HCHWA-I, Aβ deposits are found in cerebral parenchyma and, extensively, in meningocortical vessels where the Aβ seems to be rather amorphous than fibrillar. Patients suffer from stroke, cognitive decline, and some of them develop seizures. At the same location, another mutation has been discovered in a family from northern Sweden. In the so called the APP E693G Arctic mutation, glutamic acid is substituted for glycine [108]. Affected subjects have clinical features of early-onset AD, however, no signs of strokes or vascular lesions were found on brain imaging. The APP D694N Iowa mutation at position 23 of Aβ [46] causes severe amyloid angiopathy, dementia, occipital calcifications, and small ischemic infarctions in an Iowa family. Only microscopic foci of hemorrhage but no major hemorrhagic stroke is observed. Aβ plaques are sparse and of a diffuse type [138]. The same mutation has recently been found in a Spanish pedigree [52]. Interestingly, these patients show similar pathological features but in addition, develop symptomatic intracerebral hemorrhagic stroke.

### 2.3.3. Presenilin Mutations Involved in CAA Formation

Severe CAA is not only the result of APP mutations but can also be associated with AD that is caused by mutations in the presenilin-1 (PS1) and presenilin-2 (PS2) genes. The PS1 mutations L282V [21], Q184D [192], and the PS1 deletion ΔI83/ΔM84 [144] cause extensive and widespread CAA, however, in affected patients, amyloid plaques are abundant as well. A study in which 25 PS1 mutations were investigated has suggested that CAA pathology is more severe in cases in which

the mutation is located beyond codon 200 of the PS1 gene [88]. Further, CAA is also a consistent feature in a Volga-German family that develops familial AD due to the N141I mutation in the PS2 gene. In this family, cerebral hemorrhage has been reported in one mutation carrier [109].

## 2.4. Familial CAAs Caused by Proteins Different from Aβ

Besides Aβ-CAA other forms of familial CAAs, in which amyloid proteins different from Aβ are deposited, are known (Table 1, Fig. 4). The most common diseases caused by these amyloid proteins are described below.

### 2.4.1. HCHWA-I

HCHWA-Icelandic type (HCHWA-I) is an autosomal dominant disorder of early onset. Fatal cerebral hemorrhage occurs in about half of the mutation carriers in their twenties or thirties. Cognitive decline and dementia may occur in patients that survive the hemorrhages. HCHWA-I brains show severe amyloid deposits within small arteries and arterioles of leptomeninges, cerebral cortex, basal ganglia, brainstem, and cerebellum. Asymptomatically, amyloid deposition can occur in peripheral tissues, including skin, lymphoid tissues, salivary glands, and testes [30]. The amyloid protein deposited in HCHWA-I (ACys, Fig. 4B) is an N-terminal truncated form of cystatin C bearing a single glutamine for leucine amino acid substitution due to an A for T point mutation at codon 68 of the cystatin C gene [38,80]. Cystatin C belongs to the type II family of cysteine protease inhibitors and is produced by different cell types, including cortical neurons and is present in biological fluids [38], such as the CSF. Cystatin C levels in CSF of HCHWA-I patients have been found to be half of those measured in control patients [5]. Wild-type and variant cystatin C form concentration dependent inactive dimers; however, variant cystatin C dimerizes at lower concentrations and forms fibrils in conditions in which the wild-type protein forms amorphous aggregates [10]. Cystatin C may also play a role in the pathogenesis of other amyloidoses since it is present in parenchymal and vascular Aβ deposits in AD [81] and in the cerebral amyloid lesions in familial British dementia [39]. A polymorphism in the cystatin C gene might be a risk factor for AD [15].

### 2.4.2. CAA in Familial British and Familial Danish Dementia

Familial British dementia (FBD) and familial Danish dementia (FDD) belong to a novel group of hereditary dementias in which severe CAA is one of the defining pathological hallmarks [123]. In both diseases, the 266 amino-acid-long precursor protein (BriPP) is elongated due to genetic abnormalities. In FBD, a T to A point mutation in the BRI2 stop codon results in the production

of a mutated longer precursor protein, 277 amino acids in length (ABriPP). FDD is caused by a 10-nucleotide duplication occurring between codons 265 and 266 of the same gene. The resulting frame-shift abolishes the normal stop codon which as well leads to the production of a 277 amino acid long precursor protein (ADanPP) [164,166]. C-terminal cleavage of both wild-type and mutated precursor proteins by furin results in the secretion of 23 amino acid long wild-type and 34 amino acid long mutated (ABri, ADan, Fig. 4E, F) peptides [73].

FBD is clinically characterized by progressive memory loss, spastic tetraparesis, and cerebellar ataxia with a disease onset in the sixth decade [97]. In spite of severe CAA, significant cerebral hemorrhage is relatively rare [97,114]. Histologically, the major pathological changes are similar to AD including severe and widespread CAA, amyloid plaques, as well as neurofibrillary degeneration. Vascular amyloid is found in small arteries and arterioles in the leptomeninges and both gray and white matter throughout the CNS with some exceptions, such as the striatum [58]. Some veins and capillaries are affected as well. Double barreling or complete luminal obstruction of vessels is seen. In the retina, blood vessels are heavily affected by CAA [58], and moreover, vascular amyloid is also found in systemic organs [40]. All vascular amyloid is stained with antibodies recognizing ABri. Argyrophilic, ABri-positive amyloid plaques are mainly found in limbic areas. ABri-positive but Silver and Congo red-negative diffuse deposits occur in several regions, including the entorhinal cortex and fusiform gyrus, where they represent the main parenchymal lesion type [58]. Topographically, both fibrillar and non-fibrillar ABri deposits are closely associated with neurofibrillary degeneration.

The major histological features of FDD are similar to those seen in FBD. They include widespread CAA, that can be labeled with antibodies to ADan, and neurofibrillary degeneration. However, there are also differences. In FDD the predominant hippocampal parenchymal ADan deposits are Congo red and thioflavin S-negative, suggesting that they are non-fibrillar rather than fibrillar, which is different from the ABri containing amyloid plaques in FBD. Abnormal neurites primarily cluster around vascular amyloid and are absent around non-fibrillar diffuse ADan parenchymal deposits. The retinal changes, with marked ADan amyloid angiopathy and parenchymal damage, are more severe in FDD than in FBD [59]. A feature of the FDD cases is the deposition of Aβ, either isolated or in combination with ADan, in vessels and brain parenchyma. In both disorders and similar to AD and sporadic CAA, amyloid lesions contain amyloid-associated proteins, including heparan sulfate proteoglycans, ApoE, ApoJ, vitronectin, and components of the classical and alternative complement pathways, suggesting in situ complement activation [124,128].

### 2.4.3. CAA Related to Prion Protein Amyloidosis

In the human prion diseases, which include Creutzfeldt-Jakob disease (CJD), the Gerstmann-Sträussler-Scheinker syndrome (GSS), fatal familial insomnia, kuru and variant CJD, deposition of pathogenic prion protein ($PrP^{SC}$) isoform is documented only in one pedigree with GSS [123]. This GSS variant is caused by a T to G mutation occurring at codon 145 of the PRNP gene which leads to a newly formed stop codon (Y145STOP) and the production of an N- and C-terminally truncated PrP consisting of 70 amino acids. The main neuropathological findings include PrP-immunoreactive CAA, mainly affecting small- and medium-sized vessels of the cerebral and cerebellar grey matter, together with prominent perivascular PrP deposition and neurofibrillary tangle pathology. Leptomeningeal vessels are less severely affected [36].

### 2.4.4. CAA in Transthyretin and Gelsolin-Related Amyloidoses

Gelsolin-related amyloidosis or familial amyloidosis-Finnish type (FAF) is a rare disorder, reported worldwide in kindreds carrying a G654A or G654T gelsolin gene mutation. Affected patients show widespread deposition of gelsolin-related amyloid (AGel, Fig. 4D) in spinal, cerebral, and meningeal amyloid angiopathy, with marked extravascular deposits in the dura, spinal nerve roots, and sensory ganglia. The amyloid deposits are also variably immunoreactive for ApoE, alpha1-antichymotrypsin, and cystatin C [75].

Amyloidoses due to mutations of the transthyretin (TTR) gene are late-onset autosomal dominant systemic diseases characterized by deposition of transthyretin protein (ATTR) in the extracellular space of several organs [3]. In the Hungarian (D18G) (Fig. 4C) and the Ohio pedigrees (V30G), involvement of the meninges and the brain parenchyma is prominent. In patients of the Hungarian family the peripheral nerves, organs, and eye are not affected [35,113,165].

## 2.5. Sporadic Forms of CAA

The majority of CAA, however, is sporadic and is a common neuropathological finding in elderly individuals with or without evidence of AD. Not only its incidence that, depending on the study, is varying from about 10 to 60%, but also both its extent and severity steadily increase with age [53,68,92,153,168,172]. A close association between CAA and AD has been shown by several reports demonstrating that CAA is present in 80 up to 100% of AD cases and moderate to severe CAA is seen in a quarter to three quarters of all AD brains [4,23,26,43,68,151,152,190].

## 2.6. The Risk Factor ApoE

Apolipoprotein E (ApoE) is a genetic risk factor for both sporadic and familial late-onset AD [89]. The ApoE gene is located on chromosome 19 and exists as three alleles termed as ApoE ε2, ε3 and ε4 that differ from each other in only one amino acid. The ApoE ε4 allele, a known a risk factor for AD, is linked to CAA and CAA-associated hemorrhages which result possibly from increased Aβ deposition in the cerebral vasculature [50,51,118,194]. ApoE ε2, however, might promote CAA-associated hemorrhage by causing amyloid-laden vessels to undergo vasculopathic changes that lead to rupture. [54,93-95,105]. Different from the ApoE ε4 allele, ApoE ε2 is believed to be a risk factor for CAA-related hemorrhage independent of AD.

## 2.7. Clinical Consequences of CAA

Intracerebral hemorrhage (Fig. 6A, B) is the most severe clinical consequence of CAA, particularly in patients over the age of 75 years [48,96,171]. CAA-related intracerebral hemorrhage is seen in four to a twenty percent of all spontaneous (nontraumatic) cerebral hemorrhages in the elderly [23,63,67,68,78,172]. It is typically observed in the cortical or cortico-subcortical brain regions which are most heavily affected by CAA. Brains with intracerebral hemorrhage caused by CAA show extensive amyloid in blood vessel walls as well as evidence of breakdown of amyloid-containing vessels such as concentric cracking, microaneurysms and fibrinoid necrosis [85,169,172]. There is accumulating evidence supporting an additional role for CAA in producing vessel dysfunction, reduced cerebral blood flow and ischemia [49]. Ischemic lesions are characteristic of sporadic CAA [9,110] and several hereditary CAA syndromes, including HCHWA-D and the familial disorder caused by APP D694N Iowa mutation that is associated with dementia, but not with hemorrhagic stroke [49]. Pathological evidence suggest that occlusion of vessel lumens is an important mechanism for the ischemic lesions in these patients [46,47,55,85]. Even though occurring to minor degree, other lesions have been linked to CAA. A subset of CAA patients with clinically distinct symptoms show CAA-related perivascular inflammation that can cause vascular dysfunction [24], and CAA has also been shown to be associated with giant cell arteritis [2]. In addition, the effects CAA has upon the blood supply of the brain and on interstitial fluid (ISF) drainage have been emphasized particularly in relation to white matter abnormalities (Fig. 6C, D) [126,167].

It has been proposed that cerebral hemorrhage related to severe CAA consists of at least three distinct phases [1]: 1. initial seeding of Aβ42, occurring in a subset of vessels or their segments; 2. expansion of the vascular amyloid deposits through the incorporation of Aβ40 to replace the

vessel wall, a process that is enhanced by the possession of ApoE ε4; and 3. rupture of the vessel wall with hemorrhage, for which ApoE ε2 is a risk factor.

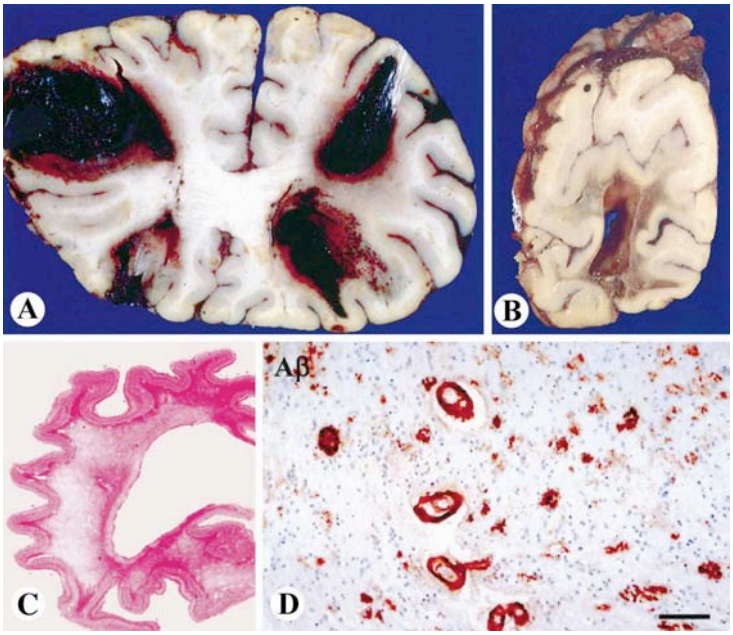


**Figure 6.** Multiple cerebral hemorrhages of varying ages in a case with severe sporadic CAA (**A**, **B**). White matter atrophy and degeneration (**C**) and severe CAA (**D**) in a case of familial AD with PS1 E280G mutation (D: Aβ immunohistochemistry, scale bar represents 70 μm). (from Revesz *et al.*, 2003).

# 3. Mechanisms of CAA Formation

The origin of the different amyloid proteins deposited in the cerebral vasculature is still poorly understood. As most cell types are able to express APP and potentially could release Aβ, several hypothesis for mechanisms leading to CAA have been suggested. The three major hypotheses are termed systemic, vascular, and drainage hypothesis (Fig. 7). These mechanisms are not necessarily thought to be mutually exclusive and might even occur at the same time.

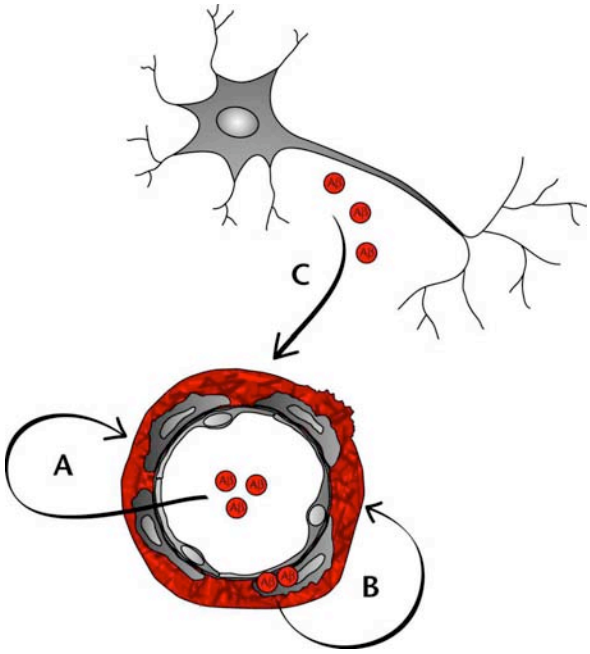


**Figure 7.** Possible mechanisms that could lead to cerebrovascular Aβ deposition. (**A)** The systemic hypothesis proposes that vascular Aβ originates from blood. (**B**) The vascular hypothesis suggests that cerebrovascular cells produce Aβ themselves. (**C**) The drainage hypothesis assumes that neuronally produced Aβ drains and accumulates along perivascular spaces.

## 3.1. Systemic Hypothesis

The systemic hypothesis proposes that Aβ is transferred from blood to the vasculature. In support of this hypothesis is the observation that APP is found in almost all cell types of the body and that Aβ is present in the circulation [84,196]. In vivo studies have shown a receptor-mediated bidirectional transport of Aβ across the blood brain barrier (BBB) including RAGE (receptor for advanced glycation end-products), LRP-1 (low-density lipoprotein receptor related protein-1), SR (scavenger receptor), and megalin receptors [83,137,196,197]. ApoE, a LRP-1 ligand and risk factor for AD and CAA, modulates the rate of Aβ transport [195]. The exchange of Aβ between central nervous system (CNS), cerebrospinal fluid (CSF), and blood is an important process determining concentration of Aβ in the brain. After intravenous injection of Aβ in rodents and primates, the peptide has been detected within cerebral vessel walls and the brain parenchyma [84,86,90,115,129]. Alternatively, blood-borne Aβ may enter the brain if the BBB integrity is compromised which indeed has been shown to be the case in AD and in the brains of Tg2576 transgenic mice [145,156]. Leakage of the BBB can also be mediated by Aβ itself by impairing endothelial regulatory function and endothelial cell death [6,66,150]. Theoretically, vascular Aβ could originate as well from CSF, where it is found in both AD patients and non-demented individuals [62,135,140].

There are several arguments against a hematogenous origin of Aβ. Initial vascular Aβ deposits are seen in the abluminal basement membrane of the vessels which is in favor of the idea that Aβ has its origin within the CNS itself [179,191]. An argument against a CSF origin of Aβ is the observation that arteries are affected more frequently by vascular amyloid than veins in the subarachnoid space. Additionally, smaller arteries are more affected by CAA than larger ones in the same locations [179]. Furthermore, transgenic mice that constitutively overproduce C99 in multiple tissues show exceptionally high levels of Aβ peptides in the plasma (approximately 17 times or more compared with the human plasma level). Although amyloidosis was observed in the intestine, no cerebral Aβ deposits were found in transgenic mice up to the age 29 months [33].

## 3.2. Vascular Hypothesis

The vascular hypothesis proposes local production of Aβ from cerebrovascular cells. Several observations support this view. APP has been detected in extracts from vessels of AD and HCHWA-D brains and in vessels walls, APP coexisted with amyloid fibrils [28,148]. It has been suggested that Aβ in CAA is derived from smooth muscle cells (SMCs) in the media of cerebral arteries [183]. They are closely associated with vascular amyloid, and have been shown to express APP and to produce Aβ [70,72,182,184]. Cultured degenerating SMCs and human brain pericytes (HBPs) have been demonstrated to overexpress APP and moreover, SMCs to overproduce Aβ [18,162]. In addition to myocytes and pericytes, endothelial, adventitial, and perivascular cells have been shown to express APP [103].

Arguments against the vascular hypothesis are that large arteries, although having several layers of SMCs, are less severely affected by CAA than smaller ones and that capillaries exhibit Aβ deposits [189]. In addition, neither CAA nor Aβ is detected in extra-cranial blood vessels [139]. This indicates that neural factors may be important in initiating vascular Aβ deposition.

## 3.3. Drainage Hypothesis

The drainage hypothesis suggests that neuronally produced Aβ drains with the interstitial fluid (ISF) along perivascular spaces of parenchymal and leptomeningeal vessels to cervical lymph nodes (Fig. 8A). CAA occurs due to deposition of Aβ along these drainage pathways [179]. In favor of the drainage hypothesis is the presence of CAA in transgenic mice which express human APP in the brain, in most instances under the control of neuron-specific promoters [11,32,157].

Based on the drainage hypothesis, a detailed mechanism for the formation of CAA and its relevance for AD has been proposed by Nicoll and co-workers [107]: "Aβ produced by neurons passes from the extracellular spaces in the brain parenchyma into the capillary basement membrane. Aβ and interstitial fluid would normal pass along the capillary basement membrane into the basement membranes on the outer aspect of the artery wall. Joined by Aβ from SMCs, Aβ and interstitial fluid would flow freely out of the brain along periarterial pathways driven by the pulsations of the arteries. With the onset of arteriosclerosis, the artery walls become more rigid, the amplitude of pulsations is reduced and the passage of Aβ along the vessel walls is slowed. Such slowing allows the soluble Aβ in the vessel walls to precipitate as insoluble or β-pleated sheet amyloid resulting in CAA. The amyloid then blocks the elimination of Aβ leading to increased concentration of soluble Aβ in the brain. The increase in soluble Aβ, which may by itself be associated with dementia, also leads to precipitation of Aβ in the form of plaques, the development of tau pathology and neuronal and synaptic loss."

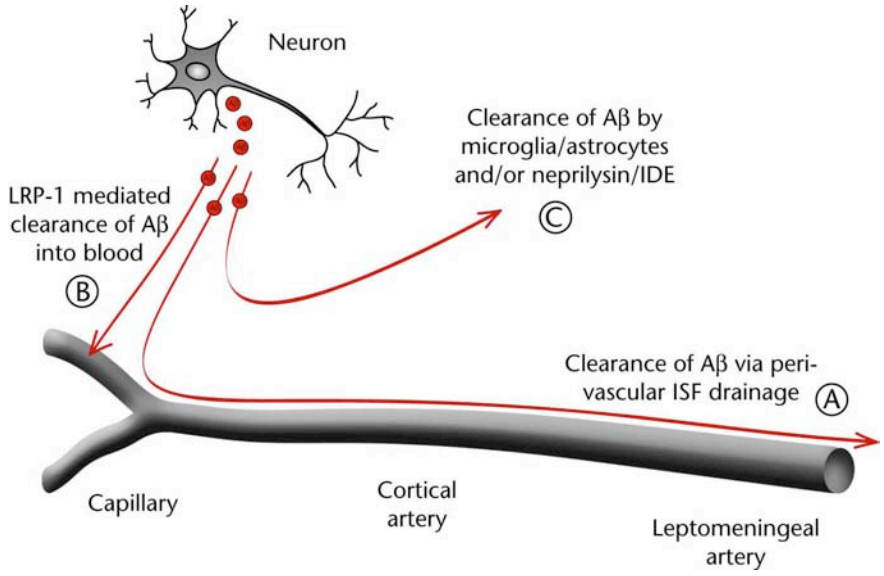


**Figure 8.** There is evidence for several routes of elimination of Aβ from the brain. (**A**) Drainage with the interstitial fluid along the perivascular pathway. (**B**) LRP-1-mediatet clearance across the blood brain barrier into the blood. (**C**) Clearance by microglia/astrocytes and/or neprilysin/IDE. (modified from Nicoll *et al.*, 2004).

In addition to the clearance of soluble Aβ by perivascular interstitial drainage pathways, other mechanisms for the elimination of Aβ from the brain exist [106]. Aβ can be absorbed into the blood via the low-density-lipoprotein receptor-related protein-1 (LRP-1) [137]. Further, Aβ has been shown to be degraded in the extracellular space of the brain by neprilysin [64] and insulin-degrading enzyme (IDE) [27]. Moreover, it has been proposed that Aβ can be cleared by microglia [180] and astrocytes [187].

# 4. Animal and Experimental Models of CAA

## 4.1. Naturally Occurring CAA in Aged Dogs and Non-Human Primates

Aged dogs develop CAA and amyloid plaques, however, few canine plaques attain the classical form with congophilic amyloid and abnormal neurites. Vascular amyloid is located in parenchymal and meningeal arterioles and in capillaries [102,173]. Amyloid accumulation starts in large vessels, particularly in the basal lamina of the tunica media of large arteries, and SMCs in the area of Aβ accumulation degenerate and die [178]. Aβ induces a segmental loss of leptomeningeal vessel wall viability [119]. The increase in the numerical density of amyloid-positive cortical and leptomeningeal vessels correlates with age [178] and CAA is often accompanied by cerebral hemorrhage [16,155].

CAA also occurs in non-human primates, ranging from lemurs to chimpanzees. Intriguingly, whether amyloid is deposited mainly in the parenchyma of the brain or in the vascular wall is species-specific to a certain degree [173]. The best-characterized primate models of CAA are squirrel and rhesus monkeys. In aged squirrel monkeys, amyloid is associated primarily with intracerebral and meningeal capillaries and arterioles and occurs to a lesser degree as small and/or diffuse deposits in the neural parenchyma and in the dense cores of senile plaques. The pattern of CAA localization is comparable to that in humans. In contrast to squirrel monkeys, aged rhesus monkeys develop mostly parenchymal amyloid deposits and have relatively less vascular amyloid. This species difference in the histological distribution of amyloid suggests that separate mechanisms may influence the accumulation of amyloid in cerebral blood vessels and in the neural parenchyma [174]. In addition to non-human primates and dogs, CAA has also been found in aged polar bears and wolverines [125,134].

The major disadvantage of studying CAA in animal models with naturally occurring CAA is the variability of the extent of vascular amyloid. Studies have to be performed with relatively large groups of old animals. Therefore, several transgenic mice showing AD-like pathology have been developed, some off which also develop CAA.

## 4.2. CAA in Transgenic Mice

A lot of different transgenic mouse model of AD have been developed. All of them overexpress human APP (hAPP) containing familial AD-causing mutations in their brains. In the majority of

cases the transgenes are expressed by neuron-specific promoters, and as a result thereof, Aβ deposits are observed in form of amyloid plaques in the brain parenchyma. CAA, however, is often not a prominent feature in these mice.

The first mouse model that has been reported to develop significant CAA, in addition to parenchymal plaques, is the APP23 mouse model that overexpresses hAPP bearing the Swedish K670N/M671L double mutation from the neuron-specific Thy-1 promoter [11,146]. As observed in humans, severe CAA in APP23 mice causes loss of SMCs and hemorrhages [181]. A detailed analysis of CAA and associated pathology in APP23 is described in the experimental section of this thesis.

A second mouse model overexpresses hAPP with the V717I London mutation under control of the Thy-1 promoter (APP/Ld mice) [157]. Besides amyloid plaques, aging APP/Ld mice also develop CAA that is predominantly seen in arterioles and ranges in extent from small focal to circumferential Aβ deposits. Like APP23 mice, loss of SMCs is seen in cerebral blood vessels of APP/Ld mice, however, no hemorrhages are observed. The major Aβ species that is deposited in the vessel wall is Aβ40. APP/Ld x PS1 A246E double-transgenic mice show higher Aβ42 levels that cause an increase in CAA and senile plaque formation.

The PDAPP [34] and the Tg2576 mouse model [60] were the first transgenic mice reported to develop significant AD-like pathology. PDAPP mice overexpress hAPP V717F from the platelet-derived growth factor (PDGF)-β promoter, while in Tg2576 mice hAPP K670N/M671L is overexpressed by hamster prion protein (PrP) promoter. In addition to amyloid plaques, both models develop an age-dependent increase in CAA with associated microhemorrhage, with the Tg2576 model having an earlier and more severe phenotype [32] and showing SMC degeneration [13]. Interestingly, when Tg2576 and PDAPP mice are bred onto an ApoE -/- background, no CAA is detected through 24 months of age, and there is little to no evidence of microhemorrhage. Biochemical analysis of isolated cerebral vessels from both PDAPP and Tg2576 mice with CAA revealed that, as in human CAA, the ratio of Aβ40:42 was elevated relative to brain parenchyma. In contrast, the ratio of Aβ40:42 from cerebral vessels isolated from old PDAPP/ApoE -/- mice was extremely low. These findings demonstrate that murine ApoE markedly promotes the formation of CAA and associated vessel damage and that the effect of ApoE combined with the level of Aβ40 or the ratio of Aβ40:42 facilitates this process [32].

Another approach reports that astroglial overproduction of the transforming growth factor (TGF)-β1 induces Aβ deposition in cerebral blood vessels and meninges of aged transgenic mice. Co-expression of TGF-β1 in transgenic mice overexpressing hAPP accelerates the deposition of Aβ [188]. Interestingly, aged double-transgenic hAPP/TGF-β1 mice show a three-fold reduction in

the number of parenchymal amyloid plaques and a 50% reduction in the overall Aβ load in the hippocampus and neocortex. In these mice, Aβ accumulates substantially in cerebral blood vessels. The reduction of parenchymal plaques is associated with a strong activation of microglia and an increase in inflammatory mediators [186]. In cerebral microvessels from young amyloid pre-depositing TGF-β1-transgenic mice, which display a prominent perivascular astrocytosis, an accumulation of basement membrane proteins and thickening of capillary basement membranes is observed. In amyloid depositing mice, various degenerative changes in microvascular cells of the brain can be observed [185].

All the mouse models described above develop both parenchymal amyloid and to a varying degree, cerebrovascular amyloid. Herein we describe now for the first time the generation of transgenic mice that develop significant CAA in the absence of compact parenchymal amyloid. These mice overexpress hAPP containing the APP E693Q Dutch mutation in neurons of the brain (APPDutch mice). A detailed characterization of APPDutch mice is given in the experimental section of this thesis.

To a certain degree, CAA can also be studied with the help of different *in vitro* systems as described below.

## 4.3. In Vitro Models of CAA

### 4.3.1. Smooth Muscle Cells and Human Brain Pericytes

Primary cultures of human cerebrovascular SMCs and HBPs are used as a model to investigate cellular pathologic processes associated with CAA. SMCs can be isolated from human parenchymal arterioles or leptomeningeal vessels and HBPs, which are phenotypically related to SMCs, from brain capillaries. Soluble Aβ42, but not Aβ40, causes rapid degeneration of cultured SMCs [18,158] and HBPs [162]. Interestingly, pre-aggregation of Aβ abolished its toxic effects [19]. Compared to Aβwt42, AβDutch40 even shows enhanced pathologic properties towards SMCs [17,175] and HBPs [163]. At low concentrations, only AβDutch40, but not Aβwt40 selectively binds and assembles into abundant fibrils on the surfaces of cultured human cerebrovascular SMCs. However, in a cell-free assay and at the same dilution, Aβ does not aggregate into fibrils. Addition of the dye Congo red prevents the cell surface fibril assembly of AβDutch40 and moreover, blocks the key pathologic responses induced by AβDutch40 in these cells [159]. Similarly, catalase and insulin are able to inhibit both, fibril formation and the toxic effect of AβDutch40 on HBPs [121,122]. Surprisingly, AβDutch42, like Aβwt40, shows no pathologic effect on

SMCs and HBPs [162]. In contrast to neurons, oxidative stress seems not to be important in Aβ-induced degeneration of SMCs and HBPs, since antioxidants could not inhibit Aβ-induced toxicity [122]. In summary, the pathogenic Aβ-fibril formation at the surface of cerebrovascular SMCs and HBPs seems to be essential for its toxicity to these cells.

### 4.3.2. Endothelial Cells

Aggregates of Aβwt40, Aβwt42, and AβDutch40 have been shown to be toxic to cultured human cerebrovascular endothelial cells (ECs), even at doses lower than those that are toxic to CNS neurons or leptomeningeal SMCs. Soluble AβDutch40 is equally toxic to ECs, whereas soluble Aβwt40 is toxic only at higher doses. This toxicity of AβDutch40 is seen at the lowest dose of 20 nM. Other than Aβwt40, soluble AβDutch40 aggregates on the surface of cultured ECs, and its toxicity can be blocked by Congo red, which inhibits amyloid fibril formation [22,100]. Unfortunately, no experiments have been performed with AβDutch42. In contrast to SMCs and HBPs, some antioxidants that inhibit free radical formation, such as vitamin E [101], *n*-propyl gallate and phenylbutyl *tert*-nitrone [6,22], and superoxid dismutase [147] can inhibit Aβ-induced toxicity *in vitro*, indicating that Aβ causes oxidative stress in ECs.

### 4.3.3. Whole Vessel Cultures

The effect of Aβ on the vasculature has also been studied in whole vessel cultures of rat aorta or on isolated human cerebral arteries collected following rapid autopsies. These studies demonstrate that freshly solubilized Aβ has vasoactive properties eliciting vasoconstriction, and they suggest that Aβ vasoactivity is mediated via the stimulation of a proinflammatory pathway. In addition, a similar proinflammatory response appears to be mediated by Aβ in isolated human brain microvessels [111,150,154].

# 5. References


1. Alonzo, N. C., Hyman, B. T., Rebeck, G. W. & Greenberg, S. M. Progression of cerebral amyloid angiopathy: accumulation of amyloid-β40 in affected vessels. *J Neuropathol Exp Neurol* **57**, 353-9 (1998).

2. Anders, K. H. et al. Giant cell arteritis in association with cerebral amyloid angiopathy: immunohistochemical and molecular studies. *Hum Pathol* **28**, 1237-46 (1997).

3. Benson, M. D. Leptomeningeal amyloid and variant transthyretins. *Am J Pathol* **148**, 351-4 (1996).

4. Bergeron, C., Ranalli, P. J. & Miceli, P. N. Amyloid angiopathy in Alzheimer's disease. *Can J Neurol Sci* **14**, 564-9 (1987).

5. Bjarnadottir, M. et al. The cerebral hemorrhage-producing cystatin C variant (L68Q) in extracellular fluids. *Amyloid* **8**, 1-10 (2001).

6. Blanc, E. M., Toborek, M., Mark, R. J., Hennig, B. & Mattson, M. P. Amyloid β-peptide induces cell monolayer albumin permeability, impairs glucose transport, and induces apoptosis in vascular endothelial cells. *J Neurochem* **68**, 1870-81 (1997).

7. Bornebroek, M. et al. White matter lesions and cognitive deterioration in presymptomatic carriers of the amyloid precursor protein gene codon 693 mutation. *Arch Neurol* **53**, 43-8 (1996).

8. Bugiani, O. et al. An Italien type of HCHWA. *Neurobiol Aging* **19**, S238 (1998).

9. Cadavid, D., Mena, H., Koeller, K. & Frommelt, R. A. Cerebral β amyloid angiopathy is a risk factor for cerebral ischemic infarction. A case control study in human brain biopsies. *J Neuropathol Exp Neurol* **59**, 768-73 (2000).

10. Calero, M. et al. Distinct properties of wild-type and the amyloidogenic human cystatin C variant of hereditary cerebral hemorrhage with amyloidosis, Icelandic type. *J Neurochem* **77**, 628-37 (2001).

11. Calhoun, M. E. et al. Neuronal overexpression of mutant amyloid precursor protein results in prominent deposition of cerebrovascular amyloid. *Proc Natl Acad Sci U S A* **96**, 14088-93 (1999).

12. Castano, E. M. et al. The length of amyloid-β in hereditary cerebral hemorrhage with amyloidosis, Dutch type. Implications for the role of amyloid-β 1-42 in Alzheimer's disease. *J Biol Chem* **271**, 32185-91 (1996).

13. Christie, R., Yamada, M., Moskowitz, M. & Hyman, B. Structural and functional disruption of vascular smooth muscle cells in a transgenic mouse model of amyloid angiopathy. *Am J Pathol* **158**, 1065-71 (2001).

14. Cras, P. et al. Presenile Alzheimer dementia characterized by amyloid angiopathy and large amyloid core type senile plaques in the APP 692Ala-->Gly mutation. *Acta Neuropathol (Berl)* **96**, 253-60 (1998).

15. Crawford, F. C. et al. A polymorphism in the cystatin C gene is a novel risk factor for late-onset Alzheimer's disease. *Neurology* **55**, 763-8 (2000).

16. Dahme, E. & Schroder, B. [Congophilic angiopathy, cerebrovascular microaneurysms and cerebral hemorrhages in old dogs]. *Zentralbl Veterinarmed A* **26**, 601-13 (1979).

17. Davis, J. & Van Nostrand, W. E. Enhanced pathologic properties of Dutch-type mutant amyloid β-protein. *Proc Natl Acad Sci U S A* **93**, 2996-3000 (1996).

18. Davis-Salinas, J., Saporito-Irwin, S. M., Cotman, C. W. & Van Nostrand, W. E. Amyloid β-protein induces its own production in cultured degenerating cerebrovascular smooth muscle cells. *J Neurochem* **65**, 931-4 (1995).

19. Davis-Salinas, J. & Van Nostrand, W. E. Amyloid β-protein aggregation nullifies its pathologic properties in cultured cerebrovascular smooth muscle cells. *J Biol Chem* **270**, 20887-90 (1995).

20. De Strooper, B. Aph-1, Pen-2, and Nicastrin with Presenilin generate an active gamma-Secretase complex. *Neuron* **38**, 9-12 (2003).

21. Dermaut, B. et al. Cerebral amyloid angiopathy is a pathogenic lesion in Alzheimer's disease due to a novel presenilin 1 mutation. *Brain* **124**, 2383-92 (2001).

22. Eisenhauer, P. B., Johnson, R. J., Wells, J. M., Davies, T. A. & Fine, R. E. Toxicity of various amyloid β peptide species in cultured human blood-brain barrier endothelial cells: increased toxicity of dutch-type mutant. *J Neurosci Res* **60**, 804-10 (2000).

23. Ellis, R. J. et al. Cerebral amyloid angiopathy in the brains of patients with Alzheimer's disease: the CERAD experience, Part XV. *Neurology* **46**, 1592-6 (1996).

24. Eng, J. A., Frosch, M. P., Choi, K., Rebeck, G. W. & Greenberg, S. M. Clinical manifestations of cerebral amyloid angiopathy-related inflammation. *Ann Neurol* **55**, 250-6 (2004).

25. Esch, F. S. et al. Cleavage of amyloid β peptide during constitutive processing of its precursor. *Science* **248**, 1122-4 (1990).

26. Esiri, M. M. & Wilcock, G. K. Cerebral amyloid angiopathy in dementia and old age. *J Neurol Neurosurg Psychiatry* **49**, 1221-6 (1986).

27. Evin, G. & Weidemann, A. Biogenesis and metabolism of Alzheimer's disease Aβ amyloid peptides. *Peptides* **23**, 1285-97 (2002).

28. Frackowiak, J., Zoltowska, A. & Wisniewski, H. M. Non-fibrillar β-amyloid protein is associated with smooth muscle cells of vessel walls in Alzheimer disease. *J Neuropathol Exp Neurol* **53**, 637-45 (1994).

29. Francis, R. et al. aph-1 and pen-2 are required for Notch pathway signaling, gamma-secretase cleavage of βAPP, and presenilin protein accumulation. *Dev Cell* **3**, 85-97 (2002).

30. Frangione, B. et al. Familial cerebral amyloid angiopathy related to stroke and dementia. *Amyloid* **8 Suppl 1**, 36-42 (2001).

31. Fraser, P. E. et al. Fibril formation by primate, rodent, and Dutch-hemorrhagic analogues of Alzheimer amyloid β-protein. *Biochemistry* **31**, 10716-23 (1992).

32. Fryer, J. D. et al. Apolipoprotein E markedly facilitates age-dependent cerebral amyloid angiopathy and spontaneous hemorrhage in amyloid precursor protein transgenic mice. *J Neurosci* **23**, 7889-96 (2003).

33. Fukuchi, K. et al. High levels of circulating β-amyloid peptide do not cause cerebral β-amyloidosis in transgenic mice. *Am J Pathol* **149**, 219-27 (1996).

34. Games, D. et al. Alzheimer-type neuropathology in transgenic mice overexpressing V717F β-amyloid precursor protein. *Nature* **373**, 523-7 (1995).

35. Garzuly, F., Vidal, R., Wisniewski, T., Brittig, F. & Budka, H. Familial meningocerebrovascular amyloidosis, Hungarian type, with mutant transthyretin (TTR Asp18Gly). *Neurology* **47**, 1562-7 (1996).

36. Ghetti, B. et al. Vascular variant of prion protein cerebral amyloidosis with tau-positive neurofibrillary tangles: the phenotype of the stop codon 145 mutation in PRNP. *Proc Natl Acad Sci U S A* **93**, 744-8 (1996).

37. Ghiso, J. & Frangione, B. Cerebral amyloidosis, amyloid angiopathy, and their relationship to stroke and dementia. *J Alzheimers Dis* **3**, 65-73 (2001).

38. Ghiso, J., Jensson, O. & Frangione, B. Amyloid fibrils in hereditary cerebral hemorrhage with amyloidosis of Icelandic type is a variant of gamma-trace basic protein (cystatin C). *Proc Natl Acad Sci U S A* **83**, 2974-8 (1986).

39. Ghiso, J., Plant, G. T., Revesz, T., Wisniewski, T. & Frangione, B. Familial cerebral amyloid angiopathy (British type) with nonneuritic amyloid plaque formation may be due to a novel amyloid protein. *J Neurol Sci* **129**, 74-5 (1995).

40. Ghiso, J. A. et al. Systemic amyloid deposits in familial British dementia. *J Biol Chem* **276**, 43909-14 (2001).

41. Glenner, G. G. Amyloid deposits and amyloidosis. The β-fibrilloses (first of two parts). *N Engl J Med* **302**, 1283-92 (1980).

42. Glenner, G. G. Amyloid deposits and amyloidosis: the β-fibrilloses (second of two parts). *N Engl J Med* **302**, 1333-43 (1980).

43. Glenner, G. G., Henry, J. H. & Fujihara, S. Congophilic angiopathy in the pathogenesis of Alzheimer's degeneration. *Ann Pathol* **1**, 120-9 (1981).

44. Glenner, G. G. & Wong, C. W. Alzheimer's disease: initial report of the purification and characterization of a novel cerebrovascular amyloid protein. *Biochem Biophys Res Commun* **120**, 885-90 (1984).

45. Goutte, C., Tsunozaki, M., Hale, V. A. & Priess, J. R. APH-1 is a multipass membrane protein essential for the Notch signaling pathway in Caenorhabditis elegans embryos. *Proc Natl Acad Sci U S A* **99**, 775-9 (2002).

46. Grabowski, T. J., Cho, H. S., Vonsattel, J. P., Rebeck, G. W. & Greenberg, S. M. Novel amyloid precursor protein mutation in an Iowa family with dementia and severe cerebral amyloid angiopathy. *Ann Neurol* **49**, 697-705 (2001).

47. Gray, F., Dubas, F., Roullet, E. & Escourolle, R. Leukoencephalopathy in diffuse hemorrhagic cerebral amyloid angiopathy. *Ann Neurol* **18**, 54-9 (1985).

48. Greenberg, S. M. Cerebral amyloid angiopathy: prospects for clinical diagnosis and treatment. *Neurology* **51**, 690-4 (1998).

49. Greenberg, S. M. Cerebral amyloid angiopathy and vessel dysfunction. *Cerebrovasc Dis* **13 Suppl 2**, 42-7 (2002).

50. Greenberg, S. M. et al. Apolipoprotein E epsilon 4 is associated with the presence and earlier onset of hemorrhage in cerebral amyloid angiopathy. *Stroke* **27**, 1333-7 (1996).

51. Greenberg, S. M., Rebeck, G. W., Vonsattel, J. P., Gomez-Isla, T. & Hyman, B. T. Apolipoprotein E epsilon 4 and cerebral hemorrhage associated with amyloid angiopathy. *Ann Neurol* **38**, 254-9 (1995).

52. Greenberg, S. M. et al. Hemorrhagic stroke associated with the Iowa amyloid precursor protein mutation. *Neurology* **60**, 1020-2 (2003).

53. Greenberg, S. M. & Vonsattel, J. P. Diagnosis of cerebral amyloid angiopathy. Sensitivity and specificity of cortical biopsy. *Stroke* **28**, 1418-22 (1997).

54. Greenberg, S. M. et al. Association of apolipoprotein E epsilon2 and vasculopathy in cerebral amyloid angiopathy. *Neurology* **50**, 961-5 (1998).

55. Greenberg, S. M., Vonsattel, J. P., Stakes, J. W., Gruber, M. & Finklestein, S. P. The clinical spectrum of cerebral amyloid angiopathy: presentations without lobar hemorrhage. *Neurology* **43**, 2073-9 (1993).

56. Haass, C. et al. Amyloid β-peptide is produced by cultured cells during normal metabolism. *Nature* **359**, 322-5 (1992).

57. Hendriks, L. et al. Presenile dementia and cerebral haemorrhage linked to a mutation at codon 692 of the β-amyloid precursor protein gene. *Nat Genet* **1**, 218-21 (1992).

58. Holton, J. L. et al. Regional distribution of amyloid-Bri deposition and its association with neurofibrillary degeneration in familial British dementia. *Am J Pathol* **158**, 515-26 (2001).

59. Holton, J. L. et al. Familial Danish dementia: a novel form of cerebral amyloidosis associated with deposition of both amyloid-Dan and amyloid-β. *J Neuropathol Exp Neurol* **61**, 254-67 (2002).

60. Hsiao, K. et al. Correlative memory deficits, Aβ elevation, and amyloid plaques in transgenic mice. *Science* **274**, 99-102 (1996).

61. Hutton, M. Missense and splice site mutations in tau associated with FTDP-17: multiple pathogenic mechanisms. *Neurology* **56**, S21-5 (2001).

62. Ida, N. et al. Analysis of heterogeneous A4 peptides in human cerebrospinal fluid and blood by a newly developed sensitive Western blot assay. *J Biol Chem* **271**, 22908-14 (1996).

63. Ishii, N., Nishihara, Y. & Horie, A. Amyloid angiopathy and lobar cerebral haemorrhage. *J Neurol Neurosurg Psychiatry* **47**, 1203-10 (1984).

64. Iwata, N., Takaki, Y., Fukami, S., Tsubuki, S. & Saido, T. C. Region-specific reduction of Aβ-degrading endopeptidase, neprilysin, in mouse hippocampus upon aging. *J Neurosci Res* **70**, 493-500 (2002).

65. Iwatsubo, T. et al. Visualization of Aβ42(43) and Aβ40 in senile plaques with end-specific Aβ monoclonals: evidence that an initially deposited species is Aβ42(43). *Neuron* **13**, 45-53 (1994).

66. Jancso, G. et al. β-amyloid (1-42) peptide impairs blood-brain barrier function after intracarotid infusion in rats. *Neurosci Lett* **253**, 139-41 (1998).

67. Jellinger, K. Cerebrovascular amyloidosis with cerebral hemorrhage. *J Neurol* **214**, 195-206 (1977).

68. Jellinger, K. A. Alzheimer disease and cerebrovascular pathology: an update. *J Neural Transm* **109**, 813-36 (2002).

69. Joachim, C. L., Duffy, L. K., Morris, J. H. & Selkoe, D. J. Protein chemical and immunocytochemical studies of meningovascular β-amyloid protein in Alzheimer's disease and normal aging. *Brain Res* **474**, 100-11 (1988).

70. Kalaria, R. N., Premkumar, D. R., Pax, A. B., Cohen, D. L. & Lieberburg, I. Production and increased detection of amyloid β protein and amyloidogenic fragments in brain microvessels, meningeal vessels and choroid plexus in Alzheimer's disease. *Brain Res Mol Brain Res* **35**, 58-68 (1996).

71. Kang, J. et al. The precursor of Alzheimer's disease amyloid A4 protein resembles a cell-surface receptor. *Nature* **325**, 733-6 (1987).

72. Kawai, M. et al. Degeneration of vascular muscle cells in cerebral amyloid angiopathy of Alzheimer disease. *Brain Res* **623**, 142-6 (1993).

73. Kim, S. H. et al. Furin mediates enhanced production of fibrillogenic ABri peptides in familial British dementia. *Nat Neurosci* **2**, 984-8 (1999).

74. Kimberly, W. T., Zheng, J. B., Guenette, S. Y. & Selkoe, D. J. The intracellular domain of the β-amyloid precursor protein is stabilized by Fe65 and translocates to the nucleus in a notch-like manner. *J Biol Chem* **276**, 40288-92 (2001).

75. Kiuru, S., Salonen, O. & Haltia, M. Gelsolin-related spinal and cerebral amyloid angiopathy. *Ann Neurol* **45**, 305-11 (1999).

76. Koo, E. H. & Squazzo, S. L. Evidence that production and release of amyloid β-protein involves the endocytic pathway. *J Biol Chem* **269**, 17386-9 (1994).

77. Kumar-Singh, S. et al. Dense-core senile plaques in the Flemish variant of Alzheimer's disease are vasocentric. *Am J Pathol* **161**, 507-20 (2002).

78. Lee, S. S. & Stemmermann, G. N. Congophilic angiopathy and cerebral hemorrhage. *Arch Pathol Lab Med* **102**, 317-21 (1978).

79. Levy, E. et al. Mutation of the Alzheimer's disease amyloid gene in hereditary cerebral hemorrhage, Dutch type. *Science* **248**, 1124-6 (1990).

80. Levy, E., Lopez-Otin, C., Ghiso, J., Geltner, D. & Frangione, B. Stroke in Icelandic patients with hereditary amyloid angiopathy is related to a mutation in the cystatin C gene, an inhibitor of cysteine proteases. *J Exp Med* **169**, 1771-8 (1989).

81. Levy, E. et al. Codeposition of cystatin C with amyloid-β protein in the brain of Alzheimer disease patients. *J Neuropathol Exp Neurol* **60**, 94-104 (2001).

82. Luyendijk, W. & Schoen, J. H. Intracerebral Hematomas. A Clinical Study of 40 Surgical Cases. *Psychiatr Neurol Neurochir* **67**, 445-68 (1964).

83. Mackic, J. B. et al. Human blood-brain barrier receptors for Alzheimer's amyloid-β 1- 40. Asymmetrical binding, endocytosis, and transcytosis at the apical side of brain microvascular endothelial cell monolayer. *J Clin Invest* **102**, 734-43 (1998).

84. Mackic, J. B. et al. Cerebrovascular accumulation and increased blood-brain barrier permeability to circulating Alzheimer's amyloid β peptide in aged squirrel monkey with cerebral amyloid angiopathy. *J Neurochem* **70**, 210-5 (1998).

85. Mandybur, T. I. Cerebral amyloid angiopathy: the vascular pathology and complications. *J Neuropathol Exp Neurol* **45**, 79-90 (1986).

86. Maness, L. M., Banks, W. A., Podlisny, M. B., Selkoe, D. J. & Kastin, A. J. Passage of human amyloid β-protein 1-40 across the murine blood-brain barrier. *Life Sci* **55**, 1643-50 (1994).

87. Mann, D. M. et al. Predominant deposition of amyloid-β 42(43) in plaques in cases of Alzheimer's disease and hereditary cerebral hemorrhage associated with mutations in the amyloid precursor protein gene. *Am J Pathol* **148**, 1257-66 (1996).

88. Mann, D. M., Pickering-Brown, S. M., Takeuchi, A. & Iwatsubo, T. Amyloid angiopathy and variability in amyloid β deposition is determined by mutation position in presenilin-1-linked Alzheimer's disease. *Am J Pathol* **158**, 2165-75 (2001).

89. Marin, D. B. et al. The relationship between apolipoprotein E, dementia, and vascular illness. *Atherosclerosis* **140**, 173-80 (1998).

90. Martel, C. L., Mackic, J. B., McComb, J. G., Ghiso, J. & Zlokovic, B. V. Blood-brain barrier uptake of the 40 and 42 amino acid sequences of circulating Alzheimer's amyloid β in guinea pigs. *Neurosci Lett* **206**, 157-60 (1996).

91. Masters, C. L. et al. Amyloid plaque core protein in Alzheimer disease and Down syndrome. *Proc Natl Acad Sci U S A* **82**, 4245-9 (1985).

92. Masuda, J., Tanaka, K., Ueda, K. & Omae, T. Autopsy study of incidence and distribution of cerebral amyloid angiopathy in Hisayama, Japan. *Stroke* **19**, 205-10 (1988).

93. McCarron, M. O. & Nicoll, J. A. Apolipoprotein E genotype and cerebral amyloid angiopathy-related hemorrhage. *Ann N Y Acad Sci* **903**, 176-9 (2000).

94. McCarron, M. O. et al. Cerebral amyloid angiopathy-related hemorrhage. Interaction of APOE epsilon2 with putative clinical risk factors. *Stroke* **30**, 1643-6 (1999).

95. McCarron, M. O. et al. Amyloid β-protein length and cerebral amyloid angiopathy-related haemorrhage. *Neuroreport* **11**, 937-40 (2000).

96. McCarron, M. O. et al. The apolipoprotein E epsilon2 allele and the pathological features in cerebral amyloid angiopathy-related hemorrhage. *J Neuropathol Exp Neurol* **58**, 711-8 (1999).

97. Mead, S. et al. Familial British dementia with amyloid angiopathy: early clinical, neuropsychological and imaging findings. *Brain* **123 ( Pt 5)**, 975-91 (2000).

98. Melchor, J. P., McVoy, L. & Van Nostrand, W. E. Charge alterations of E22 enhance the pathogenic properties of the amyloid β-protein. *J Neurochem* **74**, 2209-12 (2000).

99. Merlini, G. & Bellotti, V. Molecular mechanisms of amyloidosis. *N Engl J Med* **349**, 583-96 (2003).

100. Miravalle, L. et al. Substitutions at codon 22 of Alzheimer's Aβ peptide induce diverse conformational changes and apoptotic effects in human cerebral endothelial cells. *J Biol Chem* **275**, 27110-6 (2000).

101. Munoz, F. J. et al. Vitamin E but not 17β-estradiol protects against vascular toxicity induced by β-amyloid wild type and the Dutch amyloid variant. *J Neurosci* **22**, 3081-9 (2002).

102. Nakamura, S. et al. Deposition of amyloid β protein (Aβ) subtypes [Aβ40 and Aβ42(43)] in canine senile plaques and cerebral amyloid angiopathy. *Acta Neuropathol (Berl)* **94**, 323-8 (1997).

103. Natte, R. et al. Amyloid β precursor protein-mRNA is expressed throughout cerebral vessel walls. *Brain Res* **828**, 179-83 (1999).

104. Natte, R. et al. Ultrastructural evidence of early non-fibrillar Aβ42 in the capillary basement membrane of patients with hereditary cerebral hemorrhage with amyloidosis, Dutch type. *Acta Neuropathol (Berl)* **98**, 577-82 (1999).

105. Nicoll, J. A. et al. High frequency of apolipoprotein E epsilon 2 allele in hemorrhage due to cerebral amyloid angiopathy. *Ann Neurol* **41**, 716-21 (1997).

106. Nicoll, J. A. & Weller, R. O. A new role for astrocytes: β-amyloid homeostasis and degradation. *Trends Mol Med* **9**, 281-2 (2003).

107. Nicoll, J. A., Yamada, M., Frackowiak, J., Mazur-Kolecka, B. & Weller, R. O. Cerebral amyloid angiopathy plays a direct role in the pathogenesis of Alzheimer's disease; Pro-CAA position statement. *Neurobiol Aging* **25**, 589-97 (2004).

108. Nilsberth, C. et al. The 'Arctic' APP mutation (E693G) causes Alzheimer's disease by enhanced Aβ protofibril formation. *Nat Neurosci* **4**, 887-93 (2001).

109. Nochlin, D., Bird, T. D., Nemens, E. J., Ball, M. J. & Sumi, S. M. Amyloid angiopathy in a Volga German family with Alzheimer's disease and a presenilin-2 mutation (N141I). *Ann Neurol* **43**, 131-5 (1998).

110. Okazaki, H., Reagan, T. J. & Campbell, R. J. Clinicopathologic studies of primary cerebral amyloid angiopathy. *Mayo Clin Proc* **54**, 22-31 (1979).

111. Paris, D. et al. Vasoactive effects of Aβ in isolated human cerebrovessels and in a transgenic mouse model of Alzheimer's disease: role of inflammation. *Neurol Res* **25**, 642-51 (2003).

112. Perez, R. G. et al. Mutagenesis identifies new signals for β-amyloid precursor protein endocytosis, turnover, and the generation of secreted fragments, including Aβ42. *J Biol Chem* **274**, 18851-6 (1999).

113. Petersen, R. B. et al. Transthyretin amyloidosis: a new mutation associated with dementia. *Ann Neurol* **41**, 307-13 (1997).

114. Plant, G. T., Revesz, T., Barnard, R. O., Harding, A. E. & Gautier-Smith, P. C. Familial cerebral amyloid angiopathy with nonneuritic amyloid plaque formation. *Brain* **113 ( Pt 3)**, 721-47 (1990).

115. Pluta, R., Barcikowska, M., Januszewski, S., Misicka, A. & Lipkowski, A. W. Evidence of blood-brain barrier permeability/leakage for circulating human Alzheimer's β-amyloid-(1-42)-peptide. *Neuroreport* **7**, 1261-5 (1996).

116. Postina, R. et al. A disintegrin-metalloproteinase prevents amyloid plaque formation and hippocampal defects in an Alzheimer disease mouse model. *J Clin Invest* **113**, 1456-64 (2004).

117. Prelli, F., Castano, E., Glenner, G. G. & Frangione, B. Differences between vascular and plaque core amyloid in Alzheimer's disease. *J Neurochem* **51**, 648-51 (1988).

118. Premkumar, D. R., Cohen, D. L., Hedera, P., Friedland, R. P. & Kalaria, R. N. Apolipoprotein E-epsilon4 alleles in cerebral amyloid angiopathy and cerebrovascular pathology associated with Alzheimer's disease. *Am J Pathol* **148**, 2083-95 (1996).

119. Prior, R., D'Urso, D., Frank, R., Prikulis, I. & Pavlakovic, G. Loss of vessel wall viability in cerebral amyloid angiopathy. *Neuroreport* **7**, 562-4 (1996).

120. Rensink, A. A., de Waal, R. M., Kremer, B. & Verbeek, M. M. Pathogenesis of cerebral amyloid angiopathy. *Brain Res Brain Res Rev* **43**, 207-23 (2003).

121. Rensink, A. A. et al. Insulin inhibits amyloid β-induced cell death in cultured human brain pericytes. *Neurobiol Aging* **25**, 93-103 (2004).

122. Rensink, A. A. et al. Inhibition of amyloid-β-induced cell death in human brain pericytes in vitro. *Brain Res* **952**, 111-21 (2002).

123. Revesz, T. et al. Cerebral amyloid angiopathies: a pathologic, biochemical, and genetic view. *J Neuropathol Exp Neurol* **62**, 885-98 (2003).

124. Revesz, T. et al. Sporadic and familial cerebral amyloid angiopathies. *Brain Pathol* **12**, 343-57 (2002).

125. Roertgen, K. E. et al. Aβ-associated cerebral angiopathy and senile plaques with neurofibrillary tangles and cerebral hemorrhage in an aged wolverine (Gulo gulo). *Neurobiol Aging* **17**, 243-7 (1996).

126. Roher, A. E. et al. Cortical and leptomeningeal cerebrovascular amyloid and white matter pathology in Alzheimer's disease. *Mol Med* **9**, 112-22 (2003).

127. Roks, G. et al. Presentation of amyloidosis in carriers of the codon 692 mutation in the amyloid precursor protein gene (APP692). *Brain* **123 ( Pt 10)**, 2130-40 (2000).

128. Rostagno, A. et al. Complement activation in chromosome 13 dementias. Similarities with Alzheimer's disease. *J Biol Chem* **277**, 49782-90 (2002).

129. Saito, Y., Buciak, J., Yang, J. & Pardridge, W. M. Vector-mediated delivery of 125I-labeled β-amyloid peptide Aβ 1-40 through the blood-brain barrier and binding to Alzheimer disease amyloid of the Aβ 1-40/vector complex. *Proc Natl Acad Sci U S A* **92**, 10227-31 (1995).

130. Sastre, M. et al. Presenilin-dependent gamma-secretase processing of β-amyloid precursor protein at a site corresponding to the S3 cleavage of Notch. *EMBO Rep* **2**, 835-41 (2001).

131. Scholz, W. Studien zur Pathologie der Hirngefässe. II. Die drusige Entartung der Hirnarterien und -capillaren. *Zeitschrift für gesamte Neurologie und Psychiatrie* **162**, 694-715 (1938).

132. Selkoe, D. J. Alzheimer's disease: genes, proteins, and therapy. *Physiol Rev* **81**, 741-66 (2001).

133. Selkoe, D. J. Folding proteins in fatal ways. *Nature* **426**, 900-4 (2003).

134. Selkoe, D. J., Bell, D. S., Podlisny, M. B., Price, D. L. & Cork, L. C. Conservation of brain amyloid proteins in aged mammals and humans with Alzheimer's disease. *Science* **235**, 873-7 (1987).

135. Seubert, P. et al. Isolation and quantification of soluble Alzheimer's β-peptide from biological fluids. *Nature* **359**, 325-7 (1992).

136. Sherrington, R. et al. Cloning of a gene bearing missense mutations in early-onset familial Alzheimer's disease. *Nature* **375**, 754-60 (1995).

137. Shibata, M. et al. Clearance of Alzheimer's amyloid-β(1-40) peptide from brain by LDL receptor-related protein-1 at the blood-brain barrier. *J Clin Invest* **106**, 1489-99 (2000).

138. Shin, Y., Cho, H. S., Rebeck, G. W. & Greenberg, S. M. Vascular changes in Iowa-type hereditary cerebral amyloid angiopathy. *Ann N Y Acad Sci* **977**, 245-51 (2002).

139. Shinkai, Y. et al. Amyloid β-proteins 1-40 and 1-42(43) in the soluble fraction of extra- and intracranial blood vessels. *Ann Neurol* **38**, 421-8 (1995).

140. Shoji, M. et al. Production of the Alzheimer amyloid β protein by normal proteolytic processing. *Science* **258**, 126-9 (1992).

141. Sinha, S. et al. Purification and cloning of amyloid precursor protein β-secretase from human brain. *Nature* **402**, 537-40 (1999).

142. Sisodia, S. S., Koo, E. H., Beyreuther, K., Unterbeck, A. & Price, D. L. Evidence that β-amyloid protein in Alzheimer's disease is not derived by normal processing. *Science* **248**, 492-5 (1990).

143. Soto, C., Castano, E. M., Frangione, B. & Inestrosa, N. C. The alpha-helical to β-strand transition in the amino-terminal fragment of the amyloid β-peptide modulates amyloid formation. *J Biol Chem* **270**, 3063-7 (1995).

144. Steiner, H. et al. A pathogenic presenilin-1 deletion causes abberrant Aβ42 production in the absence of congophilic amyloid plaques. *J Biol Chem* **276**, 7233-9 (2001).

145. Stewart, P. A., Hayakawa, K., Akers, M. A. & Vinters, H. V. A morphometric study of the blood-brain barrier in Alzheimer's disease. *Lab Invest* **67**, 734-42 (1992).

146. Sturchler-Pierrat, C. et al. Two amyloid precursor protein transgenic mouse models with Alzheimer disease-like pathology. *Proc Natl Acad Sci U S A* **94**, 13287-92 (1997).

147. Sutton, E. T., Hellermann, G. R. & Thomas, T. β-amyloid-induced endothelial necrosis and inhibition of nitric oxide production. *Exp Cell Res* **230**, 368-76 (1997).

148. Tagliavini, F. et al. Coexistence of Alzheimer's amyloid precursor protein and amyloid protein in cerebral vessel walls. *Lab Invest* **62**, 761-7 (1990).

149. Tagliavini, F. et al. A new βPP mutation related to hereditary cerebral hemorrhage. *Alzheimers Rep* **2** (1999).

150. Thomas, T., Thomas, G., McLendon, C., Sutton, T. & Mullan, M. β-Amyloid-mediated vasoactivity and vascular endothelial damage. *Nature* **380**, 168-71 (1996).

151. Tian, J., Shi, J., Bailey, K. & Mann, D. M. Relationships between arteriosclerosis, cerebral amyloid angiopathy and myelin loss from cerebral cortical white matter in Alzheimer's disease. *Neuropathol Appl Neurobiol* **30**, 46-56 (2004).

152. Tomimoto, H. et al. Vascular changes in white matter lesions of Alzheimer's disease. *Acta Neuropathol (Berl)* **97**, 629-34 (1999).

153. Tomonaga, M. Cerebral amyloid angiopathy in the elderly. *J Am Geriatr Soc* **29**, 151-7 (1981).

154. Townsend, K. P. et al. Proinflammatory and vasoactive effects of Aβ in the cerebrovasculature. *Ann N Y Acad Sci* **977**, 65-76 (2002).

155. Uchida, K., Nakayama, H. & Goto, N. Pathological studies on cerebral amyloid angiopathy, senile plaques and amyloid deposition in visceral organs in aged dogs. *J Vet Med Sci* **53**, 1037-42 (1991).

156. Ujiie, M., Dickstein, D. L., Carlow, D. A. & Jefferies, W. A. Blood-brain barrier permeability precedes senile plaque formation in an Alzheimer disease model. *Microcirculation* **10**, 463-70 (2003).

157. Van Dorpe, J. et al. Prominent cerebral amyloid angiopathy in transgenic mice overexpressing the london mutant of human APP in neurons. *Am J Pathol* **157**, 1283-98 (2000).

158. Van Nostrand, W. E., Davis-Salinas, J. & Saporito-Irwin, S. M. Amyloid β-protein induces the cerebrovascular cellular pathology of Alzheimer's disease and related disorders. *Ann N Y Acad Sci* **777**, 297-302 (1996).

159. Van Nostrand, W. E., Melchor, J. P. & Ruffini, L. Pathologic amyloid β-protein cell surface fibril assembly on cultured human cerebrovascular smooth muscle cells. *J Neurochem* **70**, 216-23 (1998).

160. Vassar, R. The β-secretase, BACE: a prime drug target for Alzheimer's disease. *J Mol Neurosci* **17**, 157-70 (2001).

161. Vassar, R. et al. β-secretase cleavage of Alzheimer's amyloid precursor protein by the transmembrane aspartic protease BACE. *Science* **286**, 735-41 (1999).

162. Verbeek, M. M., de Waal, R. M., Schipper, J. J. & Van Nostrand, W. E. Rapid degeneration of cultured human brain pericytes by amyloid β protein. *J Neurochem* **68**, 1135-41 (1997).

163. Verbeek, M. M., Van Nostrand, W. E. & De Waal, R. M. W. in *Cerebral amyloid angiopathy in Alzheimer's disease and related disorders* (eds. Verbeek, M. M., De Waal, R. M. W. & Vinters, H. V.) 265-279 (Kluwer Academic Publisher, Dordrecht, The Netherlands, 2000).

164. Vidal, R. et al. A stop-codon mutation in the BRI gene associated with familial British dementia. *Nature* **399**, 776-81 (1999).

165. Vidal, R. et al. Meningocerebrovascular amyloidosis associated with a novel transthyretin mis-sense mutation at codon 18 (TTRD 18G). *Am J Pathol* **148**, 361-6 (1996).

166. Vidal, R. et al. A decamer duplication in the 3' region of the BRI gene originates an amyloid peptide that is associated with dementia in a Danish kindred. *Proc Natl Acad Sci U S A* **97**, 4920-5 (2000).

167. Vinters, H. V. Cerebral amyloid angiopathy: a microvascular link between parenchymal and vascular dementia? *Ann Neurol* **49**, 691-3 (2001).

168. Vinters, H. V. & Gilbert, J. J. Cerebral amyloid angiopathy: incidence and complications in the aging brain. II. The distribution of amyloid vascular changes. *Stroke* **14**, 924-8 (1983).

169. Vinters, H. V. et al. Secondary microvascular degeneration in amyloid angiopathy of patients with hereditary cerebral hemorrhage with amyloidosis, Dutch type (HCHWA-D). *Acta Neuropathol (Berl)* **95**, 235-44 (1998).

170. Vinters, H. V. & Vonsattel, J. P. in *Cerebral amyloid angiopathy in Alzheimer's disease and related disorders* (eds. Verbeek, M. M., de Waal, R. M. W. & Vinters, H. V.) 137-155 (Kluwer Academic Publishers, Dordrecht, The Netherlands, 2000).

171. Vinters, H. V., Wang, Z. Z. & Secor, D. L. Brain parenchymal and microvascular amyloid in Alzheimer's disease. *Brain Pathol* **6**, 179-95 (1996).

172. Vonsattel, J. P. et al. Cerebral amyloid angiopathy without and with cerebral hemorrhages: a comparative histological study. *Ann Neurol* **30**, 637-49 (1991).

173. Walker, L. C. Animal models of cerebral β-amyloid angiopathy. *Brain Res Brain Res Rev* **25**, 70-84 (1997).

174. Walker, L. C., Masters, C., Beyreuther, K. & Price, D. L. Amyloid in the brains of aged squirrel monkeys. *Acta Neuropathol (Berl)* **80**, 381-7 (1990).

175. Wang, Z., Natte, R., Berliner, J. A., van Duinen, S. G. & Vinters, H. V. Toxicity of Dutch (E22Q) and Flemish (A21G) mutant amyloid β proteins to human cerebral microvessel and aortic smooth muscle cells. *Stroke* **31**, 534-8 (2000).

176. Wattendorff, A. R., Bots, G. T., Went, L. N. & Endtz, L. J. Familial cerebral amyloid angiopathy presenting as recurrent cerebral haemorrhage. *J Neurol Sci* **55**, 121-35 (1982).

177. Wattendorff, A. R., Frangione, B., Luyendijk, W. & Bots, G. T. Hereditary cerebral haemorrhage with amyloidosis, Dutch type (HCHWA-D): clinicopathological studies. *J Neurol Neurosurg Psychiatry* **58**, 699-705 (1995).

178. Wegiel, J. et al. The origin of amyloid in cerebral vessels of aged dogs. *Brain Res* **705**, 225-34 (1995).

179. Weller, R. O. et al. Cerebral amyloid angiopathy: amyloid β accumulates in putative interstitial fluid drainage pathways in Alzheimer's disease. *Am J Pathol* **153**, 725-33 (1998).

180. Weller, R. O. & Nicoll, J. A. Cerebral amyloid angiopathy: pathogenesis and effects on the ageing and Alzheimer brain. *Neurol Res* **25**, 611-6 (2003).

181. Winkler, D. T. et al. Spontaneous hemorrhagic stroke in a mouse model of cerebral amyloid angiopathy. *J Neurosci* **21**, 1619-27 (2001).

182. Wisniewski, H. M., Frackowiak, J. & Mazur-Kolecka, B. In vitro production of β-amyloid in smooth muscle cells isolated from amyloid angiopathy-affected vessels. *Neurosci Lett* **183**, 120-3 (1995).

183. Wisniewski, H. M. & Wegiel, J. b-amyloid formation by myocytes of leptomeningeal vessels. *Acta Neuropathol (Berl)* **87**, 233-41 (1994).

184. Wisniewski, H. M., Wegiel, J. & Kotula, L. Review. David Oppenheimer Memorial Lecture 1995: Some neuropathological aspects of Alzheimer's disease and its relevance to other disciplines. *Neuropathol Appl Neurobiol* **22**, 3-11 (1996).

185. Wyss-Coray, T., Lin, C., Sanan, D. A., Mucke, L. & Masliah, E. Chronic overproduction of transforming growth factor-β1 by astrocytes promotes Alzheimer's disease-like microvascular degeneration in transgenic mice. *Am J Pathol* **156**, 139-50 (2000).

186. Wyss-Coray, T. et al. TGF-β1 promotes microglial amyloid-β clearance and reduces plaque burden in transgenic mice. *Nat Med* **7**, 612-8 (2001).

187. Wyss-Coray, T. et al. Adult mouse astrocytes degrade amyloid-β in vitro and in situ. *Nat Med* **9**, 453-7 (2003).

188. Wyss-Coray, T. et al. Amyloidogenic role of cytokine TGF-β1 in transgenic mice and in Alzheimer's disease. *Nature* **389**, 603-6 (1997).

189. Xu, H. Q. & Wang, Y. S. Pathological study on cerebral amyloid angiopathy. *Chin Med J (Engl)* **104**, 842-5 (1991).

190. Yamada, M., Tsukagoshi, H., Otomo, E. & Hayakawa, M. Cerebral amyloid angiopathy in the aged. *J Neurol* **234**, 371-6 (1987).

191. Yamaguchi, H., Yamazaki, T., Lemere, C. A., Frosch, M. P. & Selkoe, D. J. β amyloid is focally deposited within the outer basement membrane in the amyloid angiopathy of Alzheimer's disease. An immunoelectron microscopic study. *Am J Pathol* **141**, 249-59 (1992).

192. Yasuda, M. et al. A novel missense mutation in the presenilin-1 gene in a familial Alzheimer's disease pedigree with abundant amyloid angiopathy. *Neurosci Lett* **232**, 29-32 (1997).

193. Yu, G. et al. Nicastrin modulates presenilin-mediated notch/glp-1 signal transduction and βAPP processing. *Nature* **407**, 48-54 (2000).

194. Zarow, C., Zaias, B., Lyness, S. A. & Chui, H. Cerebral amyloid angiopathy in Alzheimer disease is associated with apolipoprotein E4 and cortical neuron loss. *Alzheimer Dis Assoc Disord* **13**, 1-8 (1999).

195. Zlokovic, B. V. Vascular disorder in Alzheimer's disease: role in pathogenesis of dementia and therapeutic targets. *Adv Drug Deliv Rev* **54**, 1553-9 (2002).

196. Zlokovic, B. V. et al. Blood-brain barrier transport of circulating Alzheimer's amyloid β. *Biochem Biophys Res Commun* **197**, 1034-40 (1993).

197. Zlokovic, B. V. et al. Glycoprotein 330/megalin: probable role in receptor-mediated transport of apolipoprotein J alone and in a complex with Alzheimer disease amyloid β at the blood-brain and blood-cerebrospinal fluid barriers. *Proc Natl Acad Sci U S A* **93**, 4229-34 (1996).

# Experimental Section

# 6. Spontaneous Hemorrhagic Stroke in a Mouse Model of Cerebral Amyloid Angiopathy

Manuscript published in: *The Journal of Neuroscience*, **21**, 1619-1627 (2001)

**David T. Winkler[1,4], Luca Bondolfi[1,4], Martin C. Herzig[1,4], Lukas Jann[1], Michael E. Calhoun[1,2], Karl-Heinz Wiederhold[3], Markus Tolnay[1], Matthias Staufenbiel[3], and Mathias Jucker[1]**

[1] Department of Neuropathology, Institute of Pathology, University of Basel, CH-4003 Basel, Switzerland, [2] Kastor Neurobiology of Aging Laboratories, Mount Sinai School of Medicine, New York, New York 10029,and [3]Nervous System Research, Novartis Pharma Ltd., CH-4002 Basel, Switzerland

[4]The first three authors contributed equally to this work.

## Abstract

A high risk factor for spontaneous and often fatal lobar hemorrhage is cerebral amyloid angiopathy (CAA). We now report that CAA in an amyloid precursor protein transgenic mouse model (APP23 mice) leads to a loss of vascular smooth muscle cells, aneurysmal vasodilatation, and in rare cases, vessel obliteration and severe vasculitis. This weakening of the vessel wall is followed by rupture and bleedings that range from multiple, recurrent microhemorrhages to large hematomas. Our results demonstrate that, in APP transgenic mice, the extracellular deposition of neuron-derived β-amyloid in the vessel wall is the cause of vessel wall disruption, which eventually leads to parenchymal hemorrhage. This first mouse model of CAA-associated hemorrhagic stroke will now allow development of diagnostic and therapeutic strategies.

*Key words: cerebral amyloid angiopathy; hemorrhage; stroke; bleeding; Alzheimer's disease; amyloid; amyloid precursor protein; smooth muscle cells; mouse; brain; CNS*

## Introduction

In the rapidly growing segment of elderly people in industrialized countries, hemorrhagic stroke is an increasing threat. Nontraumatic etiologies for cerebral hemorrhage include hypertension and cerebral amyloid angiopathy (CAA). In contrast to hypertensive small-vessel disease, in which bleeding is predominantly found in the basal ganglia, cerebellum, or pons, CAA leads to spontaneous and often fatal lobar hemorrhage [1-4]. CAA as a major cause of hemorrhagic stroke has not been fully appreciated in the past, with previous estimates in the range of 10% as a cause of all nontraumatic intracerebral hemorrhages [1,3,5].

The most common form of CAA is of the β-amyloid (Aβ) type [6,7]. Aβ is a 40to 42amino acid peptide derived from the longer amyloid precursor protein (APP) [8,9]. CAA occurs sporadically and can be detected to various degrees in approximately half of all individuals beyond 70years [5,10]. In addition, CAA can be detected in up to 90% of Alzheimer's disease (AD) patients [1,10]. In normal aging and AD, CAA occurs in conjunction with parenchymal amyloid plaques. However, CAA can also occur in the absence of compact plaques, as evidenced by patients with hereditary cerebral hemorrhage with amyloidosis-Dutch type (HCHWA-D) caused by a point mutation within Aβ at codon 693of APP (E693Q) [11]. These patients develop a severe form of CAA and suffer recurrent intracerebral hemorrhages, leading to death between the ages of 45and 55 [12].

Progress in CAA and CAA-related spontaneous hemorrhage has been slow because of the lack of useful animal models [13]. We have reported recently cerebral deposition of amyloid in plaques and vessels in an APP transgenic mouse model (APP23 mice) [14]. In the present study, we report that CAA in these mice consistently leads to multiple and recurrent spontaneous cerebral hemorrhages. This first mouse model of CAA-associated hemorrhagic stroke provides clues to the mechanism of CAA-related hemorrhage, as well as a needed model for testing diagnostic and therapeutic interventions.

## Results

### Age-related increase in CAA frequency and severity in APP23mice

In 8-month-old APP23 mice, cerebrovascular amyloid was generally absent with the exception of rare focal deposits in leptomeningeal vessels. In contrast, in the 19-and 27-month-old groups, cerebrovascular amyloid was found consistently throughout the neocortex, hippocampus, and thalamus (Fig. 1), and to a lesser degree in other regions such as septum, striatum, brainstem, and white matter. Leptomeningeal vessels were always heavily affected

(Fig. 2). Cerebrovascular amyloid was almost exclusively Congo red-positive, suggesting that amyloid is of a compact -pleated nature. Robust staining of vascular amyloid was found with both Aβ40- and Aβ42-specific antibodies. Aβ40 exceeded Aβ42 staining intensity, suggesting a predominance of Aβ40 over Aβ42 in vascular amyloid similar to that reported in humans [27]. Antibodies to cystatin C revealed appreciable staining of cerebrovascular amyloid, suggesting that mouse cystatin C is part of the amyloid. However, the cystatin C immunoreactivity was restricted to a subpopulation of amyloid-laden vessels predominantly in the thalamus and was clearly less intense than Aβ staining. Antibodies to SAP did not reveal any appreciable amyloid staining.

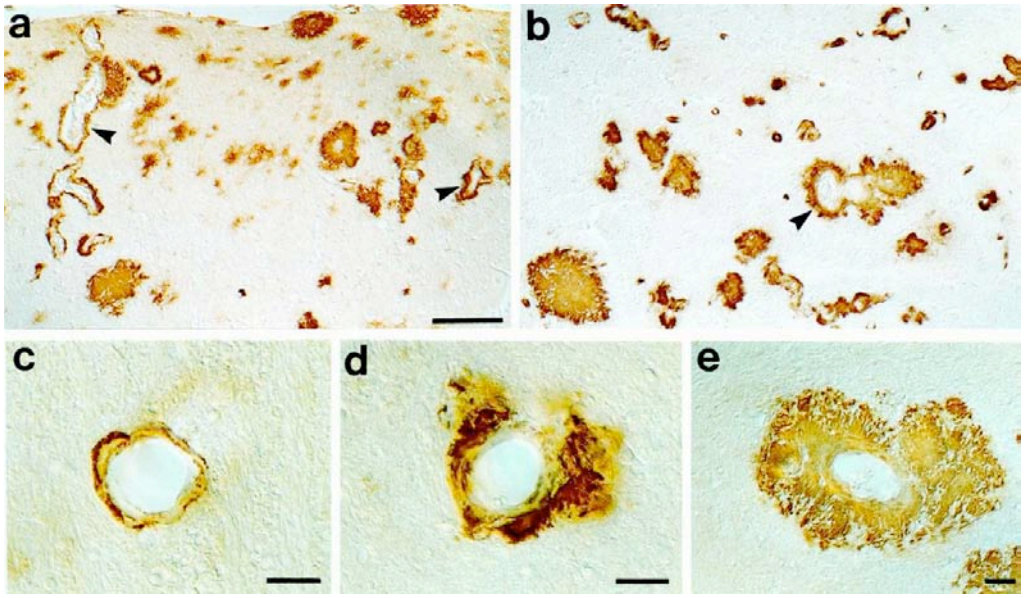


**Figure 1**. Cerebral amyloid angiopathy in APP23 mice. Aβ staining reveals significant CAA (*arrowheads)* in neocortex (*a*) and thalamus (*b*) in aged 27-month-old APP23 mice. Within these regions, CAA showed a great variability (*c-e)*, ranging from vessels with a thin rim of amyloid in the vessel wall (*c*; severity grade, 1), to vascular amyloid with amyloid infiltrating the surrounding neuropil (*d*; severity grade, 2), and to dyshoric amyloid with amyloid deposition within the vessel wall and with a thick and complete amyloid coat around the vessel wall (*e*; severity grade, 3). Scale bars: *a*, *b*, 100µm; *c-e*, 10µm.

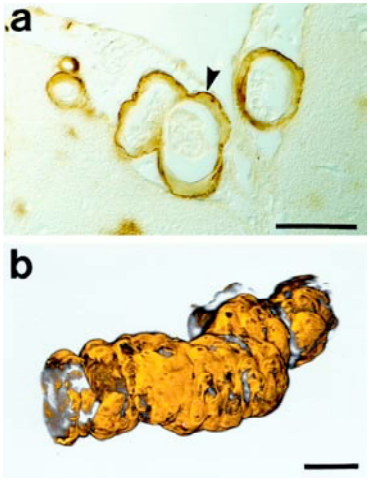


**Figure 2**. Cerebrovascular amyloid in leptomeningeal vessels. Leptomeningeal vessels are the most consistent and the first to exhibit cerebrovascular amyloid in APP23 mice. Shown in *a* are leptomeningeal vessels at the surface of the cingulate cortex of a 19-month-old APP23 mouse. Note that the amyloid is mostly confined to the outer vessel wall (*arrowhead)*, consistent with CAA in humans in which initial deposits are found in the outer basement membrane [28]. *b*, 3D reconstruction of an Aβ-stained (*orange* pseudocolored) heavily affected leptomeningeal vessel in an aged APP23 mouse. Note that nearly the entire surface is covered by a thick amyloid coat. The reconstruction consists of 198optical slices (< 0.7 μm), with a sampling interval of 0.35μm. Scale bars, 25μm.

Quantification of CAA frequency in systematically sampled sections revealed a striking age-related increase in neocortex (Fig. 3*a*), hippocampus, and thalamus (data not shown). CAA severity also increased with aging (Fig. 3*b*), indicating that not only are more vessels affected with aging but also that the amyloid burden of individual vessels increased with aging. Interestingly, thalamic vessels revealed a greater CAA severity compared with neocortical vessels in both the 19-and 27-month-old mice ($p<0.001$; CAA severity for thalamus, 1.59±0.08and 1.82±0.05, respectively). This observation was all the more interesting because the thalamus does not express the APP transgene (see Discussion). No difference in CAA frequency and severity was found between males and females ($p>0.05$), consistent with no significant sex predilection of CAA in humans [1,10].

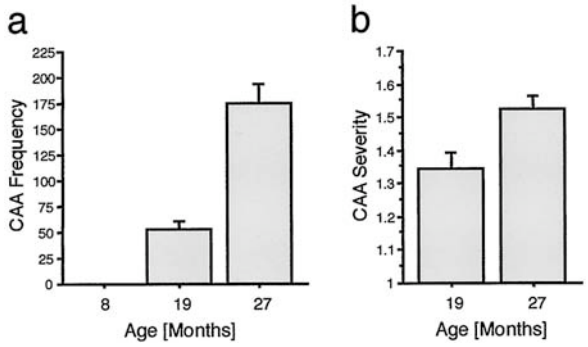


**Figure 3**. Age-related increase in CAA frequency and severity in APP23 mice. *a*, Number of amyloid affected vessels (CAA frequency) was quantified in systematically sampled sections through the neocortex of young (8months), adult (19months), and aged (27months) APP23 mice. ANOVA revealed a significant affect of age ($F(2,38) = 41.6$; $p<0.001$). *b*, A grading score was then used to assess severity of affected vessels (for details, see Fig. 1*c-e* and Materials and Methods). The mean CAA severity is indicated for the 19-and 27-month-old groups and revealed a significant age-related increase ($t(29) = 2.95$; $p<0.01$).

Similar to the striking increase in CAA with aging, a robust age-related increase in total amyloid load has been reported in these mice [15]. However, we did not find a significant correlation between CAA frequency or severity and amyloid load within age groups (data not shown), confirming previous age-corrected linear regression analysis [14].

**CAA leads to smooth muscle cell degeneration and aneurysm-likevasodilatation**

Confocal microscopy using double-labeling for Aβ and smooth muscle cell actin revealed an extensive loss of smooth muscle cells in the tunica media of amyloid-laden vessels (Fig. 4). Whereas in 19-month-old mice a focal discontinuity of the smooth muscle cell layer was typically observed (Fig. 4*b*), in 27-month-old mice, we often observed a dramatic loss of smooth muscle cells, with only patchy staining for smooth muscle cell actin remaining (Fig. 4*c*). Such a loss of smooth muscle cells concomitant with an increasing amyloid burden in the vessel wall was evident in leptomeningeal vessels and in vessels throughout neocortex, hippocampus, and thalamus, very similar to CAA in humans [29,30]. Interestingly, even in the heavily affected mice, there were often individual smooth muscle cell containing vessels that were not affected by CAA (Fig. 4*d*, *e*).

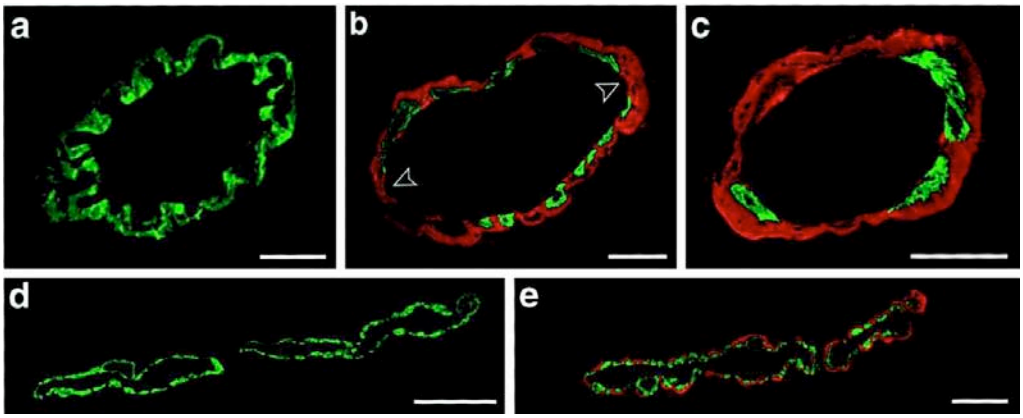


**Figure 4**. Cerebrovascular amyloid leads to smooth muscle cell loss. Confocal microscopy of double-immunolabeled vessels (*green*, smooth muscle actin; *red*, amyloid) in APP23 mice. *a*, Leptomeningeal vessel in an 8-month-old mouse shows no amyloid deposition and a complete layer of smooth muscle cells. *b*, Leptomeningeal vessel in a 19-month-old mouse shows focal disappearance of smooth muscle cells at the site of cerebrovascular amyloid (*arrowheads)*. *c*, In 27-month-old mice, smooth muscle cells have greatly disappeared, and a thick sheet of amyloid covers the wall of a leptomeningeal vessel. *d*, *e*, Parenchyma in the neocortex of a 19-month-old mouse showing an unaffected (*d*) and an amyloid-laden vessel (*e*) in close anatomical proximity. Shown are superpositions of 0.9-to 5-µm-thick optical sections. Scale bars: *a*, 10µm; *b-e*, 20µm.

We have shown previously a dystroglycan-mediated linkage between perivascular astrocytes and the vascular basement membrane [21]. Such a tight linkage between the vessel wall and astrocytic end feet is clearly important for vessel stabilization and nutrient trafficking. To study a potential disruption of this glia-vascular interface by cerebrovascular amyloid, we have used double-labeling for GFAP, β-dystroglycan, and Aβ . In cases in which the amyloid was confined to the vessel wall, no apparent changes in perivascular glia staining was apparent. However, when the vascular amyloid infiltrated the parenchyma, GFAP-positive glial processes were no longer tightly associated with the vessel parenchymal basement membrane, and there was a focal loss of β-dystroglycan (data not shown).

Loss of smooth muscle cells and disruption of the glia-vascular interface leads to vessel wall weakening. In the 27-month-old mice, a significant number of vessels with aneurysm-like enlargements were most often found in the thalamus and also neocortex (Fig. 5*c*). In such dilated vessels, the smooth muscle layer was in most cases absent, and vasodilatation often reached dramatic sizes of up to 200µm (Fig. 5*c*). No loss of smooth muscle cells or aneurysm type of vasodilatation was found in nontransgenic mice of any age.

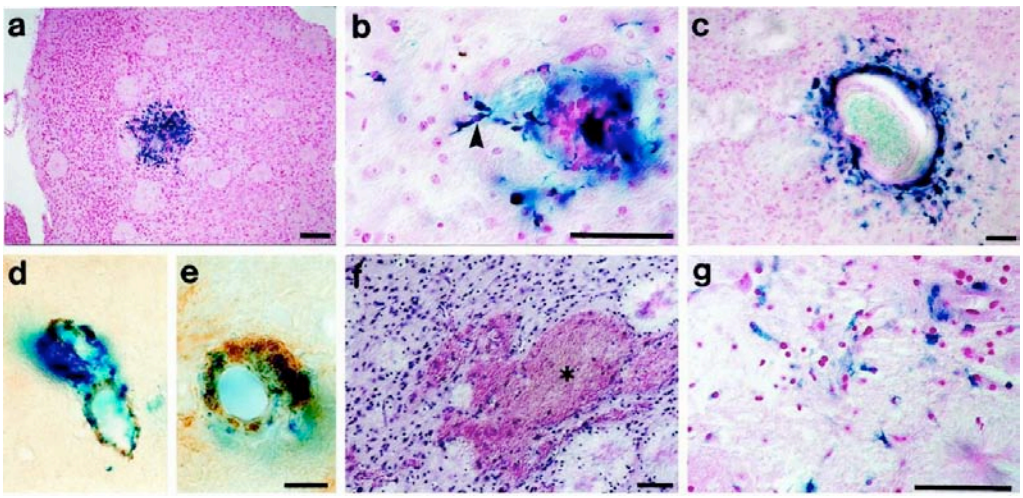


**Figure 5**. CAA-related hemorrhage in APP23 mice. *a*, Hemosiderin staining (*blue)* in the frontal cortex of a 27-month-old mouse indicative of an old hemorrhage. The section is counterstained with nuclear fast red. *b*, Perivascular hemosiderin-positive microglia (*arrowhead)* in close vicinity of a small vessel in a 27-month-old mouse. *c*, Hemosiderin-positive microglia surrounding an enlarged neocortical vessel of aneurysm-like appearance. *d*, *e*, Double-labeling for amyloid (*brown)* and hemosiderin (*blue)* localized bleedings to amyloid-laden vessels. *f*, Evidence for acute hematoma was assessed in H&E-stained sections. A significant hemorrhage (*asterisk)* in the frontal cortex of a 27-month-old APP23 mouse is shown. *g*, An adjacent section to *f* was stained with Berlin blue and revealed an old hemorrhage in the same region. Scale bars: *a*, 100µm; *b*, *c*, *f*, *g*, 50µm; *d*, *e*, 5µm.

### CAA-related cerebral hemorrhage in APP23mice

The high incidence of cerebrovascular amyloid and the loss of smooth muscle cells led us to examine whether CAA in aged APP23 mice also causes hemorrhage similar to that described in humans [1,3,5,31]. Old cerebral hemorrhages were studied using Perls's iron staining, which identifies residual hemosiderin. Acute bleeding was assessed in H&E-stained sections. No evidence for both old and acute hemorrhages were found in 8-month-old mice. In contrast, 19-month-old APP23 mice revealed several focal hemosiderin deposits in neocortex and thalamus, most of which were localized to the cytoplasm of perivascular microglial cells. Strikingly, when we looked at 27-month-old mice, we found a dramatic increase in the frequency but also size of such hemosiderin clusters (Figs. 5, 6*a*). Hemosiderin-positive microglia were often in close contact to vessels that had formed aneurysm-like enlargements (Fig. 5*c*). In several aged mice, we also found evidence for acute bleeding (Fig. 5*f*). Mice with acute hematomas also revealed numerous hemosiderin deposits throughout the neocortex, suggesting multiple recurrent bleedings over time. Acute and old bleedings were sometimes colocalized, suggesting recurrent bleeding in the same region (Fig. 5*f*, *g*). No such bleedings were observed in nontransgenic control mice of any age.

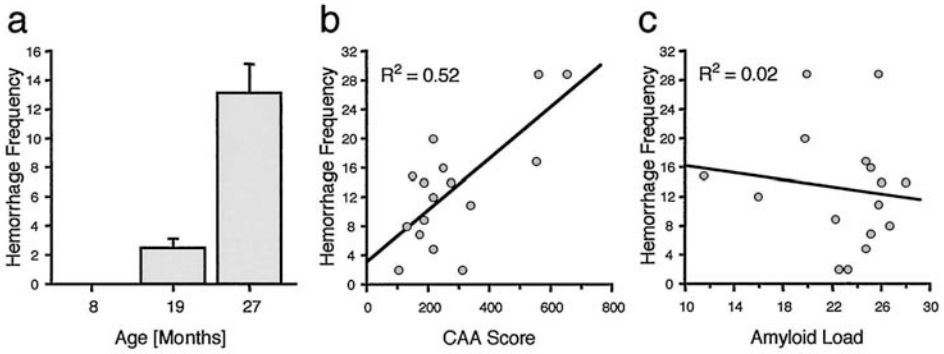


**Figure 6**. Age-related increase in hemorrhage in neocortex of APP23 mice. *a*, Frequency of perivascular hemosiderin-positive staining was assessed in systematically sampled sections through the neocortex. No evidence of old bleedings (hemosiderin) was found in the 8-month-old mice. From 19to 27months of age, there appears a striking increase in frequency of intracerebral hemorrhages (ANOVA; $F(2,38)= 26.1$; $p<0.001$). Because the sampling was done in the right hemisphere only and in every 10th section, total incidence of hemorrhages in the neocortex of 27-month-old mice can be estimated to be > 100. *b*, Significant positive relationship between CAA score (frequencyxseverity) and hemorrhage number in neocortex of the 27-month-old mice ($p<0.01$). Similar positive correlations were found between CAA frequency and hemorrhage and between CAA severity and hemorrhage (for both $R2=0.44$). *c*, In contrast, no relationship between neocortical amyloid plaque load and hemorrhages was found ($p>0.05$).

The anatomical distribution of the hemorrhages (primarily neocortex and thalamus, and to a lesser degree pia, hippocampus, and striatum) appeared very similar to the distribution of CAA. Correlative analysis between hemorrhage number and CAA score (frequencyxseverity) in neocortex of the 27-month-old group of mice revealed a significant positive correlation (Fig. 6*b*). A similar significant positive relationship was found in the thalamus (data not shown). These observations are in line with the morphological analysis, in which in most cases hemosiderin could clearly be assigned to amyloid-laden vessels (Fig. 5*d*, *e*). Interestingly, and consistent with the independence of amyloid plaque and CAA development, no significant relationship was observed between total amyloid load and hemorrhages (Fig. 6*c*).

It is difficult to establish whether an acute hemorrhagic stroke was the cause of spontaneous death in some of the aged APP23 mice. Most of the hematomas were small, reaching only a "subclinical" state. However, a large neocortical hematoma may have been the cause of the spontaneous death of at least one mouse.

**CAA-associatedvasculitis**

A granulomatous giant cell vasculitis has been reported in some cases of human CAA. This observation has been attributed to a coexistence of vasculitis and CAA or to an immunological

reaction and complication of CAA [32-34]. In 3of the 25aged APP23 mice, all of them with a high CAA score, we have found evidence of CAA-associated vasculitis. In particular, one mouse, examined after its spontaneous death, exhibited a severe lymphocytic vasculitis throughout subcortical, cortical, and leptomeningeal vessels (Fig. 7). In this case, lymphocytes were found in the vessel wall, indicative of endovasculitis. Affected vessels appeared thickened, partially necrotic, and sometimes obliterated (Fig. 7). There were no multinucleated giant cells or neutrophils. Because vasculitis was not observed in nontransgenic mice and only in transgenic mice with significant CAA, it does not appear to be the cause but an occasional consequence of CAA in our mouse model.

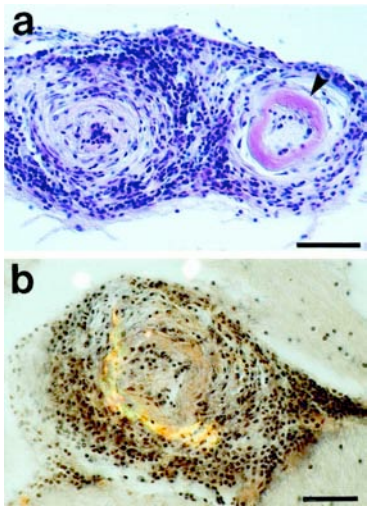


**Figure 7**. Vasculitis in aged APP23 mice with severe CAA. *a*, H&E staining of two vessels affected by a chronic lymphocytic vasculitis. Lymphocytic infiltrates are seen throughout the entire vessel walls. The vessel wall on the *left* appears thickened and the lumen is obliterated. There is severe amyloid deposition in the *right* vessel wall (*arrowhead)*. *b*, Double-staining for H&E and for Congo red (*green-yellow* birefringence) reveals amyloid deposits in a vessel heavily affected by a lymphocytic vasculitis. Scale bars, 50µm.

**BBBleakage**

Breakdown of the BBB with transition of blood protein into the vessel wall and brain parenchyma has been implicated as a key step in the pathogenesis leading to cerebral hemorrhage [35]. However, the present results using two different methods of BBB testing did not reveal any obvious leakage of the BBB unless an acute bleeding was present. We noticed that trypan blue labeled more vessels in the aged APP23 mice compared with age-matched controls and that the labeling was preferentially associated with amyloid-laden vessels. However, neither the dye nor HRP significantly infiltrated the neuropil, and the punctate staining for HRP in the

vessel wall was consistent with the reported normal incorporation of blood-derived HRP by endocytic vesicles of the vascular endothelia [25].

## Discussion

### Progression of CAA in APP23 mice is similar to CAA inhumans

CAA in APP23 mice shows striking similarities to human CAA [1,27,36]. It is mostly congophilic and consists mainly of Aβ40. Initial deposition occurs in the abluminal part of smooth muscle cell-containing vessels, and leptomeningeal vessels are the first to be affected. Later, many smaller vessels and capillaries become affected. CAA in mice and humans occurs in the neocortex and to a lesser degree in hippocampus, striatum, basal forebrain, brainstem, and white matter. There are, however, also differences in the anatomical distribution of CAA between mouse and human. For example, CAA in thalamus is much more prominent in mouse than human. Vice versa, there is almost no CAA in mouse cerebellum, whereas CAA occurs in human cerebellum. These differences might be explained by the anatomically restricted transgene expression [37] but also by species-differences in Aβ transport and drainage along perivascular spaces [14,38,39].

In both APP23 mouse and human, there is a striking age-related increase in frequency and severity of CAA [1,10]. Such an increase may reflect a stochastic seeding process in the vessel wall and subsequent Aβ accumulation [40]. In addition, an age-related decrease in perivascular drainage of Aβ by a thickening of the vessel basement membrane and/or by an impaired vessel motility in the aging brain may significantly contribute to the increase in CAA with aging [38,41].

Interestingly, in both mouse and human, development of CAA and amyloid plaques appear to be independent processes, both naturally depending on Aβ levels and on age as common risk factors [14,42]. Consistently, it has been demonstrated that overexpression of TGF-β1 increases CAA but decreases amyloid plaque formation in APP/TGF-β1 double-transgenic mice [14,42-44]. The different pathogeneses of vascular amyloid and parenchymal amyloid have important consequences for therapeutic intervention in CAA-associated hemorrhagic stroke (see below).

### CAA is the cause of hemorrhagic stroke in APP23mice

The strongest causal link between CAA and cerebral hemorrhage in humans comes from the observation that HCHWA-D patients with a point mutation at position 22of Aβ (position 693of APP) develop severe CAA and suffer fatal lobar hemorrhagic strokes early in their fifties [12,45].

Cerebral hemorrhage is also a frequent finding in sporadic CAA and AD. However in these patients, CAA appears to be a prerequisite but not sufficient for vessel rupture, with additional factors such as hypertension, vascular abnormalities, fibrinoid necrosis, infarcts, trauma, vasculitis, and apolipoprotein E (ApoE) genotype playing an important role [5,31,36,46]. Whether these factors contribute to vessel rupture independently of CAA or secondary to CAA is not clear.

In APP23 mice, CAA is the only factor to which the hemorrhage could be attributed. Hemorrhage was only found in aged transgenic mice with CAA and was not observed in aged control mice. Both hemorrhage and CAA increase very similarly and almost exponentially with aging. Hemorrhage was predominantly found in brain regions in which CAA is most severe, i.e., in the neocortex and thalamus. In areas with no CAA (such as the cerebellum), no hemorrhages were detected. There was a significant correlation between CAA and hemorrhage in the neocortex and thalamus, and in most cases, bleeding could be clearly allocated to individual amyloid-laden vessels. It may be argued that APP overexpression (albeit restricted to neurons in APP23 mice) or amyloid deposition in the brain parenchyma predispose vessels to rupture. However, the findings of severe CAA and hemorrhages in the thalamus, which lacks transgene expression [14], and lack of a correlation between amyloid plaques and hemorrhage argues against this possibility. In summary, these observations demonstrate that CAA is the driving force of vessel rupture and hemorrhage in the APP23 mouse.

**Pathogenesis of CAA-inducedhemorrhage**

The present results indicate that the loss of smooth muscle cells is an early and severe consequence of cerebrovascular amyloid deposition, as described in CAA in humans [29,30]. In human CAA, it has been suggested that increased Aβ production of smooth muscle cells leads to smooth muscle degeneration [29,30,47]. However, this cannot be the case in APP23 mice because transgenic Aβ in the mice is of neuronal origin and is not produced by smooth muscle cells [14]. Alternatively, it has been suggested that smooth muscle cells internalize neuron-derived Aβ and that release of Aβ may trigger smooth muscle cell degeneration [48]. Again, this is unlikely to be the mechanism in the mice, because we did not find any evidence for Aβ within smooth muscle cells. In contrast, our results suggest that extracellular Aβ is toxic to smooth muscle cells. This toxicity may either be mediated by soluble Aβ, which drains along perivascular spaces [14,38,47], or by Aβ fibril assembly at the surface of smooth muscle cells [49]. It is also conceivable that smooth muscle cells degenerate by purely mechanical constriction by the surrounding amyloid coat or by focal ischemia. Regardless of the exact mechanism, our results suggest that smooth muscle cell degeneration can be driven by extracellular amyloid of neuronal origin.

The disruption of the tight link between perivascular astrocytic end feet and the vessel wall appears somewhat later in the pathogenesis of CAA-induced hemorrhage and occurs to a significant degree only when the vascular amyloid infiltrates the neuropil. Such dyshoric amyloid also leads to perivascular microglial activation [14]. Disruption of the tight glial-vascular interface, together with the replacement of the media by amyloid, leads to a weakening of the vessel wall, which occasionally leads to aneurysmal dilatations in aged APP23 mice. In addition, the present results show that a severe endovasculitis with vessel obliteration develops in ~10% of the aged mice with CAA. Both the frequency and morphology of such CAA-associated endovasculitis appears to be very similar to sporadic human CAA [32-34] and also greatly contributes to vessel weakening and rupture.

In humans, it has been suggested that cerebrovascular amyloid leads to "cracks" in the vessel wall, with plasma enzymes leaking into and digesting the wall [35,36]. In APP23 mice, significant BBB leakage and fibrinoid necrosis were absent. Consistent with no gross BBB leakage, we did not find SAP to be a component of cerebrovascular amyloid in the APP23 mice. In contrast, SAP is a component of human CAA and has been implicated in the protection of the amyloid fibrils from degradation [50-52].

It has been suggested that fatal hemorrhage in sporadic CAA and HCHWA-D is associated with the presence of cystatin C as a component of the vessel amyloid [5,53-55]. The present results indicate that cystatin C is also a component of CAA in APP23 transgenic mice, but a clear relationship between cystatin C and hemorrhage was not obvious. In future studies, it will be instrumental to develop mouse model of CAA other than of the Aβ type, which will help to illuminate the mechanisms of CAA and CAA-induced hemorrhages [6]. For example, it is not clear why HCHWA-Iceland type patients, who develop CAA composed of mutated cystatin C, suffer fatal hemorrhages much earlier than HCHWA-D patients [56]. In contrast, patients with dementia of the British and Danish types, who develop severe CAA composed of ABri and ADan, respectively, do not develop significant hemorrhage [57,58]. Thus, the risk of hemorrhage may be predicted by the type of amyloid, the amount of amyloid, the participation of cofactors such as pathological chaperones, or the anatomical distribution of the amyloid within the vessel or certain brain regions.

**Diagnostic and therapeutic potential of mouse models ofCAA**

CAA does not naturally occur in rodents but has been reported in aged dogs and nonhuman primates [13]. CAA-related spontaneous hemorrhage has only consistently been reported in aged

dogs beyond 13years of age [59,60]. The present findings of robust CAA with multiple and recurrent hemorrhages in aged APP23 transgenic mice make this the first useful and genetically defined animal model to study diagnostic and therapeutic strategies of CAA-associated hemorrhage [3,4].

In terms of diagnostic potential, the APP23 mouse model should be well suited for the development of *in vivo* detection of cerebrovascular amyloid [61] and noninvasive markers for the progression of CAA-induced hemorrhages. There is a great need for diagnostic tools because, for example, it has been reported that recurrent bleedings are more severe than initial bleedings and more often fatal [62,63]. Recently, progress in noninvasive detection of hemosiderin has been reported using gradient-echo magnetic resonance imaging [63].

Potential treatments for CAA-related hemorrhage can be divided into strategies of inhibiting the deposition of amyloid in the vessel wall and in blocking subsequent pathogenesis leading to vessel wall rupture [3]. It has been reported recently that vaccination of PDAPP transgenic mice leads to a significant reduction of amyloid plaques presumably by phagocytotic microglia [64,65]. Unfortunately, PDAPP transgenic mice do not develop significant CAA, and the outcome of vaccination on CAA is uncertain. If vaccination indeed has the potential to "clear" even vascular amyloid, great caution has to be devoted to potential induction of bleeding attributable to removal of the amyloid coat, which presumably give the amyloid-laden vessel some stability. Regarding therapies aimed at reducing the risk of vessel rupture, the genetically defined APP23 mice offers a great potential to identify molecular factors involved in vessel rupture. For example, it has been suggested recently that the ApoE 2 genotype predisposes an amyloid-laden vessel to rupture [46].

Finally, mouse models of CAA and CAA-related hemorrhagic stroke will now allow to study the functional consequences of CAA and related hemorrhage in more detail. We have shown previously that CAA in adult APP23 mice (in the absence of bleeding) leads to perivascular neurodegeneration, including neuron loss, dystrophic terminals, and microglial activation [14,66]. In the present study, we have demonstrated multiple and recurrent bleeding in APP23 mice as they age, which in turn induces additional neurodegeneration. These observations suggest that a significant portion of the cognitive impairment in APP23 mice [67,68] may be caused by a chronic toxic effect of CAA on the parenchyma and by CAA-induced multiple hemorrhages. It is also striking that several forms of dementia have been described recently, all of which exhibit severe amyloid angiopathy but lack significant neuritic plaque pathology [57,58,69]. All of these observations point to the need to reevaluate the role of CAA in AD dementia.

## Materials and Methods

*Animals.* Generation of B6,D2-TgN(Thy1-APP Swe)23 transgenic mice (APP23 mice) has been described previously [15]. APP23 mice overexpress $APP_{751}$ with the Swedish double-mutation under the control of a neuron-specific Thy-1 promoter element [14,15]. The mice have been backcrossed with C57BL/6J mice. A total of 101heterozygous male and female APP23 mice and nontransgenic control mice ranging from 8to 28months of age from generation F6-F12 have been used in this study. Nontransgenic control mice were either littermate control mice or control mice from another litter of the same generation of backcrossing.

*Histology and immunohistochemistry.* Mice were overdosed with pentobarbital. Brains were removed, immersion fixed for 2d in 4% paraformaldehyde, and embedded in paraffin [16]. Coronal serial sections of 25µm thickness were cut with a microtome throughout the brain. For three-dimensional (3D) confocal reconstruction (see below), some brains were post-fixed, cryoprotected, frozen, and sectioned at 100µm with a freezing-sliding microtome [17].

Cresyl violet, hematoxylin and eosin (H&E), and Congo red staining were done according to standard protocols [18]. The Berlin Blue method of Perls's was used to visualize ferric iron in hemosiderin [18,19]. Immunohistochemistry on paraffin and fixed-frozen sections was done according to previously published protocols [16,17] by using the avidin-biotin-peroxidase complex method (Vector Laboratories, Burlingame, CA) with diaminobenzidine as chromogen. The following antibodies were used: polyclonal antibodies to Aβ (NT-11/12) [15], polyclonal antibody AS42/14 specifically to Aβ 42 [15]; polyclonal antibody FCA3340 and FCA3542 specifically to Aβ40 and to Aβ42, respectively [20] [generous gift from F.Checlair]; mouse monoclonal antibody to α-smooth muscle actin (clone 1A4; Sigma, St. Louis, MO), mouse monoclonal antibody to β-dystroglycan (Novocastra, Newcastle upon Tyne, UK) [21]; polyclonal antibody to glial fibrillary acidic protein (GFAP) (Dako, Glostrup, Denmark); polyclonal antibodies to cystatin C (Accurate Chemicals, Westbury, NY and Dako); and polyclonal antibody to mouse serum amyloid P component (SAP) (Calbiochem, La Jolla, CA).

*Confocal microscopy.* Double-labeling for Aβ and smooth muscle cells was achieved by incubating paraffin sections simultaneously with polyclonal antibody to Aβ (NT12) and mouse monoclonal antibody to -smooth muscle actin. The secondary antibodies were Alexa 568goat anti-rabbit IgG and Alexa 488goat anti-mouse IgG (1:500; Molecular Probes, Eugene, OR). Sections were mounted with Vectashield (Vector Laboratories) and analyzed with a Confocal Laser Scanning Microscope LSM 510,inverted Axiovert 100M (Zeiss, Oberkochen, Germany). For 3D reconstruction of amyloid-laden vessels, thick, fixed frozen sections were incubated with

NT12 antibody, followed by Alexa 488goat anti-rabbit IgG. The 3D reconstruction was done by using the Full3D function of the Imaris 3.0software (Bitplane AG, Zürich, Switzerland).

*Quantitative analysis of CAA and total amyloid burden.* Groups of young (8.0months; *n*=10), adult (19.2±0.2months; *n*= 15), and aged (27.1±0.2months; *n*=16) APP23 mice were used, with males and females balanced in all groups. Age-matched nontransgenic young (8.0months; *n*=10), adult (19.8±0.4months; *n*=8), and aged (26.9±0.4months; *n*=10) mice were used. Frequency and severity of CAA were quantified on systematically sampled serial Aβ-immunostained sections (NT12 antibody) throughout the region of interest (every 20th section through the neocortex; every 10 th section through the hippocampus; every 10th section through the thalamus; yielding 7-10 sections per region). A rating scale was used that was similar to that described previously [14,22]. "CAA frequency" was calculated by counting the total number of Aβ-positive vessels in the entire set of systematically sampled sections. To calculate "CAA severity," A-positive vessels were divided in one of three severity grades: 1,A β immunoreactivity confined to the vessel wall; 2,granular Aβ immunoreactivity in and around vessel wall with focal infiltration of the amyloid into the neuropil; and 3,extensive infiltration of amyloid into the neuropil with a complete amyloid coat around the vessel (see Fig. 1*c-e)*. The mean for all vessels was taken as CAA severity. Finally, "CAA score" was calculated by multiplying CAA frequency with CAA severity. All of the quantification was done on the right hemisphere only. This grading system was used by two independent raters and yielded similar results. Total amyloid burden (percentage) was quantified on the same set of systematically sampled Aβ-immunostained sections using a point grid as described previously [23].

*Quantitation of cerebral hemorrhage.* Cerebral hemorrhage is accompanied by a delayed appearance of hemosiderin-positive microglia [24]. Perls's Berlin blue-stained clusters of hemosiderin staining were quantified on sets of systematically sampled sections (every 10th section throughout the neocortex, hippocampus, and thalamus). All numbers are again for the right hemisphere only. An additional set of every 10th section was stained for H&E and screened for acute intraparenchymal bleedings (presence of large accumulation of erythrocytes in brain parenchyma). In addition to the groups of 8-,19-,and 27-month-old APP23 and control mice, we also assessed hemorrhage number in aged APP23 mice and age-matched controls that were collected after their spontaneous death (APP23, *n*=9; mean age, 24.6±0.7months; controls, *n*=4; 24.0±1.5months). Brains of these mice were immersion-fixed in 4% paraformaldehyde for several weeks, paraffin-embedded, and serially cut.

*Assessment of the blood-brain barrier.* Three 24-month-old female APP23 mice and three littermate controls were used. Mice received an intravenous injection of horseradish peroxidase

(HRP) (type IV-A; Sigma) in the tail vein (0.4mg/gm body weight). Thirty minutes later, mice were overdosed with pentobarbital and perfused with PBS, followed by 2% paraformaldehyde plus 2% glutaraldehyde. Brains were post-fixed, cryoprotected, frozen, and cut with a freezing-sliding microtome. Blood-brain barrier (BBB) leakage was studied by incubating sections in PBS with 0.05% DAB and 0.03% hydrogen peroxide [25]. One transgenic and one aged control mouse were perfused with 10ml of 0.4% trypan blue (Fluka, Buchs, Switzerland) in PBS, followed by 2% paraformaldehyde plus 2% glutaraldehyde [26]. Brains were post-fixed, cut with a vibratome, and examined for BBB leakage of the dye.

*Statistical analysis.* All statistical analysis was done with STATVIEW 5.01.Significance levels were set at $p<0.05$.Indicated is the mean± SEM.

## Footnotes

This work was supported by Swiss National Science Foundation Grants 3100-44526.95and 3130-56753.99,the Fritz Thyssen Foundation (Cologne, Germany), and the Swiss Academy of Medical Sciences. D.T.W. was supported by MD/PhD Grant 3135-54877.98from the Swiss National Science Foundation. We thank A.Probst (Basel, Switzerland), L.Walker (Ann Arbor, MI), and R.Kalaria (Newcastle, UK) for discussions and comments on this manuscript. We also thank D. Abramowski, C.Stürchler-Pierrat, C.Mistl, W.Kränger (Basel, Switzerland), and M.Pepys (London, UK) for experimental help and advice. The antibody donation of F.Checlair (Valbonne, France) is greatly acknowledged.

D.T.W., L.B., and M.C.H. contributed equally to this work

## References

1. Vinters, H. V. Cerebral amyloid angiopathy. A critical review. *Stroke* **18**, 311-24 (1987).

2. Massaro, A. R. et al. Clinical discriminators of lobar and deep hemorrhages: the Stroke Data Bank. *Neurology* **41**, 1881-5 (1991).

3. Greenberg, S. M. Cerebral amyloid angiopathy: prospects for clinical diagnosis and treatment. *Neurology* **51**, 690-4 (1998).

4. Sacco, R. L. Lobar intracerebral hemorrhage. *N Engl J Med* **342**, 276-9 (2000).

5. Itoh, Y., Yamada, M., Hayakawa, M., Otomo, E. & Miyatake, T. Cerebral amyloid angiopathy: a significant cause of cerebellar as well as lobar cerebral hemorrhage in the elderly. *J Neurol Sci* **116**, 135-41. (1993).

6. Burgermeister, P., Calhoun, M. E., Winkler, D. T. & Jucker, M. Mechanisms of cerebrovascular amyloid deposition. Lessons from mouse models. *Ann N Y Acad Sci* **903**, 307-16 (2000).

7. Yamada, M. Cerebral amyloid angiopathy: an overview. *Neuropathology* **20**, 8-22 (2000).

8. Price, D. L., Tanzi, R. E., Borchelt, D. R. & Sisodia, S. S. Alzheimer's disease: genetic studies and transgenic models. *Annu Rev Genet* **32**, 461-93 (1998).

9. Selkoe, D. J. Translating cell biology into therapeutic advances in Alzheimer's disease. *Nature* **399**, A23-31 (1999).

10. Yamada, M., Tsukagoshi, H., Otomo, E. & Hayakawa, M. Cerebral amyloid angiopathy in the aged. *J Neurol* **234**, 371-6 (1987).

11. Levy, E. et al. Mutation of the Alzheimer's disease amyloid gene in hereditary cerebral hemorrhage, Dutch type. *Science* **248**, 1124-6 (1990).

12. Wattendorff, A. R., Frangione, B., Luyendijk, W. & Bots, G. T. Hereditary cerebral haemorrhage with amyloidosis, Dutch type (HCHWA-D): clinicopathological studies. *J Neurol Neurosurg Psychiatry* **58**, 699-705 (1995).

13. Walker, L. C. Animal models of cerebral β-amyloid angiopathy. *Brain Res Brain Res Rev* **25**, 70-84 (1997).

14. Calhoun, M. E. et al. Neuronal overexpression of mutant amyloid precursor protein results in prominent deposition of cerebrovascular amyloid. *Proc Natl Acad Sci U S A* **96**, 14088-93 (1999).

15. Sturchler-Pierrat, C. et al. Two amyloid precursor protein transgenic mouse models with Alzheimer disease-like pathology. *Proc Natl Acad Sci U S A* **94**, 13287-92 (1997).

16. Calhoun, M. E. et al. Hippocampal neuron and synaptophysin-positive bouton number in aging C57BL/6 mice. *Neurobiol Aging* **19**, 599-606 (1998).

17. Jucker, M. et al. Age-related deposition of glia-associated fibrillar material in brains of C57BL/6 mice. *Neuroscience* **60**, 875-89 (1994).

18. Carson, F. L. Histotechnology, 2nd edition, ASCP Press, Chicago, USA. (1996).

19. Gomori, G. Microtechnical demonstration of iron. *Am J Pathol* **12**, 655-663 (1936).

20. Barelli, H. et al. Characterization of new polyclonal antibodies specific for 40 and 42 amino acid-long amyloid β peptides: their use to examine the cell biology of presenilins and the immunohistochemistry of sporadic Alzheimer's disease and cerebral amyloid angiopathy cases. *Mol Med* **3**, 695-707 (1997).

21. Tian, M. et al. Dystroglycan in the cerebellum is a laminin alpha 2-chain binding protein at the glial-vascular interface and is expressed in Purkinje cells. *Eur J Neurosci* **8**, 2739-47 (1996).

22. Olichney, J. M. et al. The apolipoprotein E epsilon 4 allele is associated with increased neuritic plaques and cerebral amyloid angiopathy in Alzheimer's disease and Lewy body variant. *Neurology* **47**, 190-6 (1996).

23. Calhoun, M. E. et al. Neuron loss in APP transgenic mice. *Nature* **395**, 755-6 (1998).

24. Koeppen, A. H., Dickson, A. C. & McEvoy, J. A. The cellular reactions to experimental intracerebral hemorrhage. *J Neurol Sci* **134 Suppl**, 102-112 (1995).

25. Banks, W. A. & Broadwell, R. D. Blood to brain and brain to blood passage of native horseradish peroxidase, wheat germ agglutinin, and albumin: pharmacokinetic and morphological assessments. *J Neurochem* **62**, 2404-19 (1994).

26. Reynolds, D. S. & Morton, A. J. Changes in blood-brain barrier permeability following neurotoxic lesions of rat brain can be visualised with trypan blue. *J Neurosci Methods* **79**, 115-21 (1998).

27. Alonzo, N. C., Hyman, B. T., Rebeck, G. W. & Greenberg, S. M. Progression of cerebral amyloid angiopathy: accumulation of amyloid-β40 in affected vessels. *J Neuropathol Exp Neurol* **57**, 353-9 (1998).

28. Yamaguchi, H., Yamazaki, T., Lemere, C. A., Frosch, M. P. & Selkoe, D. J. β amyloid is focally deposited within the outer basement membrane in the amyloid angiopathy of Alzheimer's disease. An immunoelectron microscopic study. *Am J Pathol* **141**, 249-59 (1992).

29. Kawai, M. et al. Degeneration of vascular muscle cells in cerebral amyloid angiopathy of Alzheimer disease. *Brain Res* **623**, 142-6 (1993).

30. Wisniewski, H. M. & Wegiel, J. β-amyloid formation by myocytes of leptomeningeal vessels. *Acta Neuropathol (Berl)* **87**, 233-41 (1994).

31. Vonsattel, J. P. et al. Cerebral amyloid angiopathy without and with cerebral hemorrhages: a comparative histological study. *Ann Neurol* **30**, 637-49 (1991).

32. Probst, A. & Ulrich, J. Amyloid angiopathy combined with granulomatous angiitis of the central nervous system: report on two patients. *Clin Neuropathol* **4**, 250-9 (1985).

33. Mandybur, T. I. & Balko, G. Cerebral amyloid angiopathy with granulomatous angiitis ameliorated by steroid-cytoxan treatment. *Clin Neuropharmacol* **15**, 241-7 (1992).

34. Yamada, M. et al. Immune reactions associated with cerebral amyloid angiopathy. *Stroke* **27**, 1155-62 (1996).

35. Maeda, A. et al. Computer-assisted three-dimensional image analysis of cerebral amyloid angiopathy. *Stroke* **24**, 1857-64 (1993).

36. Mandybur, T. I. Cerebral amyloid angiopathy: the vascular pathology and complications. *J Neuropathol Exp Neurol* **45**, 79-90 (1986).

37. Andra, K. et al. Expression of APP in transgenic mice: a comparison of neuron-specific promoters. *Neurobiol Aging* **17**, 183-90 (1996).

38. Weller, R. O. et al. Cerebral amyloid angiopathy: amyloid β accumulates in putative interstitial fluid drainage pathways in Alzheimer's disease. *Am J Pathol* **153**, 725-33 (1998).

39. Weller, R. O. Pathology of cerebrospinal fluid and interstitial fluid of the CNS: significance for Alzheimer disease, prion disorders and multiple sclerosis. *J Neuropathol Exp Neurol* **57**, 885-94 (1998).

40. Lansbury, P. T., Jr. Structural neurology: are seeds at the root of neuronal degeneration? *Neuron* **19**, 1151-4 (1997).

41. Kalaria, R. N. Cerebral vessels in ageing and Alzheimer's disease. *Pharmacol Ther* **72**, 193-214 (1996).

42. Greenberg, S. M., Rebeck, G. W., Vonsattel, J. P., Gomez-Isla, T. & Hyman, B. T. Apolipoprotein E epsilon 4 and cerebral hemorrhage associated with amyloid angiopathy. *Ann Neurol* **38**, 254-9 (1995).

43. Wyss-Coray, T. et al. Amyloidogenic role of cytokine TGF-β1 in transgenic mice and in Alzheimer's disease. *Nature* **389**, 603-6 (1997).

44. Wyss-Coray, T. et al. Transforming growth factor TGF-β1 modifies Alzheimer's-type pathology in transgenic mice and humans. *Neurobiol Aging* **21**, S125 (2000).

45. Vinters, H. V. et al. Secondary microvascular degeneration in amyloid angiopathy of patients with hereditary cerebral hemorrhage with amyloidosis, Dutch type (HCHWA-D). *Acta Neuropathol (Berl)* **95**, 235-44 (1998).

46. O'Donnell, H. C. et al. Apolipoprotein E genotype and the risk of recurrent lobar intracerebral hemorrhage. *N Engl J Med* **342**, 240-5 (2000).

47. Davis-Salinas, J., Saporito-Irwin, S. M., Cotman, C. W. & Van Nostrand, W. E. Amyloid β-protein induces its own production in cultured degenerating cerebrovascular smooth muscle cells. *J Neurochem* **65**, 931-4 (1995).

48. Urmoneit, B. et al. Cerebrovascular smooth muscle cells internalize Alzheimer amyloid β protein via a lipoprotein pathway: implications for cerebral amyloid angiopathy. *Lab Invest* **77**, 157-66 (1997).

49. Van Nostrand, W. E., Melchor, J. P. & Ruffini, L. Pathologic amyloid β-protein cell surface fibril assembly on cultured human cerebrovascular smooth muscle cells. *J Neurochem* **70**, 216-23 (1998).

50. Coria, F. et al. Isolation and characterization of amyloid P component from Alzheimer's disease and other types of cerebral amyloidosis. *Lab Invest* **58**, 454-8 (1988).

51. Tennent, G. A., Lovat, L. B. & Pepys, M. B. Serum amyloid P component prevents proteolysis of the amyloid fibrils of Alzheimer disease and systemic amyloidosis. *Proc Natl Acad Sci U S A* **92**, 4299-303 (1995).

52. Verbeek, M. M., Otte-Holler, I., Veerhuis, R., Ruiter, D. J. & De Waal, R. M. Distribution of A β-associated proteins in cerebrovascular amyloid of Alzheimer's disease. *Acta Neuropathol (Berl)* **96**, 628-36 (1998).

53. Maruyama, K., Ikeda, S., Ishihara, T., Allsop, D. & Yanagisawa, N. Immunohistochemical characterization of cerebrovascular amyloid in 46 autopsied cases using antibodies to β protein and cystatin C. *Stroke* **21**, 397-403 (1990).

54. Vinters, H. V., Secor, D. L., Pardridge, W. M. & Gray, F. Immunohistochemical study of cerebral amyloid angiopathy. III. Widespread Alzheimer A4 peptide in cerebral microvessel walls colocalizes with gamma trace in patients with leukoencephalopathy. *Ann Neurol* **28**, 34-42 (1990).

55. Maat-Schieman, M. L., van Duinen, S. G., Rozemuller, A. J., Haan, J. & Roos, R. A. Association of vascular amyloid β and cells of the mononuclear phagocyte system in hereditary cerebral hemorrhage with amyloidosis (Dutch) and Alzheimer disease. *J Neuropathol Exp Neurol* **56**, 273-84 (1997).

56. Olafsson, I., Thorsteinsson, L. & Jensson, O. The molecular pathology of hereditary cystatin C amyloid angiopathy causing brain hemorrhage. *Brain Pathol* **6**, 121-6 (1996).

57. Vidal, R. et al. A stop-codon mutation in the BRI gene associated with familial British dementia. *Nature* **399**, 776-81 (1999).

58. Vidal, R. et al. A decamer duplication in the 3' region of the BRI gene originates an amyloid peptide that is associated with dementia in a Danish kindred. *Proc Natl Acad Sci U S A* **97**, 4920-5 (2000).

59. Dahme, E. & Schroder, B. Kongophile Angiopathie, cerebrovaskuläre Mikroaneurysmen und cerebrale Blutungen beim alten Hund. *Zentralbl Veterinarmed A* **26**, 601-13 (1979).

60. Uchida, K., Miyauchi, Y., Nakayama, H. & Goto, N. Amyloid angiopathy with cerebral hemorrhage and senile plaque in aged dogs. *Nippon Juigaku Zasshi* **52**, 605-11 (1990).

61. Skovronsky, D. M. et al. In vivo detection of amyloid plaques in a mouse model of Alzheimer's disease. *Proc Natl Acad Sci U S A* **97**, 7609-14 (2000).

62. Passero, S., Burgalassi, L., D'Andrea, P. & Battistini, N. Recurrence of bleeding in patients with primary intracerebral hemorrhage. *Stroke* **26**, 1189-92 (1995).

63. Greenberg, S. M., O'Donnell, H. C., Schaefer, P. W. & Kraft, E. MRI detection of new hemorrhages: potential marker of progression in cerebral amyloid angiopathy. *Neurology* **53**, 1135-8 (1999).

64. Schenk, D. et al. Immunization with amyloid-β attenuates Alzheimer-disease-like pathology in the PDAPP mouse. *Nature* **400**, 173-7 (1999).

65. Bard, F. et al. Peripherally administered antibodies against amyloid β-peptide enter the central nervous system and reduce pathology in a mouse model of Alzheimer disease. *Nat Med* **6**, 916-9 (2000).

66. Phinney, A. L. et al. Cerebral amyloid induces aberrant axonal sprouting and ectopic terminal formation in amyloid precursor protein transgenic mice. *J Neurosci* **19**, 8552-9 (1999).

67. Kelly, P. H. et al. Progressive impairment in amyloid precursor protein transgenic mouse line APP23. *Soc Neurosci Abstr* **25**, 1291 (1999).

68. Sommer, B. et al. Transgenic approaches to model Alzheimer's disease. *Rev Neurosci* **11**, 47-51 (2000).

69. Vidal, R. et al. Senile dementia associated with amyloid β protein angiopathy and tau perivascular pathology but not neuritic plaques in patients homozygous for the APOE-epsilon4 allele. *Acta Neuropathol (Berl)* **100**, 1-12 (2000).

# 7. Neuron-derived Aβ is Targeted to the Vasculature in a Mouse Model of Hereditary Cerebral Hemorrhage With Amyloidosis-Dutch Type

In Press: *Nature Neuroscience*

**Martin C. Herzig[1,2], David T. Winkler[2], Patrick Burgermeister[2], Michelle Pfeifer[1,2], Esther Kohler[1,2], Stephen D. Schmidt[3], Simone Danner[4], Dorothee Abramowski[4], Christine Stürchler-Pierrat[4], Kurt Bürki[5], Sjoerd G. van Duinen[6], Marion L. C. Maat-Schieman[6], Matthias Staufenbiel[4], Paul M. Mathews[3], Mathias Jucker[1,2]**

[1]Department of Cellular Neurology, Hertie-Institute for Clinical Brain Research, University of Tübingen, D-72076 Tübingen, Germany; [2]Department of Neuropathology, Institute of Pathology, University of Basel, CH-4003 Basel, Switzerland; [3]Nathan Kline Institute, New York University School of Medicine, Orangeburg, NY 10962, USA; [4]Novartis Institutes for Biomedical Research, Nervous Systems Research, CH-4002 Basel, Switzerland; [5]Institute of Laboratory Animal Science, University of Zürich, CH-8057 Zürich, Switzerland; [6]Departments of Pathology and Neurology, Leiden University Medical Center, 2300 RC Leiden, The Netherlands

## Abstract

The E693Q mutation within the amyloid precursor protein (APP) leads to cerebral amyloid angiopathy (CAA) with recurrent cerebral hemorrhagic strokes and dementia in affected patients. In contrast to Alzheimer's disease (AD) patients, these Hereditary Cerebral Hemorrhage with Amyloidosis-Dutch type (HCHWA-D) patients exhibit few parenchymal amyloid plaques and show minimal neurofibrillary pathology. Here we report that neuron-restricted overexpression of human E693Q APP in transgenic mice (APPDutch mice) leads to severe CAA, smooth muscle cell degeneration, cerebral hemorrhages, and neuroinflammation. In contrast, neuronal overexpression of wild-type human APP (APPwt mice) results in predominantly parenchymal amyloidosis. In HCHWA-D and APPDutch mice the Aβ40:42 ratio is significantly

higher than in AD and APPwt mice, and significant wild-type human or murine Aβ40, respectively, is co-deposited with the AβDutch. Genetically shifting the ratio of AβDutch40:42 towards AβDutch42 by crossing APPDutch mice with mutated presenilin 1 transgenic mice redistributes the amyloid pathology from the vasculature to the parenchyma. The understanding that different Aβ species can drive amyloid pathology in different cerebral compartments has implications for current anti-amyloid therapeutic strategies. This HCHWA-D mouse model is the first to develop robust CAA in the absence of parenchymal amyloid, highlights the key role of neuronally produced Aβ to vascular amyloid pathology, and emphasizes the differing roles of Aβ40 and Aβ42 in vascular and parenchymal amyloid pathology.

## Introduction

Mutations in the amyloid precursor protein (APP) at the β- and γ-secretase sites have been shown to cause familial forms of early onset Alzheimer's disease (AD). These mutations increase the production of either total amyloid-β peptides (Aβ) or of the more amyloidogenic Aβ1-42 species. In contrast, most mutations within the Aβ domain do not result in a full range of AD pathology but characteristically result in cerebrovascular pathology [1-3]. For example, the E693Q point mutation in APP (residue 22 of Aβ) results in Hereditary Cerebral Hemorrhage with Amyloidosis-Dutch type (HCHWA-D), an autosomal dominant form of cerebral amyloid angiopathy (CAA) [4,5]. HCHWA-D patients suffer from recurrent lobar cerebral hemorrhages with an onset in the fifth decade of life [6]. At autopsy patients show extensive CAA in leptomeningeal arteries and cortical arterioles and to a lesser extent in meningocortical veins. In contrast to AD, parenchymal amyloid plaques are not prominent in HCHWA-D pathology, although diffuse parenchymal Aβ is found [7]. Because of these features of the disease, HCHWA-D has become the human genetic archetype of the Aβ congophilic angiopathy seen sporadically in many of the elderly and in the majority of AD patients [8,9].

Previous *in vitro* findings have shown that Aβ harboring the Dutch E693Q mutation (AβDutch) has been associated with enhanced aggregation properties, reduced clearance from brain, and greater toxicity towards smooth muscle cells compared to Aβ wild-type (Aβwt) [10-14]; however, the reasons for the predominant cerebral vascular amyloid deposition in HCHWA-D patients is unclear. In the present study we have generated human APP E693Q transgenic mice (APPDutch mice) to study the mechanisms underlying vascular amyloidosis and the consequences of CAA using an *in vivo* model system.

## Results

### Cerebrovascular amyloid in HCHWA-D consists of both AβDutch and Aβwt with a predominance of Aβ1-40

Cerebrovascular amyloid in HCHWA-D brain was found predominantly in leptomeningeal and cortical vessel wall, often with limited labeling of diffuse parenchymal Aβ deposits (Fig. 1*a*). Immunohistochemical staining with carboxy-terminal specific antibodies to Aβ suggest that Aβ40 predominates over Aβ42 in the cerebrovascular amyloid (Fig. 1*b,c*). To confirm this and to determine whether AβDutch is the predominant Aβ species deposited in the vessel wall, we used Bicine/Tris/urea SDS-PAGE [15] to separate various Aβ species. Analysis revealed that both HCHWA-D cortical tissue and isolated leptomeningeal vessels contained abundant AβDutch1-40 as well as significant amounts of Aβwt1-40 (Fig. 1*d*). In contrast, in sporadic AD patients both Aβ1-40 and Aβ1-42 were clearly present (Fig. 1*d*). These observations were confirmed by ELISA which showed only half as much Aβ40 compared to Aβ42 in AD while in HCHWA-D brain tissue Aβ40 exceeded Aβ42 levels by more than 18-fold (Table 1).

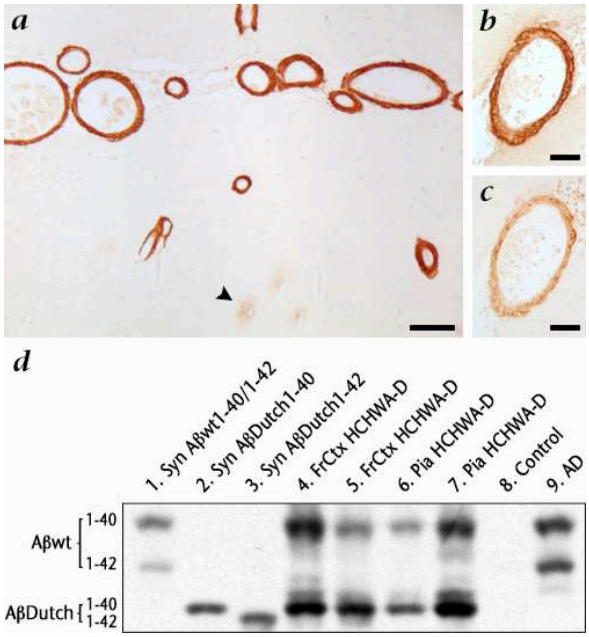


**Fig 1.** *Vascular amyloid in HCHWA-D brain consists of both AβDutch and Aβwt with Aβ1-40 being the predominant peptide*. ***a,*** Frontal cortex of HCHWA-D brain (50 year-old patient) immunostained with antibody NT12 to Aβ. Massive amyloid deposition within leptomeningeal and cortical vessel walls is observed. Only few and diffuse parenchymal Aβ deposits are observed (arrowhead) although pretreatment may increase parenchymal staining in the patients [50]. ***b, c,*** Immunolabeling of vascular amyloid with antibodies specific to Aβx-40 (R208 in *b*) and Aβx-42 (R306 in *c*) reveals that the majority of vascular amyloid ends at amino acid 40. ***d,*** Western blotting of brain homogenates. Synthetic Aβ (lane 1-3). Homogenates of frontal cortex (lane 4, 5) and pia (lane 6, 7) of

HCHWA-D patients contain both Aβwt1-40 and AβDutch1-40, but no detectable Aβwt1-42 and AβDutch1-42. This observation suggests that cerebrovascular amyloid in HCHWA-D patients consists of both Aβwt and AβDutch and is predominantly of the Aβ1-40 isoform. Control patients show no detectable Aβ (lane 8) while both Aβwt1-40 and 1-42 are found in a sporadic AD patient (lane 9). Bars are 100µm (*a*) and 50µm (*b*, *c*).

**Neuron-specific overexpression of human E693Q APP leads to CAA**

To understand the pathogenesis of HCHWA-D and the mechanisms leading to cerebrovascular amyloid, we generated transgenic (tg) mice overexpressing E693Q mutated human APP (hAPP) under the control of the neuron-specific Thy-1 promoter element (APPDutch mice). High levels of hAPP mRNA were detected in neocortex, hippocampus, and brain stem by *in situ* hybridization (Fig. 2*a*). Consistently, immunohistochemistry revealed robust hAPP expression in the same brain regions exclusively within neurons and neuronal processes. No expression of hAPP mRNA or protein was detected in vessel walls (Fig. 2*b*). Two tg lines were selected with high hAPP expression levels that remained constant with aging (Fig. 2*c*). By direct Western blot analysis, AβDutch could not be detected in young APPDutch mice. AβDutch1-40, however, was readily detectable in a 23 month-old mouse, consistent with amyloid deposition at this age (Fig. 2*c*). Morphological analysis of APPDutch mice between 22 to 30 months of age (*n*=30) showed an onset of vascular amyloid deposition at approximately 22-25 months for both lines. Amyloid deposition in the brain was largely confined to the cerebral vasculature (Fig. 2*d*), appearing first in leptomeningeal vessels followed by cortical vessel. Female mice appeared to have an earlier onset than males. Congo red (Fig. 2*g*) and Thioflavin S staining (not shown) demonstrated that much of the cerebrovascular amyloid was in a compact β-pleated sheet conformation. Similar to HCHWA-D brain and consistent with the Western blot analysis, immunoreactivity for Aβ40 was much more intense than for Aβ42 (Fig. 2*e,f*). Some amyloid-laden vessels showed a "vessel-within-vessel" configuration (Fig. 2*h*). At the electron microscopic level, an irregular thickening of the basement membrane with amorphous material was observed in some vessels while others contained amyloid fibrils within the basement membrane, predominantly on the adventitial side, while the endothelial cell layer appeared to be intact. At a more advanced stage amyloid fibrils were observed in a radial pattern in between the smooth muscle cells with some fibrils invading the parenchyma (Fig. 2*i*). In spite of a significant vascular amyloid burden, APPDutch mice did not develop compact parenchymal amyloid plaques and only rarely diffuse parenchymal Aβ deposits were observed.

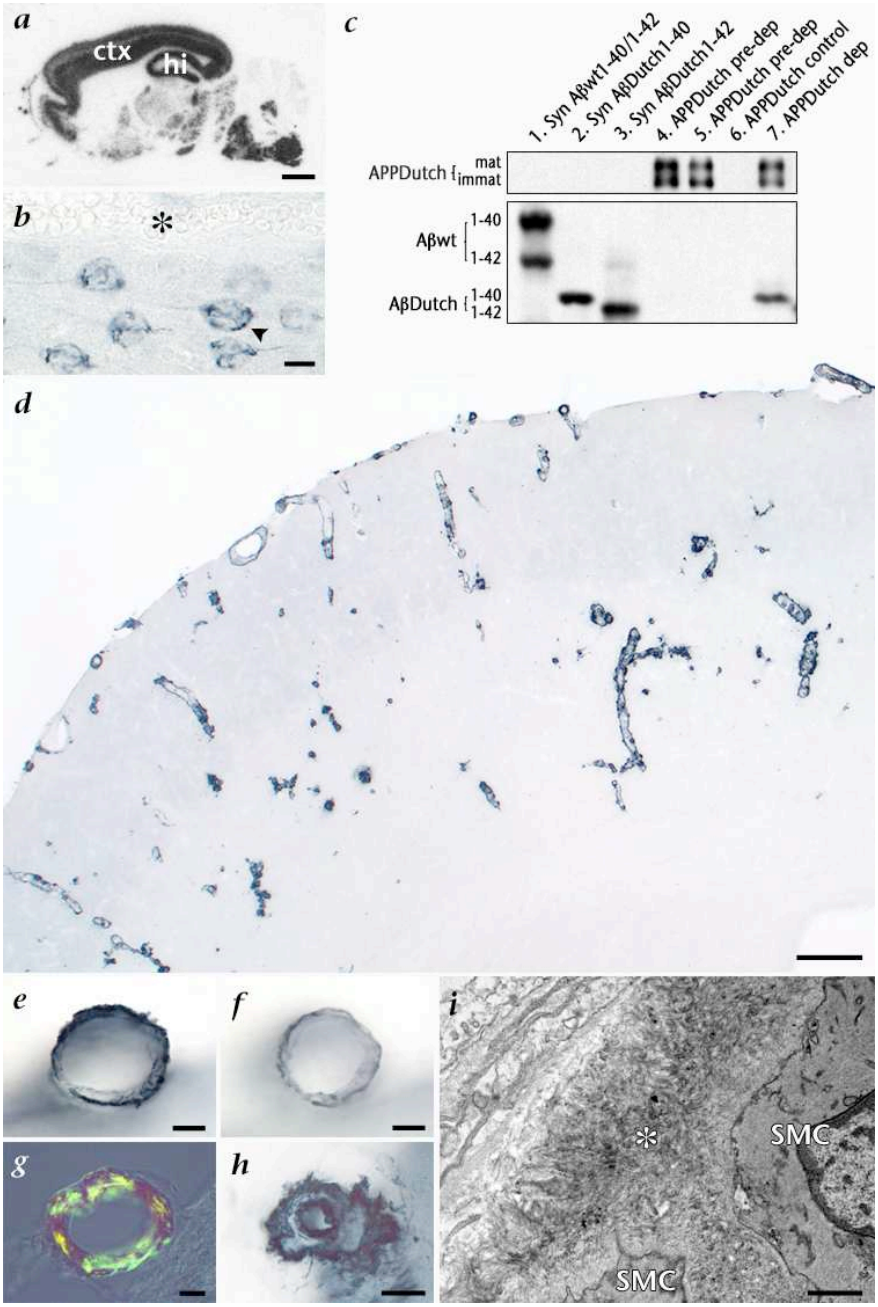


**Fig 2.** *APPDutch mice develop cerebral amyloid angiopathy.* ***a****, In situ* hybridization reveals high transgene-derived mRNA levels in neocortex (ctx) and hippocampus (hi) and brain stem. ***b****,* Immunostaining for human (h) APP in neocortex shows punctate labeling of neuronal perikarya (arrowhead) and weaker labeling of axonal processes. Consistent with the neuron-specific promoter, there was no hAPP expression in the vessel wall (the lumen of the vessel is indicated by an asterisk). ***c****,* Western blot analysis of hAPP and hAβ in mouse brain using an antibody specific to human APP/Aβ. Upper panel: APPDutch expression in APPDutch mouse line 23 (lane 4) and 33 (lane 5, 7) and a non-transgenic control littermate (lane 6). Bands demonstrate immature and mature forms of hAPP. Lower panel: Synthetic human Aβwt1-40 mixed with human Aβwt1-42, AβDutch1-40, and AβDutch1-42 peptides were used as markers (lanes 1-3). Aβ levels did not reach detection levels in pre-depositing APPDutch mice without immunoprecipitation (shown are 13 month-old mice). In contrast, in a 23 month-old amyloid depositing APPDutch mouse AβDutch1-40, but not AβDutch1-42, was readily detected (lane 7). ***d****,* Immunohistochemical analysis of a 29 month-old APPDutch mouse shows Aβ deposition largely confined to

leptomeningeal and neocortical vessels (NT12 antibody). No compact parenchymal deposits are seen. ***e, f,*** Immunolabeling of vascular amyloid with antibodies specific to Aβ40 (R208 in *e*) and Aβ42 (R306 in *f*) reveals that the majority of vascular amyloid ends at amino acid 40. ***g,*** Congo red staining of an amyloid-laden vessels demonstrates that the vast majority of the amyloid is of compact nature and congophilic. ***h,*** High magnification of amyloid-containing cortical vessel that shows a vessel-within-vessel configuration. ***i,*** Electron micrograph demonstrating abundant amyloid fibrils (asterisk) between the smooth muscle cells (SMC) in a 30 month-old APPDutch mouse. Bars are 1mm (*a*), 10µm (*b, e, f, g, h*), 200µm (*d*), 1µm (*i*).

### CAA induces hemorrhages and neuroinflammation

Amyloid-laden vessels in APPDutch mice show a severe loss of smooth muscle cells (Fig. 3*a,b*). Consistent with the loss of smooth muscle cells and a concomitant weakening of the vessel wall, fresh hemorrhages (Fig. 3*c,d*), as well as indications of previous hemorrhages (Fig. 3*e,f*) were found in three of the oldest APPDutch mice. No bleedings were found in age-matched, non-transgenic mice (not shown).

In APPDutch mice with CAA, a strong, perivascular microglial inflammatory reaction was observed (Fig. 3*g*). This microgliosis was confined to the immediate vicinity of amyloid-laden vessels and was absent adjacent to non-affected vessels (Fig. 3*h*). In addition, an activation of astrocytes was observed throughout all neocortical areas affected by CAA (Fig. 3*i*) but was absent in brain areas devoid of vascular amyloid and in non-tg control mice (Fig. 3*k*). The widespread astrocytosis in areas affected with CAA may be the result of partial ischemia and a perfusion-deficit associated with amyloid-laden vessels.

**Table 1. Aβ40:42 ratios in brains of pre-depositing and depositing transgenic mice, HCHWA-D and AD patients.** Levels of human and murine Aβ40 and Aβ42 were determined by ELISA in Aβ-depositing 18 month-old APPwt and 28 month-old APPDutch mice (*n*=5-11). Human Aβ was measured in pre-depositing 7 month-old APPwt and APPDutch mice (*n*=6-9), in pre-depositing 3 month-old and Aβ-depositing 9 month-old APPDutch/PS45 mice, in AD and HCHWA-D patients (*n*=3-9). Indicated is the mean of the individual Aβ40:42 ratios ± SEM. ** P < 0.01; *** P < 0.001. Absolute Aβ values are reported in Table 1S (supplementary material).

| | human Aβ40:42 | | murine Aβ40:42 |
|---|---|---|---|
| | pre-depositing | depositing | depositing |
| APPwt | 4.3±0.3 ] ** | 2.8±0.4 ] *** | 1.1±0.1 ] ** |
| APPDutch | 7.8±0.9 | 12.1±1.4 | 3.0±0.5 |
| APPDutch/PS45 | 0.4±0.9 | 0.4±0.02 | |
| HCHWA-D | | 18.6±7.0 | |
| AD | | 0.5±0.19 | |

**Table 1.** Aβ40:42 ratios in brains of pre-depositing and depositing transgenic mice, HCHWA-D and AD patients.

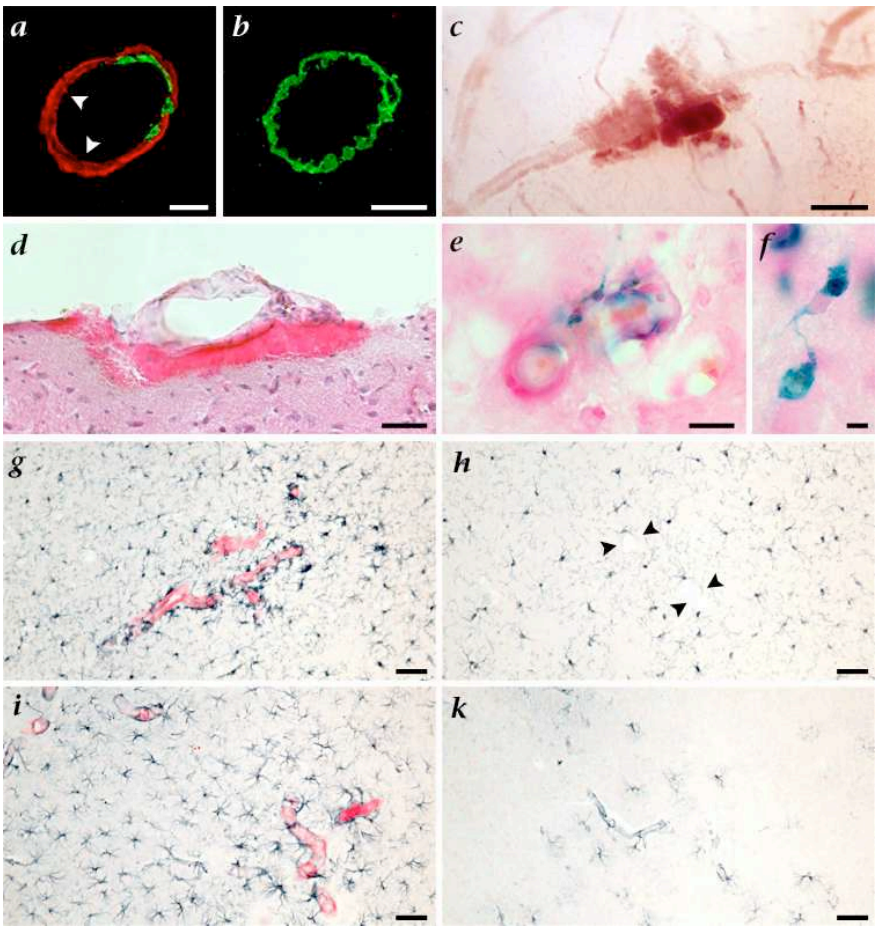


**Fig 3.** *Hemorrhages and neuroinflammation in APPDutch mice.* ***a,*** Double labeling for smooth muscle cell actin (green) and Aβ (red) in a leptomeningeal vessel of a 29 month-old APPDutch mouse reveals displacement of smooth muscle cells by vascular amyloid (arrowheads). ***b,*** Vessels that are not affected by Aβ show a continuous rim of smooth muscle cells. ***c,*** A fresh hemorrhage is shown that occurred at the surface of the brain of an 29 month-old APPDutch mouse. ***d,*** H&E staining on a cross-section through the bleeding shown in *c*. ***e,*** Microhemorrhage associated with amyloid-laden vessels visualized by Perls' Prussian blue staining for ferric iron. ***f,*** High magnification of such microbleeds reveal hemosiderin-positive microglia. ***g,*** Activated perivascular microglia (blue) in the immediate vicinity of amyloid-laden vessels (Congo red) in the neocortex of a 29 month-old APPDutch mouse. ***h,*** Such microgliosis was absent in the same mouse around non-affected vessels (arrowheads). ***i,*** Reactive astrocytes (blue) in neocortical areas with CAA (Congo red). ***k,*** In neocortical regions with no vascular amyloid no reactive astrocytes were observed. Bars are 20μm (*a, b, e*), 100μm (*c, g, h, I, k*), 50μm (*d*), 5μm (*f*).

### Increased Aβ40:42 ratio in APPDutch compared to APPwt mice

To examine the determinants that lead to vascular vs. parenchymal amyloid deposition, we compared the pattern of amyloid deposition in APPDutch mice with that of tg mice overexpressing wild-type hAPP, at levels similar to the APPDutch mice, under the same Thy-1 promoter element, and in the same C57BL/6J genetic background (APPwt mice). Aged APPwt mice developed parenchymal plaques with limited vascular deposits (Fig. 4*a*). Western blot

analysis of APPwt mice with amyloid deposits revealed both Aβwt1-40 and Aβwt1-42 while in APPDutch mice AβDutch1-40 was seen but AβDutch1-42 was below detection level (Fig. 4*b*). This was confirmed by ELISA, which revealed a more than 4-fold higher human Aβ40:42 ratio in APPDutch mice than in APPwt mice (Table 1; for absolute values see Table 1S, supplementary material). We also analyzed steady-state levels of Aβ40 and Aβ42 in APPDutch and APPwt mice at 7 mo of age, prior to detectable amyloid deposition, to determine whether this difference in the Aβ40:42 ratio is an early event or only seen after the accumulation of significant amyloid. An almost 2-fold greater ratio of Aβ40:42 was seen in young APPDutch when compared to APPwt mice of a similar age (Table 1, 1S).

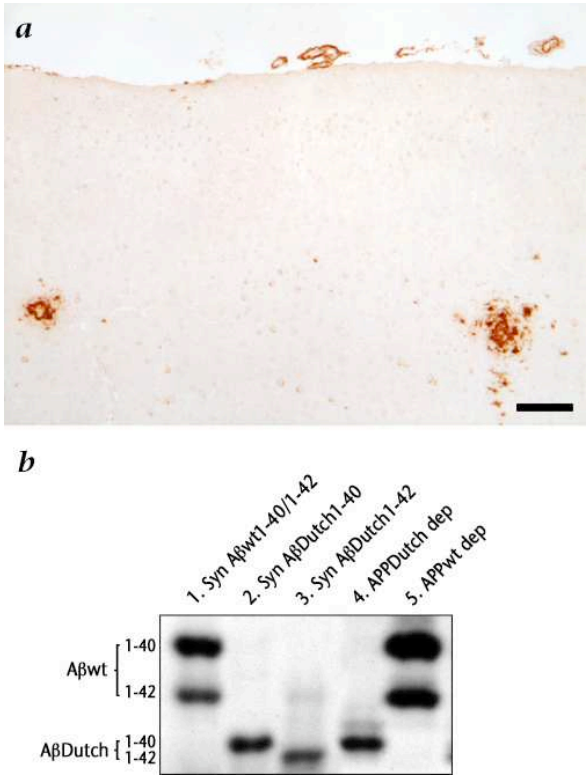


**Fig 4.** *Parenchymal and vascular amyloid deposition in APPwt mice*. ***a,*** Aβ-immunostaining of an 18 month-old APPwt mouse reveals parenchymal amyloid deposits with only scattered CAA. ***b,*** Western blot analysis of human Aβ in APPwt brain in comparison to APPDutch brain. Lanes 1-3, synthetic human Aβ. In amyloid-depositing APPwt (18 months) mice a substantial Aβwt1-40 and somewhat less Aβwt1-42 band was observed (lane 5) while in amyloid-depositing APPDutch mice (23 months) only AβDutch1-40 was detected (lane 4). Scale bar is 100μm.

**Increased AβDutch1-42 levels in APPDutch/PS45 double tg mice provoke early and massive parenchymal amyloid**

Examining our hypothesis that a high ratio of AβDutch1-40 over AβDutch1-42 is linked to and potentially necessary for the predominant vascular amyloid deposition in APPDutch mice, we crossed APPDutch mice with mice that overexpress human presenilin-1 bearing the G384A mutation (PS45 mice), which is known to increase Aβ1-42 production [16,17]. Strikingly, starting at 12 weeks of age APPDutch/PS45 double tg mice developed parenchymal amyloid in the neocortex and hippocampus. At 10 months of age massive parenchymal diffuse and compact amyloid was found in virtually all brain regions. Unlike the APPDutch single tg mice, vascular amyloid, although present, was a much less prominent feature in the APPDutch/PS45 double tg mice (Fig. 5*a*).

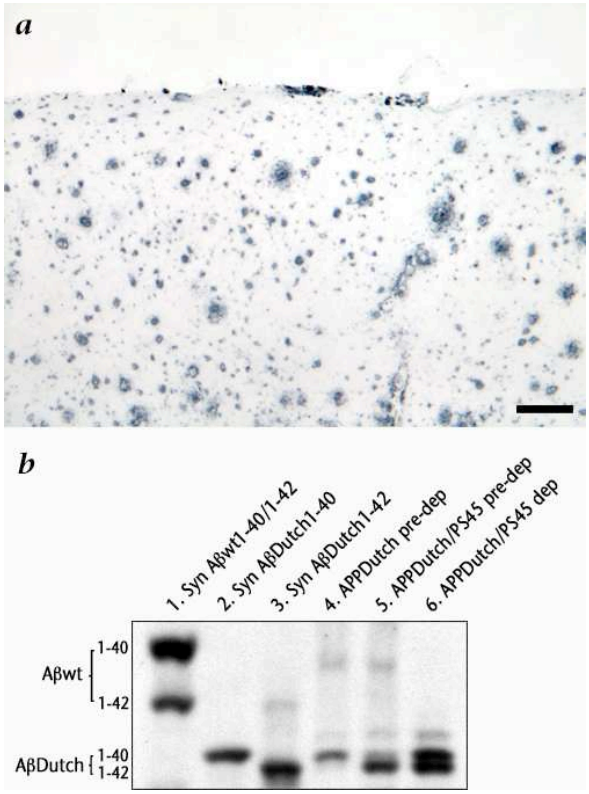


**Fig 5.** *Predominant parenchymal amyloid deposition in APPDutch/PS45 double tg mice*. ***a,*** Aβ-immunostaining of a 10 month-old APPDutch/PS45 mouse shows extensive, predominantly diffuse, but also some congophilic, parenchymal amyloid deposits with only scattered CAA. ***b,*** Western blot analysis of human Aβ in mouse brain immunoprecipitates. Lanes 1-3, synthetic human Aβ. Pre-depositing (4 month-old) APPDutch mouse reveals only AβDutch1-40 (lane 4). In contrast, both AβDutch1-40 and 1-42 are detectable in a pre-depositing 2,5 month-old (lane 5) and depositing 10 month-old (lane 6) APPDutch/PS45 double tg mice. In order to show AβDutch1-40 and 1-42 as distinct bands, the sample shown in lane 6 was highly diluted. Scale bar is 100μm.

Western blot analysis of APPDutch/PS45 brain homogenates revealed abundant AβDutch1-42 in addition to AβDutch1-40 (Fig. 5*b*). ELISA measurements confirmed this observation, with AβDutch42 at least twice as abundant as AβDutch40 in pre-depositing and depositing double tg mice (Table 1, 1S). These results demonstrate that AβDutch is capable of forming parenchymal amyloid deposits and that such deposits can be induced in APPDutch mice by increasing the production of AβDutch42 via the expression of mutant presenilin.

**Endogenous murine Aβ is co-deposited with human Aβ**

To determine whether endogenous murine Aβ, the counterpart of Aβwt derived from the wild-type allele in HCHWA-D patients, is co-deposited with transgene-derived human Aβ in APPDutch mice, we performed ELISAs specific for murine Aβ40 and Aβ42. The amount of murine Aβ was 4.4±0.1% of the human Aβ detected in APPwt mice and 8.0±1.0% in APPDutch mice. Interestingly, depositing APPDutch mice showed a roughly 3-fold increase in the ratio of murine Aβ40:42 when compared to APPwt mice (Table 1, 1S).

## Discussion

In spite of the identification of the HCHWA-D causing APP mutation more than a decade ago [4], progress toward understanding the pathogenesis of HCHWA-D has been hampered by the lack of an animal model. Here we describe a transgenic mouse model that develops extensive cerebrovascular amyloid deposits in leptomeningeal and cortical vessels, similar to that found in affected patients [5,7]. Parenchymal amyloid is nearly absent, and the few parenchymal plaques found are diffuse [7]. The observation that neuronal expression of APPDutch is sufficient for cerebrovascular amyloidosis, smooth muscle cell degeneration and hemorrhage in a mouse model strongly suggests that neurons are the source of the cerebrovascular amyloid in HCHWA-D. Moreover, these results demonstrate that smooth muscle cell degeneration does not require intracellular Aβ production but can be initiated by extracellular, neuron-derived Aβ that is transported to and accumulates at the vasculature.

Expanding upon previous research [18,19], we find that amyloid deposits in HCHWA-D brains contain not only AβDutch40 but also abundant Aβwt40, with only little Aβ42. Like the human disease, in the APPDutch mouse the vast majority of the deposited Aβ is Aβ40 with AβDutch40 12-fold more abundant than AβDutch42. This is in contrast to sporadic AD and APPwt mice or other transgenic mice expressing Swedish APP, where significantly more Aβ42 relative to Aβ40 is deposited [20-23]. In both HCHWA-D and APPDutch mice Aβwt, derived from the wild-type allele in

HCHWA-D and from the endogenous murine APP in the APPDutch mice, follows the deposition pattern of the mutated AβDutch species.

The two other mouse models we have examined in this study further highlight the important role of the Aβ40:42 ratio in determining vascular vs. parenchymal amyloid deposition. The APPwt mouse overexpresses APP at levels comparable to the APPDutch mouse but develops abundant parenchymal plaques and only sparse vascular amyloidosis suggesting that the single E693Q amino acid substitution is sufficient to target neuron-derived Aβ to the vessel wall. Strikingly, the Aβ40:42 ratio in APPwt mice was significantly lower compared to APPDutch mice. Thus, a straightforward explanation for why the Dutch mutation leads to CAA would be that it favors the production of Aβ40, which in turn is vasculotropic. To examine this hypothesis we determined the Aβ40:42 ratio in young transgenic mice before the onset of amyloid deposition, where a two-fold higher ratio of Aβ40:42 was seen in APPDutch mice when compared to APPwt mice. In conditioned media of E693Q transfected cells a similar, albeit somewhat smaller increase in the Aβ40:42 ratio has been reported [11,24] suggesting that the Dutch mutation affects Aβ40:42 ratios at the level of Aβ production or clearance. Recent results show that AβDutch40 is more resistant to proteolysis by both neprilysin and insulin-degrading enzyme [25,26] and is less efficiently cleared into the blood [13] than Aβwt40, however, similar studies with AβDutch42 have not been reported.

Familial AD-causing PS1 mutations shift the generation of Aβ to favor Aβ42, which results in early and robust parenchymal amyloid deposition in human wild-type Aβ producing tg mice [16,27,28]. Crossing the APPDutch mouse with the PS45 line resulted in, at a young age, abundant parenchymal plaque formation with limited CAA pathology. Thus, although AβDutch preferentially accumulates around cerebral vessels, genetically shifting the ratio of AβDutch40:42 to favor AβDutch42 is sufficient to alter the distribution of the resulting amyloid pathology from the vasculature to the parenchyma. Moreover, this demonstrates that AβDutch can form dense and congophilic plaques within the parenchyma and that parenchymal amyloid formation in the APPDutch mouse and HCHWA-D patients is therefore likely to be limited by the absence of Aβ42-driven parenchymal amyloid seeding. The present data do not exclude a role for Aβ42 as seed for vascular amyloid.

We have previously shown that cerebral amyloidosis is not a local process and that Aβ can be transported extracellularly and accumulate distant to its site of production [29], as must also occur in the APPDutch mouse. This observation, together with the finding of similar intraneuronal Aβ accumulation in APPDutch and APPwt tg mice (Fig. 1S, supplementary material), argues that different Aβ species interact differently with the extracellular environment, making Aβ´s movement through the different local environments in the CNS an important determinant of amyloid pathology. For instance, when Aβ42 concentration is insufficient to form and maintain parenchymal amyloid seeds, soluble Aβ is transported from neurons to the vasculature where it

is cleared into the blood or drained along perivascular spaces [30,31]. Coupled with the observation that AβDutch40 is less efficiently cleared than Aβwt40 [13], this may in part explain why AβDutch40 accumulates at the vessel wall in the APPDutch mouse but can then accumulates within the parenchyma when this mouse is crossed with the PS45 mouse.

The knowledge that both Aβ40 and Aβ42 species have the potential to drive amyloid pathology, albeit within different compartments, will undoubtedly have further implications as anti-Aβ therapies are developed. For example, anti-Aβ immunotherapy has been shown to preferentially clear Aβ42 from mice with pre-existing amyloid pathology [32,33]. While selective clearance of Aβ42 would beneficially reduce parenchymal amyloid burden, this might potentiate vascular amyloid pathology as has been alluded to in Aβ-immunotherapy studies done in mice and may have been the case for the two Aβ42-immunized patient who have gone to autopsy [32,34-36]. Given this complexity, further studies of anti-Aβ therapies will need to follow alterations in the Aβ40 to Aβ42 ratio while addressing the resulting balance of vascular and parenchymal amyloid pathology.

Most HCHWA-D patients die early due to recurrent strokes [6]. A few patients with relatively restricted stroke pathology, however, reach a considerable age. Nevertheless, these individuals show a continuous cognitive decline similar to that seen in AD patients [37]. This supports recent studies suggesting that CAA is not only a significant cause of intracerebral hemorrhage in the elderly, but also an important contributing factor to cognitive impairment and AD dementia [38]. CAA has been suggested to interfere with the anatomical integrity of the vessel wall, the physiological response to vasodilation, and can occlude affected vessels and thus induce perivascular ischemia [8,39,40]. However, these studies have been limited by their reliance on end-stage human autopsy cases and transgenic models that have severe parenchymal amyloidosis in addition to CAA [41,42]. Our APPDutch model, which recapitulates well human HCHWA-D, is likely to be an invaluable tool with which to further study the pathogenic mechanism by which CAA affects cognition and neurodegeneration and in the development of therapeutic strategies.

## Methods

**Patients.** HCHWA-D tissue of frontal cortex and pial vessels were obtained at autopsy from five patients (50 to 76 years old; post-mortem delay from 5 to <48 hrs). For comparison cortical tissue from nine autopsy confirmed AD cases (61-93 years, post-mortem delay 4-26 hrs) and two control patients (78 and 87 years, post mortem delay 4-11 hrs) were used.

**Generation of transgenic mice.** To generate Dutch-mutant APP transgenic mice, human APP751 cDNA with the E693Q mutation was inserted into the blunt-ended *Xho*I site of the

vector pTSC$\alpha$1 containing the murine Thy-1.2 minigene [43]. After removal of vector sequences by NotI/PvuI digestion, linear Thy-1-APP constructs were injected into C57BL/6J oocytes. Five positive transgenic founder mice (C57BL/6-TgN(Thy1-$APP_{E693Q}$)) were identified and expression of human APP was assessed by Western blot and immunohistochemistry. The two lines (#23, #33) with the highest transgene expression were used in this study (APPDutch mice). Expression levels in these lines are about 5-fold over endogenous APP levels (data not shown). The generation of the wild-type human APP751 transgenic mice (C57BL/6-TgN(Thy1-APP)51) has been described previously [44]. Line #16 (the APPwt mouse), which has a similar or slightly higher APP expression level than the APPDutch mice, was used in this study. APPDutch/PS45 double tg mice were obtained by crossing APPDutch mice with mice overexpressing human G384A mutated presenilin-1 under the control of the murine Thy-1 promoter (B6,D2-TgN(Thy1-presenilin-$1_{G384A}$)45). These PS45 mice were backcrossed to C57BL/6J for more than 7 generations prior to use. All mice analyzed were hemizygous for the transgene(s) of interest.

**Histology and immunohistochemistry.** Tissue was immersion fixed in 4% paraformaldehyde. Histology and immunohistochemistry was performed on either 4µm thick paraffin-embedded or 25µm free-floating frozen sections. A$\beta$ was immunostained with rabbit polyclonal antibody NT12 (NT11) [43], using standard immunoperoxidase procedures with Elite ABC kits (Vector Laboratories, Burlingame, CA), and 3,3'-diaminobenzidine (Sigma, St. Louis, MO) or Vector SG (Vector Laboratories) as substrates. For specific staining of A$\beta$x-40 or A$\beta$x-42, rabbit antisera R208 (R163) or R306 (R165), respectively, were used [45] (gift of P. Mehta, New York, NY). All A$\beta$ antibodies recognized both A$\beta$wt and A$\beta$Dutch. Human APP (hAPP) was visualized with polyclonal antibody A4CT (specific to the C-terminal 100 amino acids of APP) (courtesy of K. Beyreuther, Heidelberg, Germany). Microglia and astroglia were stained with rabbit polyclonal antibody to Iba1 [46] (courtesy of Y. Imai, Tokyo, Japan) and with rabbit polyclonal antibody to glial fibrillary acidic protein (GFAP) (Dako, Glostrup, Denmark), respectively. Double immunofluorescence labeling of A$\beta$ and smooth muscle cells was performed for confocal microscopy. NT12 and mouse monoclonal antibody to $\alpha$-smooth muscle actin (A-2547, Sigma) followed by goat anti rabbit Alexa 568 and goat anti mouse Alexa 488 (Molecular Probes, Eugene, OR) were used. Shown are superpositions of optical sections. Congo red, Thioflavin S, and Perls' Prussian blue reaction for ferric iron were performed according to standard protocols [40].

**Electron microscopy.** Mice were perfused with ice-cold PBS for 5 min. Neocortical tissue pieces were removed and immersion fixed in 4% paraformaldehyde/0.5% glutaraldehyde at 4°C. The tissue was then postfixed in 1% osmium tetroxide in 0.1 M cacodylate buffer, dehydrated, and processed for Spurr embedding. Ultrathin sections were cut from selected areas, stained with

uranyl acetate and lead citrate and examined and photographed with a Jeol JEM1011 electron microscope.

**In situ hybridization.** In situ hybridization for human APP was performed as previously described [43,47]. In brief, a $^{33}$P-labeled oligonucleotide probe, 5'-AGCCTCTTCCTCTACCTCATC-ACCATCCTCATCGTCCTCG-3', complementary to the coding sequence of hAPP between nucleotides 859 and 898 was used at a final concentration of 2pmol/ml.

**Western blot analysis.** APP expression levels in transgenic mice were analyzed using standard 8% SDS-polyacrylamide minigels followed by blotting and antibody binding as described below. For analysis of Aβ, Western blots were performed according to previously described protocols [15]. Briefly, samples of homogenized brain hemispheres were subjected to SDS-PAGE using 10%T/5%C Bicine/Tris minigels containing 8M urea in the separation gel. To detect Aβ in brains of pre-depositing mice, immunoprecipitation with antibody 6E10 was performed. Proteins were transferred to a PVDF Immobilon-P membrane (Millipore, Bedford, MA) by semi-dry blotting, incubated with antibody 6E10 (Signet, Dedham, MA) and visualized by chemiluminescence (ECL, Amersham). Antibody 6E10 recognizes residue 1-17 of Aβ, and the Dutch mutation at position 22 does not interfere with its binding. Synthetic Aβwt1-40 and Aβw1-42 peptides were purchased from Bachem (Bubendorf, Switzerland). Synthetic AβDutch1-40 and AβDutch1-42 were gifts of J. Ghiso (New York, NY) and W. E. Van Nostrand (Stony Brook, NY).

**ELISA.** Cerebral Aβ levels of patients and Aβ depositing mice were assayed by sandwich ELISA from formic-acid-extracted, sucrose homogenates prepared from cortical tissue or mouse hemi-brains lacking the cerebellum as previously described [48]. Aβ was captured with Aβ carboxy-terminal monoclonal antibodies that recognize exclusively either Aβx-40 (JRF/cAβ40/10) or Aβx-42 (JRF/cAβ42/26) and detected with horseradish peroxidase-conjugated JRF/Aβtot/17, which was raised against the amino-terminal 16 residues of human Aβ [48]. Aβ levels in mice prior to amyloid deposition were determined by preparing a sucrose homogenate from each hemibrain (without cerebellum) and then extracting this in diethylamine (DEA), as previously described [49]. Endogenous murine Aβ was similarly detected using DEA extraction and a murine-specific monoclonal antibody for detection (JRF/rAβ1-15/2) [49]. ELISA results are reported as the mean ± SEM in fmol Aβ per g wet brain, based on standard curves using synthetic Aβ1-40 and Aβ1-42 peptide standards (American Peptide Co. Sunnyvale, CA). The values were compared by non-parametric Mann-Whitney U analysis. All capture and detection antibodies were a gift from M. Mercken, Johnson and Johnson Pharmaceutical Research and Development/Janssen Pharmaceutica.

## Acknowledgments

We would like to thank H. Widmer (Bern, Switzerland) for experimental help, and L. Walker (Atlanta, GA, USA), J. Ghiso (New York, NY, USA), and T. Saido (Saitama, Japan) for comments on this manuscript. Synthetic Aβ and antibodies to APP and Aβ have been generously provided by M. Mercken (Beerse, Belgium), P. Paganetti (Basel, Switzerland), K. Beyreuther (Heidelberg, Germany), C. Labeur (Ghent, Belgium), Y. Imai (Tokyo, Japan), W. Van Nostrand (Stony Brook, NY, USA), P. Mehta (New York, NY, USA) and J. Ghiso (New York, NY, USA). We appreciate R. Nixon´s (Orangeburg, NY) support of the ELISA measurements. This work was supported by grants to MJ from the Fritz Thyssen Foundation (Cologne, Germany), *the* EU under the sixth framework programme, priority: life sciences and health, Contract No. LSHM-CT-2003-503330, the Swiss National Science Foundation, and to PM from NIA and NINDS.

## Supplemental Material

### Supplemental Figure 1S.

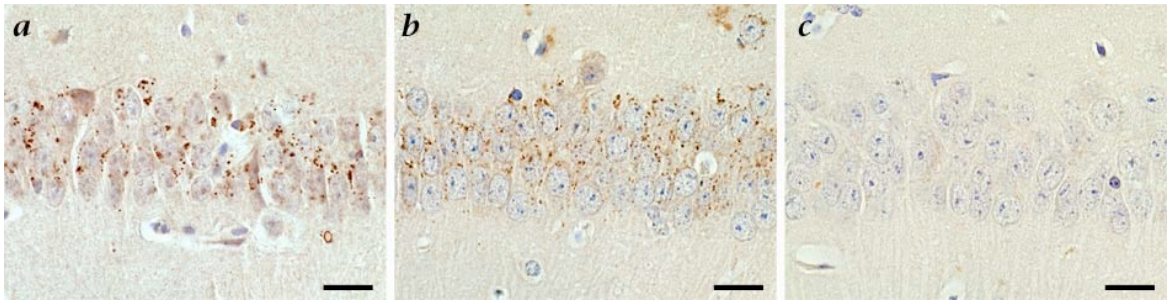


**Fig 1S.** *Intraneuronal Aβ in APPDutch and APPwt transgenic mice.* NT12-immunostaining for Aβ (brown) in hippocampal CA1 neurons reveals intracellular human Aβ in a 29 month-old APPDutch (***a***) and a 24 month-old APPwt mouse (***b***), while no Aβ is detected in a 24 month-old non-transgenic control littermate (***c***). Bars are 20 µm (*a*, *b*, *c*).

**Supplemental Table 1S.**

**Table 1S. Absolute Aβ levels in brains of pre-depositing and depositing transgenic mice, HCHWA-D and AD patients.** Levels of human (h) and murine (m) Aβ40 and Aβ42 were determined by ELISA in Aβ-depositing 18 month-old APPwt and 28 month-old APPDutch mice (*n*=5-11). Human Aβ was measured in pre-depositing 7 month-old APPwt and APPDutch mice (*n*=6-9), in pre-depositing 3 month-old and Aβ-depositing 9 month-old APPDutch/PS45 mice, in AD and HCHWA-D patients (*n*=3-9). Indicated is the mean of individual Aβ values ± SEM. Levels are reported as pmol Aβ/g wet brain.

| | pre-depositing | | depositing | | depositing | |
|---|---|---|---|---|---|---|
| | hAβ40 | hAβ42 | hAβ40 | hAβ42 | mAβ40 | mAβ42 |
| APPwt | 4.49±0.28 | 1.05±0.03 | 234±72.2 | 138±46.9 | 16.3±2.94 | 15.7±3.34 |
| APPDutch | 2.76±0.41 | 0.36±0.04 | 4'520±1326 | 461±131 | 288±60.1 | 113±26.6 |
| APPDutch/PS45 | 2.47±0.80 | 6.64±2.89 | 5'003±949 | 11'392±2740 | | |
| HCHWA-D | | | 14'437±7598 | 1'184±673 | | |
| AD | | | 1'219±467 | 3'147±401 | | |

Note that the Aβ40:42 ratios in Table 1 are the mean +/- SEM calculated from the individual Aβ40:42 ratios determined for each animal, not from the mean Aβ40 and Aβ42 measurements for each genotype given here.

## References


1. Haass, C. & Steiner, H. Protofibrils, the unifying toxic molecule of neurodegenerative disorders? *Nat Neurosci* **4**, 859-60 (2001).

2. Hardy, J. Amyloid, the presenilins and Alzheimer's disease. *Trends Neurosci* **20**, 154-9 (1997).

3. Selkoe, D.J. Translating cell biology into therapeutic advances in Alzheimer's disease. *Nature* **399**, A23-31 (1999).

4. Levy, E. et al. Mutation of the Alzheimer's disease amyloid gene in hereditary cerebral hemorrhage, Dutch type. *Science* **248**, 1124-6 (1990).

5. Wattendorff, A.R., Bots, G.T., Went, L.N. & Endtz, L.J. Familial cerebral amyloid angiopathy presenting as recurrent cerebral haemorrhage. *J Neurol Sci* **55**, 121-35 (1982).

6. Bornebroek, M., Haan, J., Maat-Schieman, M.L., Van Duinen, S.G. & Roos, R.A. Hereditary cerebral hemorrhage with amyloidosis-Dutch type (HCHWA-D): I--A review of clinical, radiologic and genetic aspects. *Brain Pathol* **6**, 111-4 (1996).

7. Maat-Schieman, M.L., van Duinen, S.G., Bornebroek, M., Haan, J. & Roos, R.A. Hereditary cerebral hemorrhage with amyloidosis-Dutch type (HCHWA-D): II--A review of histopathological aspects. *Brain Pathol* **6**, 115-20 (1996).

8. Vinters, H.V. Cerebral amyloid angiopathy. A critical review. *Stroke* **18**, 311-24 (1987).

9. Greenberg, S.M. Cerebral amyloid angiopathy: prospects for clinical diagnosis and treatment. *Neurology* **51**, 690-4 (1998).

10. Fraser, P.E. et al. Fibril formation by primate, rodent, and Dutch-hemorrhagic analogues of Alzheimer amyloid β-protein. *Biochemistry* **31**, 10716-23 (1992).

11. De Jonghe, C. et al. Flemish and Dutch mutations in amyloid β precursor protein have different effects on amyloid β secretion. *Neurobiol Dis* **5**, 281-6 (1998).

12. Watson, D.J., Selkoe, D.J. & Teplow, D.B. Effects of the amyloid precursor protein Glu693-->Gln 'Dutch' mutation on the production and stability of amyloid β-protein. *Biochem J* **340 ( Pt 3)**, 703-9 (1999).

13. Monro, O.R. et al. Substitution at codon 22 reduces clearance of Alzheimer's amyloid-β peptide from the cerebrospinal fluid and prevents its transport from the central nervous system into blood. *Neurobiol Aging* **23**, 405-12 (2002).

14. Van Nostrand, W.E., Melchor, J.P. & Ruffini, L. Pathologic amyloid β-protein cell surface fibril assembly on cultured human cerebrovascular smooth muscle cells. *J Neurochem* **70**, 216-23 (1998).

15. Klafki, H.W., Wiltfang, J. & Staufenbiel, M. Electrophoretic separation of βA4 peptides (1-40) and (1-42). *Anal Biochem* **237**, 24-9 (1996).

16. Citron, M. et al. Mutant presenilins of Alzheimer's disease increase production of 42-residue amyloid β-protein in both transfected cells and transgenic mice. *Nat Med* **3**, 67-72 (1997).

17. De Jonghe, C. et al. Evidence that Aβ42 plasma levels in presenilin-1 mutation carriers do not allow for prediction of their clinical phenotype. *Neurobiol Dis* **6**, 280-7 (1999).

18. Castano, E.M. et al. The length of amyloid-β in hereditary cerebral hemorrhage with amyloidosis, Dutch type. Implications for the role of amyloid-β 1-42 in Alzheimer's disease. *J Biol Chem* **271**, 32185-91 (1996).

19. Prelli, F. et al. Expression of a normal and variant Alzheimer's β-protein gene in amyloid of hereditary cerebral hemorrhage, Dutch type: DNA and protein diagnostic assays. *Biochem Biophys Res Commun* **170**, 301-7 (1990).

20. Jankowsky, J.L. et al. Mutant presenilins specifically elevate the levels of the 42 residue β-amyloid peptide in vivo: evidence for augmentation of a 42-specific γ secretase. *Hum Mol Genet* **13**, 159-170 (2004).

21. Johnson-Wood, K. et al. Amyloid precursor protein processing and Aβ42 deposition in a transgenic mouse model of Alzheimer disease. *Proc Natl Acad Sci U S A* **94**, 1550-5 (1997).

22. Richards, J.G. et al. PS2APP transgenic mice, coexpressing hPS2mut and hAPPswe, show age-related cognitive deficits associated with discrete brain amyloid deposition and inflammation. *J Neurosci* **23**, 8989-9003 (2003).

23. Hsiao, K. et al. Correlative memory deficits, Aβ elevation, and amyloid plaques in transgenic mice. *Science* **274**, 99-102 (1996).

24. Nilsberth, C. et al. The 'Arctic' APP mutation (E693G) causes Alzheimer's disease by enhanced Aβ protofibril formation. *Nat Neurosci* **4**, 887-93 (2001).

25. Tsubuki, S., Takaki, Y. & Saido, T.C. Dutch, Flemish, Italian, and Arctic mutations of APP and resistance of Aβ to physiologically relevant proteolytic degradation. *Lancet* **361**, 1957-8 (2003).

26. Morelli, L. et al. Differential degradation of amyloid β genetic variants associated with hereditary dementia or stroke by insulin-degrading enzyme. *J Biol Chem* **278**, 23221-6 (2003).

27. Borchelt, D.R. et al. Accelerated amyloid deposition in the brains of transgenic mice coexpressing mutant presenilin 1 and amyloid precursor proteins. *Neuron* **19**, 939-45 (1997).

28. Holcomb, L. et al. Accelerated Alzheimer-type phenotype in transgenic mice carrying both mutant amyloid precursor protein and presenilin 1 transgenes. *Nat Med* **4**, 97-100 (1998).

29. Meyer-Luehmann, M. et al. Extracellular amyloid formation and associated pathology in neural grafts. *Nat Neurosci* **6**, 370-7 (2003).

30. Shibata, M. et al. Clearance of Alzheimer's amyloid-β(1-40) peptide from brain by LDL receptor-related protein-1 at the blood-brain barrier. *J Clin Invest* **106**, 1489-99 (2000).

31. Weller, R.O. et al. Cerebral amyloid angiopathy: amyloid β accumulates in putative interstitial fluid drainage pathways in Alzheimer's disease. *Am J Pathol* **153**, 725-33 (1998).

32. Pfeifer, M. et al. Cerebral hemorrhage after passive anti-Aβ immunotherapy. *Science* **298**, 1379 (2002).

33. Das, P., Murphy, M.P., Younkin, L.H., Younkin, S.G. & Golde, T.E. Reduced effectiveness of Aβ1-42 immunization in APP transgenic mice with significant amyloid deposition. *Neurobiol Aging* **22**, 721-7 (2001).

34. Nicoll, J.A. et al. Neuropathology of human Alzheimer disease after immunization with amyloid-β peptide: a case report. *Nat Med* **9**, 448-52 (2003).

35. Koller, M.F. et al. Active immunization of mice with an Aβ-Hsp70 vaccine. *Neurobiol Dis (in press)* (2004).

36. Ferrer, I., Boada Rovira, M., Sánchez Guerra, M.L., Rey, M.J. & Costa-Jussá, F. Neuropathology and pathogenesis of encephalitis following amyloid-β immunization in Alzheimer's disease. *Brain Pathol* **14**, 11-20 (2004).

37. Natte, R. et al. Dementia in hereditary cerebral hemorrhage with amyloidosis-Dutch type is associated with cerebral amyloid angiopathy but is independent of plaques and neurofibrillary tangles. *Ann Neurol* **50**, 765-72 (2001).

38. Greenberg, S.M. Cerebral amyloid angiopathy and dementia: two amyloids are worse than one. *Neurology* **58**, 1587-8 (2002).

39. Christie, R., Yamada, M., Moskowitz, M. & Hyman, B. Structural and functional disruption of vascular smooth muscle cells in a transgenic mouse model of amyloid angiopathy. *Am J Pathol* **158**, 1065-71 (2001).

40. Winkler, D.T. et al. Spontaneous hemorrhagic stroke in a mouse model of cerebral amyloid angiopathy. *J Neurosci* **21**, 1619-27 (2001).

41. Calhoun, M.E. et al. Neuronal overexpression of mutant amyloid precursor protein results in prominent deposition of cerebrovascular amyloid. *Proc Natl Acad Sci U S A* **96**, 14088-93 (1999).

42. Van Dorpe, J. et al. Prominent cerebral amyloid angiopathy in transgenic mice overexpressing the london mutant of human APP in neurons. *Am J Pathol* **157**, 1283-98 (2000).

43. Sturchler-Pierrat, C. et al. Two amyloid precursor protein transgenic mouse models with Alzheimer disease-like pathology. *Proc Natl Acad Sci U S A* **94**, 13287-92 (1997).

44. Bodendorf, U. et al. Expression of human β-secretase in the mouse brain increases the steady-state level of β-amyloid. *J Neurochem* **80**, 799-806 (2002).

45. Mehta, P.D. et al. Plasma and cerebrospinal fluid levels of amyloid β proteins 1-40 and 1-42 in Alzheimer disease. *Arch Neurol* **57**, 100-5 (2000).

46. Ohsawa, K., Imai, Y., Kanazawa, H., Sasaki, Y. & Kohsaka, S. Involvement of Iba1 in membrane ruffling and phagocytosis of macrophages/microglia. *J Cell Sci* **113 ( Pt 17)**, 3073-84 (2000).

47. Sola, C., Mengod, G., Probst, A. & Palacios, J.M. Differential regional and cellular distribution of β-amyloid precursor protein messenger RNAs containing and lacking the Kunitz protease inhibitor domain in the brain of human, rat and mouse. *Neuroscience* **53**, 267-95 (1993).

48. Janus, C. et al. Aβ peptide immunization reduces behavioural impairment and plaques in a model of Alzheimer's disease. *Nature* **408**, 979-82 (2000).

49. Rozmahel, R. et al. Normal brain development in PS1 hypomorphic mice with markedly reduced γ-secretase cleavage of βAPP. *Neurobiol Aging* **23**, 187-94 (2002).

50. Maat-Schieman, M.L., Yamaguchi, H., van Duinen, S.G., Natte, R. & Roos, R.A. Age-related plaque morphology and C-terminal heterogeneity of amyloid β in Dutch-type hereditary cerebral hemorrhage with amyloidosis. *Acta Neuropathol (Berl)* **99**, 409-19 (2000).

# 8. Extracellular Amyloid Formation and Associated Pathology in Neural Grafts

Manuscript published in: *Nature Neuroscience*, **6**, 370-7 (2003)

**Melanie Meyer-Luehmann[1,5], Martina Stalder[1,5], Martin C. Herzig[1], Stephan A. Kaeser[1], Esther Kohler[1], Michelle Pfeifer[1], Sonia Boncristiano[1], Paul M. Mathews[2], Marc Mercken[3], Dorothee Abramowski[4], Matthias Staufenbiel[4], and Mathias Jucker[1]**

[1]Department of Neuropathology, Institute of Pathology, University of Basel, Schönbeinstrasse 40, CH-4003 Basel, Switzerland, [2]Nathan Kline Institute for Psychiatric Research, New York University School of Medicine, Orangeburg, New York 10962, USA, [3]Johnson and Johnson Pharmaceutical Research and Development, B-2340 Beerse, Belgium, [4]Novartis Pharma AG, Nervous System Research, CH-4002 Basel, Switzerland

[5]The first two authors contributed equally to this work.

## Abstract

Amyloid precursor protein (APP) processing and the generation of β-amyloid peptide (Aβ) are important in the pathogenesis of Alzheimer's disease. Although this has been studied extensively at the molecular and cellular levels, much less is known about the mechanisms of amyloid accumulation *in vivo*. We transplanted transgenic APP23 and wild-type B6 embryonic neural cells into the neocortex and hippocampus of both B6 and APP23 mice. APP23 grafts into wild-type hosts did not develop amyloid deposits up to 20 months after grafting. In contrast, both transgenic and wild-type grafts into young transgenic hosts developed amyloid plaques as early as 3 months after grafting. Although largely diffuse in nature, some of the amyloid deposits in wild-type grafts were congophilic and were surrounded by neuritic changes and gliosis, similar to the amyloid-associated pathology previously described in APP23 mice. Our results indicate that diffusion of soluble Aβ in the extracellular space is involved in the spread of Aβ pathology, and that extracellular amyloid formation can lead to neurodegeneration.

## Introduction

Alzheimer's disease (AD) is a late-onset progressive neurodegenerative disorder that is characterized by aggregation of Aβ into senile plaques and cerebrovascular amyloid. Genetic studies and results from transgenic (Tg) mice support the view that the production and/or deposition of Aβ is an early and critical process in AD pathogenesis that triggers a cascade of pathological events leading to the formation of neurofibrillary tangles, synapse and neuron loss, neuroinflammation and dementia [1,2]. A matter of controversy, however, is whether this cascade is initiated by the accumulation of Aβ in the extracellular space or by intraneuronal Aβ generation [2-11].

To investigate the mechanisms and early stages of abnormal protein deposition and related neurotoxicity, previous work used neural transplantation techniques to study prion encephalopathy [12]. In AD research, similar approaches have been pursued, but no convincing amyloid pathology has been associated with the grafts [13-16]. However, the recent generation of APP-transgenic mice that develop robust cerebral amyloid with aging [17-19] has opened new opportunities to study the mechanism of cerebral amyloidosis by using neurografting techniques. To test the hypothesis that transplanted neural tissue retains its native properties regardless of host genotype, we transplanted wild-type (WT) and APP23 Tg embryonic cortical and hippocampal brain tissue into the brains of both Tg and WT mice. Our results suggest that the phenotype of the transplanted tissue is strongly influenced by the properties of the host, and that extracellular diffusion of Aβ is centrally involved in cerebral amyloidogenesis. Moreover, we conclude that extracellular amyloid formation is closely associated with neurodegeneration.

## Results

### APP23 grafts into WT hosts show no amyloid for 20 month

Cell suspensions of APP23 embryonic cortical and hippocampal tissue were injected into the neocortex and hippocampus, respectively, of 3 month-old B6 WT mice. Grafts were analyzed 3–24 months later. All grafts integrated well into the surrounding host tissue and appeared healthy and viable by morphological analysis. Only minimal gliosis was found at the graft–host interface. Nevertheless, grafts could easily be identified in cresyl-violet stained sections due to differences in cytoarchitecture between graft and host tissue (Fig. 1a, d and g). Immunohistochemistry revealed robust and exclusive expression of human APP (hAPP) in the graft, where hAPP was restricted to neurons and their processes, consistent with the neuron-

specificity of the Thy-1 promoter used to generate APP23 mice (Fig. 1b, e and h). Cellular hAPP expression within the grafts looked very similar to that in adult APP23 mice.

Although amyloid deposition in neocortex and hippocampus of APP23 mice starts at the age of 6 months [19], we did not find any amyloid formation in hippocampal or cortical grafts up to 20 months after grafting (Fig. 1c and f and Table 1). Beyond 20 months, when hosts were more than 23 months of age, we identified two out of nine mice that developed massive amyloid in the parenchyma and vasculature within at least one graft (Fig. 1i). Interestingly, some amyloid was found outside the grafts, particularly in vessels. To study whether it is the age of the host or the post-grafting time that determines amyloid deposition in the grafts, we also placed APP23 grafts in adult and aged WT hosts (Table 1). Again, grafts were healthy, viable and well-integrated into the host. However, no amyloid formation was observed in such grafts, suggesting that it is not the age of the host, but rather the length of time that the grafts reside in the host, that determines amyloid formation.

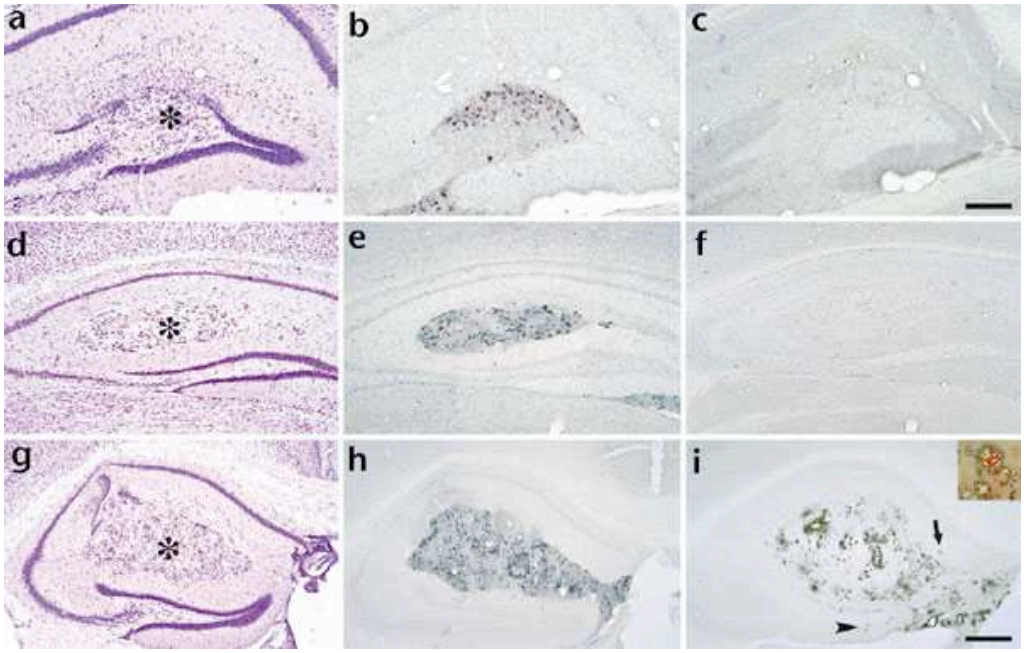


**Figure 1**. Neural grafting of APP23 tissue into B6 hosts. Embryonic APP23 hippocampal tissue was injected into the hippocampus of 3 month-old B6 WT hosts. Mice were analyzed at various times after grafting (Table 1). Shown are mice analyzed 3 months (a–c), 18 months (d–f) and 21 months (g–i) after grafting. Cresyl violet staining was used to identify the grafts (asterisks in a, d, g). Immunohistochemistry revealed strong hAPP expression restricted to neurons in the grafts (b, e, h). Nevertheless, Aβ-immunostaining did not reveal any amyloid deposits 3 and 18 months post-grafting (c, f). At 21 months postgrafting, massive amyloid deposition in both plaques and vessels was found that was to a great extent congophilic (i, insert). The bulk of the amyloid was confined to the graft, but some vessels with amyloid (arrow) and some diffuse amyloid (arrowhead) were

found outside the graft in the host tissue. Similar results were observed when cortical Tg tissue was injected into the cortex of WT mice (not shown). Scale bars, 250 μm (a–c) and 400 μm (d–i).

**Table 1. APP23 tissue transplanted into B6 brain.**

| | | Post-grafting interval (months) | | | | |
|---|---|---|---|---|---|---|
| Host | Age[a] | 3 | 6 | 12 | 18 | > 20 |
| B6 | 3 | 0[b]/12[c] | 0/6 | 0/6 | 0/20 | 2/9 |
| B6 | 16 | 0/1 | 0/2 | 0/6 | | |
| B6 | 24 | 0/2 | 0/5 | | | |

[a]Age of the host (in months) at time of transplantation.
[b]Number of mice with amyloid deposits in at least one graft.
[c]Total number of mice analyzed.

**Table 1**. APP23 tissue transplanted into B6 brain.

### APP expression and Aβ levels in APP23 grafts

We tested several hypotheses to explain the delay/lack of amyloid formation in neocortical and hippocampal APP23 grafts in WT hosts, as compared to the cerebral amyloidosis observed in APP23 mice at the age of 6 months. First, we tested the hypothesis that hAPP expression may be downregulated in grafted neurons, as compared to the expression in normal adult APP23 mice (Fig. 2a and b). However, no obvious differences in hAPP expression were found between micropunches taken from neocortical and hippocampal Tg grafts and those taken from neocortex and hippocampus of normal adult APP23 mice.

Second, we tested the hypothesis that alterations in the processing of hAPP in grafted neurons may lead to a reduction in Aβ production and/or a shift in the ratio of Aβ1-40 to Aβ1-42. To this end, Aβ was immunoprecipitated from micro-punches taken from Tg grafts and compared to micropunches taken from 4–6 month-old APP23 mice, at an age before these mice develop amyloid deposits. Results showed similar Aβ levels in the grafts as compared to young APP23 mice, with a predominance of Aβ1-40 over Aβ1-42 (Fig. 2b). Differences in Aβ1-40 levels in the grafts as compared to young APP23 mice ranged from -31% to +28% (mean, -2 ± 17%; $P > 0.05$). Interestingly, in the oldest transplant analyzed (20 months post-grafting), there was a relative increase of Aβ1-42 over Aβ1-40 (Fig. 2c). This observation is consistent with the result obtained in aged amyloid-depositing APP23 mice. Overall, these results do not support the idea that reduced Aβ production by the grafted tissue is responsible for the slow onset of amyloid deposition in APP23 grafts in WT hosts versus normal APP23 mice.

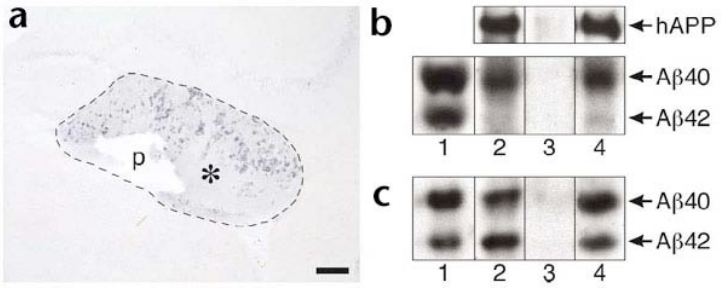


**Figure 2**. APP and Aβ levels in APP23 grafts placed in B6 hosts. (a) Hippocampus of a 15 month-old B6 WT mouse that received an APP23 graft at the age of 3 months. A micropunch (p) was taken from the graft (asterisk) and subjected to western blot analysis. The remaining tissue was immersion-fixed and immunostained for hAPP, showing that hAPP expression was exclusively confined to the graft. Scale bar, 150 µm. (b) Western blotting of the micropunch taken from the APP23 hippocampal graft shown in (a) with hAβ/APP-specific antibody 6E10. In addition, micro-punches from hippocampus were taken from young 4–6 month-old APP23 mice and control B6 mice for comparison. Lane 1, synthetic Aβ40/42. Lane 2, punch from the hippocampal APP23 graft. Lane 3, punch from B6 hippocampus (CA1 area). Lane 4, punch from APP23 hippocampus (CA1 area). Note that hAPP expression and Aβ levels in the graft (lane 2) were comparable to that in APP23 hippocampus (lane 4). In both graft and young APP23 mouse, Aβ1-40 was several fold higher than Aβ1-42. (c) Similar analysis as in (b) but for an APP23 cortical graft 20 months post-grafting. For comparison, micropunches from neocortex were taken from a 12 month-old amyloid- depositing APP23 mouse and a control B6 mouse. Lane 1, synthetic Aβ40/42. Lane 2, punch from the cortical APP23 graft. Lane 3, punch from B6 neocortex. Lane 4, punch from APP23 neocortex.

Third, we investigated the possibility that intracerebral grafting of Tg hAPP/Aβ producing tissue might evoke a humoral immune response in a WT host that has never seen hAPP/Aβ before [20], which might prevent amyloid deposition in the transplant [21]. However, serum titers of anti-Aβ antibodies in engrafted mice were not different from serum titers of normal B6 mice (both < 1:100). As a positive control, we used sera of APP23 mice passively immunized with Aβ antibodies with titers of 1:4,000 to 1:20,000 [22].

**Grafts into APP23 hosts develop amyloid after 3 months**

To study the influence of the host upon amyloid deposition in the graft, we intracerebrally grafted cortical and hippocampal APP23 (Tg) and B6 (WT) control tissue into the cortex and hippocampus, respectively, of 6 month-old APP23 mice (Fig. 3 and Table 2). Again, grafts integrated well into the surrounding host tissue and appeared healthy and viable by morphological analysis with no evidence of neurodegeneration. After only 3 months post-grafting, Tg grafts developed significant amounts of amyloid (Fig. 3a–c) and so did WT cortical and hippocampal grafts (Fig. 3d–i and Table 2). Amyloid deposition occurred throughout the grafts, with the greatest accumulation along the border of the graft. At this age, the host tissue has also developed amyloid plaques, but in most animals they were significantly fewer than in

the grafts. Semiquantitative analysis of double-stained sections for Aβ and Congo red indicated that 50% and 12% of the amyloid was compact in Tg and WT grafts, respectively (Fig. 3i insert). Immunohistochemical analysis with antibodies specifically to Aβx-40 and Aβx-42 revealed the presence of both Aβ species in the graft with a predominance of Aβx-40 over Aβx-42 (Fig. 4a and b). Immuno-labeling with an antibody that recognizes mouse but not human Aβ showed very faint labeling of the amyloid deposits, suggesting that minimal amounts of mouse Aβ may contribute to the amyloid in WT grafts (Fig. 4c), as was also seen for the host tissue amyloid. Aβ was also immunoprecipitated from micropunches taken from amyloid-bearing WT grafts. Results revealed again both human Aβ1-40 and Aβ1-42 in the graft similar to that seen in aged amyloid-depositing APP23 mice (Fig. 4d and e).

**Table 2. APP23 and B6 tissue transplanted into APP23 brain.**

| | | Grafts[b] | |
|---|---|---|---|
| **Host** | **Age[a]** | **APP23** | **B6** |
| APP23 | 6 | 7[c]/7[d] | 10/13 |

[a]Age of the host (in months) at time of transplantation.
[b]Mice were killed 3 months after grafting.
[c]Number of mice with amyloid in at least one graft.
[d]Total mice analyzed.

**Table 2**. APP23 and B6 tissue transplanted into APP23 brain.

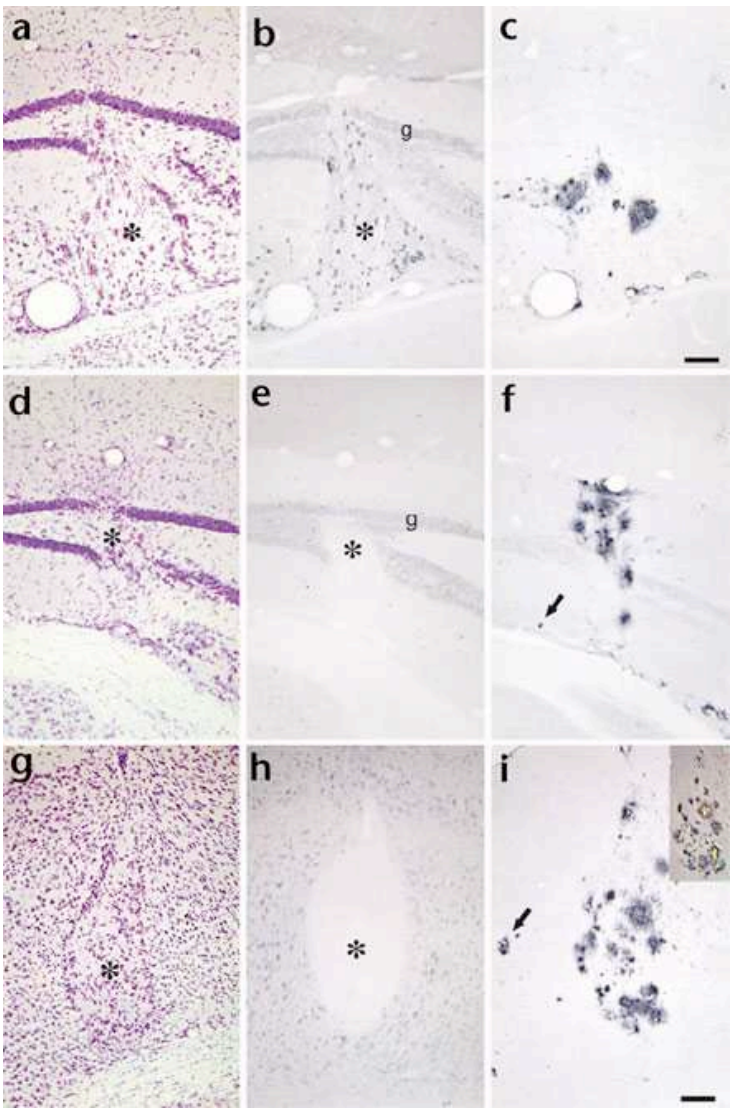


**Figure 3**. Neural grafting of APP23 and B6 tissue into APP23 hosts. Embryonic APP23 hippocampal tissue was injected into the hippocampus of a 6 month-old APP23 mouse and analyzed 3 months later (a–c). Cresyl violet staining shows the graft (asterisk) in the dentate gyrus (a). Immunohistochemistry with an antibody to hAPP shows robust neuronal expression of hAPP in the graft and host (b). Immunostaining for Aβ in adjacent sections revealed considerable amyloid deposits in the graft (c). Strikingly, amyloid deposition in the graft was also found when B6 WT hippocampal tissue was injected into the hippocampus of a 6 month-old APP23 mouse and analyzed 3 months later (d–f). In this case, no hAPP expression was found in the graft (e). The same was found when embryonic B6 WT cortical tissue was grafted into the neocortex of a 6 month-old APP23 mouse and analyzed 3 months later (g–i). Although the majority of the amyloid was of the diffuse type, some amyloid was compact and Congo red–positive. The insert in (i) shows an adjacent section stained for Congo red and viewed under cross-polarized light. Note that in most cases amyloid deposition in the graft was more intense than the scattered amyloid plaques in the 9 month-old host tissue (arrows in f and i). Scale bars, 90 μm (a–f) and 50 μm (g–i).

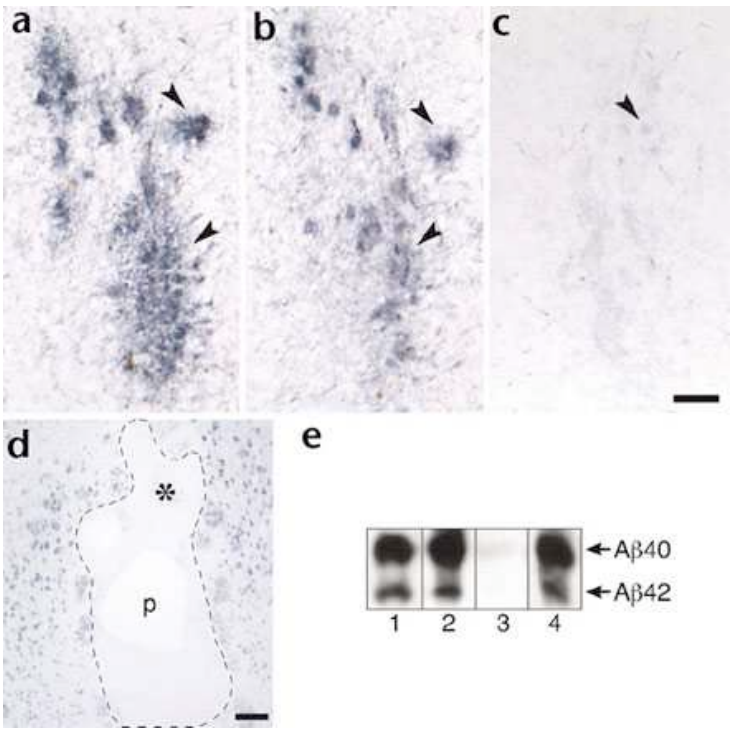


**Figure 4**. Amyloid in B6 grafts. Immunostaining with antibody JRF/cAβ40/10 specific to Aβx-40 (a) and antibody JRF/cAβ42/26 specific to Aβx-42 (b) of a B6 WT graft placed in neocortex of an APP23 host. Antibodies specific to rodent (mouse) Aβ (JRF7rAβ1-15/2) revealed only very faint labeling of the amyloid (c). Shown are adjacent sections with arrowheads indicating the same amyloid deposits. Note that the faint labeling of vessels and microglia is due to unspecific labeling of the secondary anti-mouse IgG antibody. (d) A micropunch (p) was taken from a cortical WT graft (asterisk) and subjected to western blot analysis. The remaining tissue was immersion-fixed and immunostained for hAPP, showing that hAPP expression was exclusively confined to the host. (e) Western blotting of the micropunch taken from the WT cortical graft shown in (d) with human Aβ-specific antibody 6E10. In addition, micropunches were taken from the neocortex of a 12 month-old amyloid-depositing APP23 mouse and a control B6 mouse. Lane 1, synthetic Aβ40/42. Lane 2, punch from the cortical WT graft. Lane 3, punch from B6 neocortex. Lane 4, punch from APP23 neocortex. Note the presence of both Aβ1-40 and Aβ1-42 in the WT graft. Scale bars, 20 µm (c) and 120 µm (d).

### Mechanism of amyloid formation in B6 grafts

To study whether the site of the graft placement may influence Aβ formation in the grafts, we injected hippocampal and cortical WT tissue into either the thalamus or striatum of 6 month-old APP23 mice (*n*= 4 for thalamus and *n*= 8 for striatum). Grafts were analyzed 3 months later. Thalamus and striatum were selected because they differ markedly in amyloid deposition in APP23 mice. The thalamus develops significant amyloid deposition in aged APP23 mice, whereas amyloid deposition in the striatum is low, even in aged APP23 mice [19,23]. Consistent with the idea that the properties of the surrounding host tissue influence amyloid deposition in the graft, we found that two out of four mice (50%) developed amyloid in the 'thalamic' grafts, and zero out of eight mice (0%) developed amyloid in the 'striatal' grafts (Fig. 5). To examine

whether the influence of the surrounding host tissue may be explained by differences in soluble extracellular Aβ levels among the engrafted brain regions, extracellular soluble Aβx-40 and Aβx-42 was measured by ELISA in thalamus, striatum, neocortex and hippocampus of 6 month-old pre-depositing APP23 mice. Results showed the highest Aβ levels in hippocampus (Aβx-40, 2.61 ng/g wet weight; Aβx-42, 0.41 ng/g) and neocortex (Aβx-40, 2.42 ng/g; Aβx-42, 0.42 ng/g), followed by the thalamus (Aβx-40, 1.94 ng/g; Aβx-42, 0.32 ng/g). The levels in the striatum (Aβx-40, 0.71 ng/g; Aβx-42, 0.15 ng/g) were more than 50% lower than these other regions. Recent microdialysis analysis of Aβ also shows significantly lower extracellular soluble Aβ concentrations in striatum than in hippocampus (J.R. Cirrito *et al* ., *Soc. Neurosci. Abstr.* 191.15, 2002). Thus, soluble extracellular Aβ levels in the host may determine amyloid deposition in the graft, suggesting that Aβ is transported extracellularly from the host into the graft. We also tested the hypothesis that the grafts in thalamus and striatum differ in levels of Aβ-degrading enzymes. However, no evidence of a difference was found using immunohistochemical analysis of insulin-degrading enzyme [24] and neprilysin [25] expression in graft versus host (data not shown), although expression levels do not necessarily reflect enzyme activity.

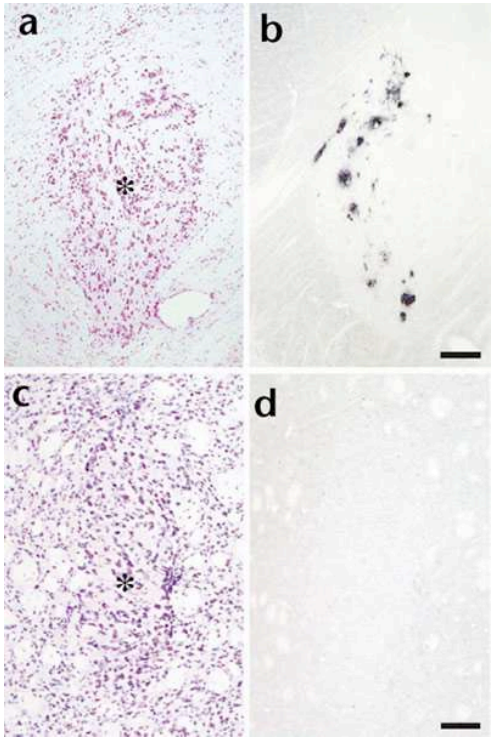


**Figure 5**. Neural grafting of B6 tissue into thalamus and striatum of APP23 hosts. (a, b) Embryonic B6 hippocampal tissue was injected into the thalamus of a 6 month-old APP23 mouse and analyzed 3 months later. Cresyl violet staining shows that the grafts were nicely integrated into the host thalamus and viable without any signs of neurodegeneration (asterisk in a). Immunostaining for Aβ in adjacent sections revealed amyloid deposits in the graft (b). In contrast, when embryonic B6 tissue was placed into the striatum of a 6 month-old APP23 mouse, no amyloid formation was observed 3 months later (c, d). Scale bars, 250 µm.

We also addressed several other possible mechanisms for Aβ transport from the host into the graft. We considered that hAPP/Aβ could be anterogradely transported from host Tg neurons into the WT graft. It has been described previously that host axons can penetrate a homotypic transplant, although in very low numbers [26]. Moreover, APP is anterogradely transported to synaptic sites where it is released [27]. Thus, we used Holmes silver staining to visualize processes between host and graft. Overall, fiber density within the graft was much lower than in the host. Although a few fibers were found to cross the host–graft boundary, most of the fibers were confined to their host or graft compartments (Fig. 6a). Moreover, immunohistochemistry did not reveal any hAPP-positive fibers that penetrated into WT grafts (Fig. 6b , but see also Fig. 3e and h).

We also considered the possibility that microglia transport APP/Aβ from the host into the graft. Thus, not the graft *per se*, but the lesion-associated gliosis or inflammation, may induce amyloid accumulation in WT grafts. In favor of this explanation is the observation that amyloid was predominantly observed at the border of the graft, an area of slightly higher microglia density than the rest of the graft. To test this possibility, we made stab wounds in the neocortex and hippocampus of 6 month-old APP23 mice and analyzed the mice 3 months later. However, in none of lesioned mice ($n$= 4) was amyloid found, despite appreciable microgliosis around the lesion site, which was more extensive than at the host–graft boundary (Fig. 6c and d). Moreover, we injected three APP23 mice with WT grafts in which cells were killed by freezing before transplantation. Again, no amyloid accumulation was found, although microgliosis was clearly present (data not shown). Thus, surgical trauma alone is not sufficient to induce β-amyloidosis in APP23 mice.

These results favor the idea that soluble and diffusible Aβ is transported extracellularly via interstitial fluid from the host into the graft where Aβ undergoes fibril formation and deposition. To exclude the possibility that host-derived soluble extracellular Aβ is internalized by WT neurons in the graft, and that such internalized Aβ is the nidus and a prerequisite for extracellular amyloid plaque formation, we used immunohistochemical staining with a variety of antibodies to Aβ, including antibodies previously suggested to recognize intracellular human Aβ [28]. We did not find any evidence for intracellular human Aβ in the WT graft (Fig. 6e and f).

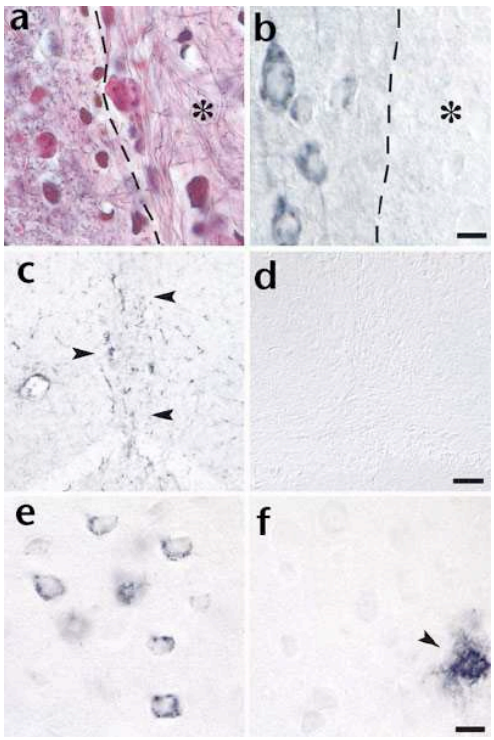


**Figure 6**. Mechanism of amyloid formation in B6 grafts. (a) Holmes silver staining of the graft–host boundary of a B6 WT graft (asterisk) in a 9 month-old APP23 host. There is a lower density of fibers in the graft than in the host. Only a few fibers crossed the host–graft boundary (dotted line) and most fibers were confined to either the host or the graft. (b) Consistent with the Holmes fiber staining, immunostaining for hAPP shows many positive neurons and processes in the host tissue, but none in the WT graft. (c) Cortical stab wound in a 6 month-old APP23 host shows an appreciable increase in CD11b-positive microglia around the lesion site 3 months after surgery (arrowheads). (d) However, immunohistochemistry for Aβ in an adjacent section does not indicate any amyloid deposition in the vicinity of the lesion. (e) Aβ immunostaining with antibody NT12 in the neocortex of a 9 month-old APP23 host reveals punctate intraneuronal staining. (f) In contrast, no evidence of intraneuronal Aβ was found in neocortical WT grafts into APP23 hosts. An amyloid plaque in the WT graft is shown by an arrowhead. The same results were observed with monoclonal antibody W0-2 specific to human Aβ. Scale bars, 10 μm (a, b), 100 μm (c, d) and 15 μm (e, f).

### Amyloid-associated pathology in B6 grafts

The presence of amyloid in WT grafts allowed us to study the impact of host-derived extracellular amyloid formation on neurodegeneration. Although most of the amyloid in WT grafts was of the diffuse type and did not induce any notable neuropil changes, some compact and congophilic amyloid plaques were observed (Figs. 3i (insert) and 7a). Only a few neuronal cells were observed in the area proximal to compact plaques, and some of them showed signs of degeneration (Fig. 7b). Moreover, plaques were surrounded by dystrophic synaptophysin-positive boutons (Fig. 7c) and abnormally thick acetylcholinesterase-positive processes (Fig. 7d). A subpopulation of these distorted neuritic structures were positive for hyperphosphorylated tau (Fig. 7e). Gliosis and neuroinflammation were also evident from clusters of darkly stained

complement receptor 3 (CD11b)-positive and ionized calcium binding adaptor molecule 1 (Iba1)-positive microglia cells with hypertrophic processes that cover the amyloid core (Fig. 7f and g). Hypertrophic reactive glial fibrillary acidic protein (GFAP)-positive astrocytes were also observed around the amyloid deposits (Fig. 7h). Overall, these changes appeared similar to the amyloid-associated degeneration, microgliosis and reactive astrocytosis previously described in amyloid-depositing APP23 mice [19,23,29-32].

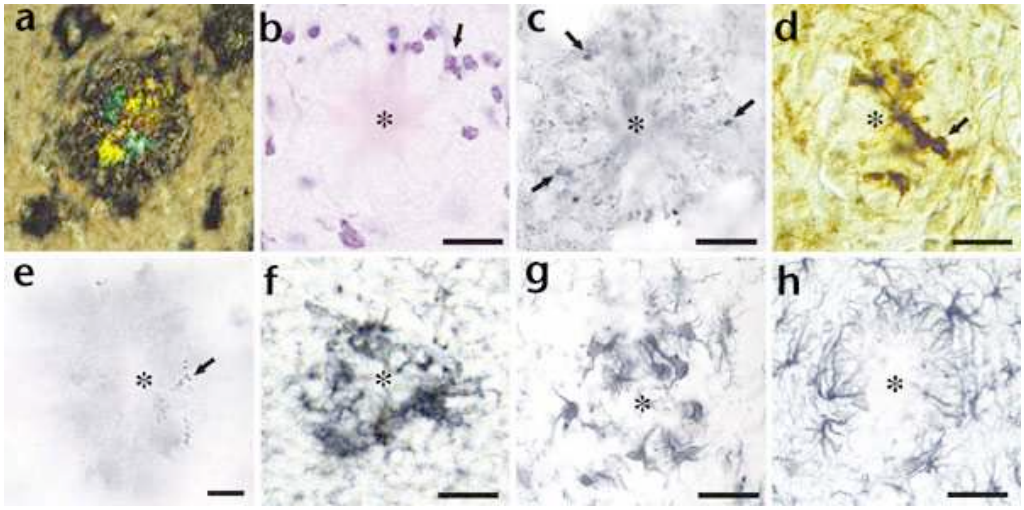


**Figure 7**. Amyloid pathology associated with congophilic amyloid plaques in B6 grafts. (a) Compact plaque in B6 WT graft in a 9 month-old APP23 host reveals bi-refringence when viewed under cross-polarized light (double staining for Aβ and Congo red). (b) Cresyl violet staining demonstrates only a few neuronal cell bodies at the plaque periphery and some of them with a dying phenotype (arrow). (c) Plaques are surrounded and interdigitated by synaptophysin-positive dystrophic boutons (arrows). (d) Acetylcholinesterase staining reveals abnormally large cholinergic processes near the plaque (arrow). (e) Some of these abnormal and distorted processes at the plaque periphery were positive for hyperphosphorylated tau (arrow). (f) CD11b-immunostaining shows hypertrophic microglia clustered around compact amyloid plaques. (g) Amyloid-associated microglia were also intensively positive for Iba1, similar to those observed in amyloid-depositing APP23 mice. (h) GFAP staining reveals hypertrophic and reactive astrocytes decorating the plaque periphery. Scale bars, 25 μm (a, b), 10 μm (c), 25 μm (d), 6 μm (e), 25 μm (f), 30 μm (g) and 25 μm (h).

## Discussion

Whether cerebral amyloidosis is initiated by a gradual increase in extracellular Aβ or by the formation of intracellular Aβ aggregates with subsequent accumulation in the extracellular space (ECS) is controversial [2-11]. Our results suggest that local intracellular Aβ is not a prerequisite for extracellular amyloid deposition and that amyloid deposition is not necessarily confined to the

region of Aβ production. Rather, Aβ can be transported and/or diffuses considerable distances in ECS of the brain before it aggregates, deposits extracellularly and causes neurodegeneration.

First, we grafted APP23 tissue into WT hosts. Because cerebral amyloidosis in the neocortex and hippocampus of APP23 mice appears at 6 months of age [19], our initial expectation was that Tg neocortical and hippocampal grafts placed in WT hosts would also develop amyloid at about 6 months post-grafting. However, no Aβ deposition was observed in the Tg grafts up to 20 months post-grafting, despite APP/Aβ production in the Tg graft similar to APP23 mice. Thus, a reasonable explanation for this lack of or delay in amyloid formation is that extracellular Aβ in the graft did not reach high enough concentrations for amyloid formation because of movement of extracellular soluble Aβ out of the graft into the large volume of surrounding host tissue. It has previously been shown that extracellular Aβ is transported via interstitial fluid to the vasculature, where Aβ is cleared by drainage along the perivascular spaces into the lymph nodes and/or by transport through the blood–brain barrier into the blood [19,33-36]. That Aβ is transported from the Tg graft into the WT host is consistent with the observation of amyloid outside the Tg graft, particularly in vessel walls.

Second, the most compelling evidence that Aβ is extracellularly transported between host and graft comes from our observation that WT grafts in Tg hosts showed amyloidosis. The amyloid in WT grafts was largely human Aβ and thus transgene- and host-derived. Moreover, amyloid in WT grafts only developed when grafts were placed in brain areas such as neocortex, hippocampus, and to some extent thalamus, which all have relative high levels of soluble extracellular Aβ. Amyloid did not develop when grafts were placed into the striatum, which has significant lower concentrations of extracellular soluble Aβ. Finally, axonal transport and transport by microglia of Aβ from the host into the graft did not appear to be significant. Thus, our results argue strongly that soluble Aβ from the Tg host is transported extracellularly via the interstitial fluid from the host into the graft, where Aβ then undergoes deposition. Previous findings suggest that synaptic dysfunction may precede frank neuronal degeneration in AD, and that this dysfunction may be caused by extracellular, diffusible oligomeric assemblies of Aβ [37]. Our results would also suggest that such soluble Aβ aggregates may diffuse over considerable distances in the ECS and therefore may have an unexpected ability to impact synapses distal to the site of Aβ production.

It could be argued that host-derived human Aβ may be internalized by neurons within the WT graft [38,39] and that such internalized human Aβ may undergo fibril formation intracellularly before being released and providing the starting point for extracellular amyloid formation [7-11,38,39]. However, we found no evidence of intracellular human Aβ in WT grafts. Additionally, we

did not find evidence that the amyloid in WT grafts consisted of significant amounts of mouse Aβ, which might have originated in neurons within the WT graft. Moreover, we have previously reported no difference in amyloid deposition between APP23 mice on a WT background and APP23 mice on an *App*-null background [36]. Thus, intraneuronal Aβ does not appear to be a prerequisite for extracellular amyloid formation. Nevertheless, a contributing role of intraneuronal Aβ to extracellular amyloid deposition cannot be entirely ruled out. The relatively lower amount of compact amyloid in the WT grafts versus Tg grafts (both in Tg hosts) may be explained by amyloid formation initiated by an intracellular nidus, leading to predominantly compact amyloid plaques, whereas amyloid formed in the ECS is largely of the diffuse type. However, these differences may also simply be explained by an Aβ concentration difference given that the Tg graft produced Aβ in addition to that provided by the surrounding host tissue.

The unexpected observation that WT grafts often had amyloid deposition before the Tg host tissue suggests that the graft provided a particularly favorable environment for amyloidogenesis. Increased levels of extracellular matrix proteins in the ECS of neural grafts [36,40,41] may act as chaperones for Aβ fibril formation or promote amyloidogenesis by inhibiting interstitial fluid transport of Aβ to the vessels and subsequent drainage [33,40-42]. Using diffusion-weighted MRI, we have recently shown that amyloidosis in APP23 mice is closely related to a decrease in brain ECS diffusion properties (T. Mueggler *et al*., unpub. data). Notably, however, the induction of extracellular matrix constituents by a stab wound or by the injection of dead cells does not promote amyloid deposition in APP23 mice. Thus, in future studies it will be important to characterize the factors that promote amyloidogenesis in the WT grafts. Identifying such amyloid-promoting factors may provide additional targets for amyloid-lowering therapies.

Whether neurodegeneration is related to intracellular Aβ generation or to its extracellular deposition is key to understanding the pathobiology of AD [2]. Oligomerization and accumulation of intracellular Aβ1-42 in AD has been consistently reported [6-8,10,43]. Based on these findings, it has been suggested that accumulation of Aβ1-42 in intracellular compartments may lead to neuronal death [8,10,11]. However, our findings of amyloid-associated nerve cell degeneration and dystrophic neuritic and synaptic structures (including hyperphosphorylated processes) in the vicinity of compact amyloid deposits in WT grafts suggest that intracellular Aβ is not a prerequisite for neurodegeneration. In fact, amyloid pathology in WT grafts is very similar to that previously described in APP Tg mice, including neuron death in the vicinity of amyloid plaques [23,32,44], synaptic abnormalities [30], dystrophic cholinergic processes [31,45] and tau hyperphosphorylated distorted neuritic structures [19]. Moreover, the gliosis and the increase in neuroinflammatory markers were also similar between WT grafts with amyloid and amyloid-depositing APP Tg mice [19,29,46].

In conclusion, our grafting experiments indicate that cerebral β-amyloidosis does not require locally generated intracellular Aβ to initiate Aβ deposition. Indeed, transport or diffusion of Aβ in the ECS of the brain is sufficient and can lead to amyloid pathology at a considerable distance from the site of Aβ generation. Overall, our findings show that factors beyond those directly involved in cellular Aβ production and intracellular Aβ metabolism are important for amyloidogenesis *in vivo*. The amyloid-associated pathology in WT grafts further suggests that neurodegeneration in AD is dependent, at least partially, upon extracellular amyloid accumulation.

## Methods

**Donor embryos for grafting.** Donor mice were C57BL/6 (B6) mice (RCC, Füllinsdorf, Switzerland) and APP23 mice [19]. APP23 mice overexpress mutated human APP (hAPP) with the Swedish double mutation under a neuron-specific murine Thy-1 promoter element. All APP23 mice were from generations 9–11 of backcrossing to B6. To produce Tg grafts, homozygous male APP23 mice were bred with hemizygous female APP23 mice. For WT grafts, B6 mice were bred. Pregnant females were staged by vaginal plugs, and embryos at E15–17 (crown-to-rump length, 13–15 mm) were taken for grafting.

**Intracerebral grafting.** Embryonic neocortices and hippocampi were dissected on ice under semi-sterile conditions in Dulbecco's modified Eagle's Medium (DMEM; Life Technologies, Basel, Switzerland). All neocortical tissue pieces from the entire litter were pooled. The same procedure was performed for the hippocampal pieces. Cell suspensions were prepared mechanically through repeated pipetting with Pasteur pipettes on ice. Total cell counts and cell viability were determined with a hemocytometer and 0.4% trypan blue stain (0.4%; Fluka, Buchs, Switzerland). Cell number was adjusted to 100,000 cells/ l, and cell viability was 80%.

Host mice (3–24 month-old females) were anaesthetized with a mixture of ketamine (10 mg/kg body weight) and xylazine (20 mg/kg body weight) in saline. Bilateral stereotaxic injections of 2.5 l cortical and hippocampal cell suspensions were placed with a Hamilton syringe into the neocortex (A/P, +1.0 mm from bregma; L, 2.0 mm; D/V, -1.5 mm) and hippocampus (A/P, -2.5 mm; L, 2.0 mm; D/V, -2.5 mm), respectively. In selected mice, cell suspensions were injected into the striatum (A/P, +1.0 mm; L, 2.0 mm; D/V, -3 mm) and thalamus (A/P, -2.5 mm; L, 1.5 mm; D/V, -3 mm). Injection speed was 1.25 l/min, and the needle was kept in place for an additional 2 min before it was slowly withdrawn. The surgical area was cleaned with sterile

saline, and the incision was sutured. As a control, some mice received stab wound lesions—the needle was lowered in the brain without injection of any cell suspension. All experiments were in compliance with protocols approved by the local Animal Care and Use Committee (Veterinäramt, Basel).

**Histology and immunohistochemistry.** At various time points after grafting, host mice were deeply anesthetized, and either they were perfused transcardially with PBS buffer (0.1 M, pH 7.4) followed by 4% paraformaldehyde in PBS (pH 7.4), or their brains were removed and immersion-fixed for 2 d in 4% paraformaldehyde in PBS. Brains were then dehydrated overnight in 30% sucrose. After freezing, 20–30 m serial coronal sections were cut through the transplants on a freeze-sliding microtome and collected in 0.1 M Tris-buffered saline (pH 7.4).

Sections were stained histologically with cresyl-violet and immunohistochemically according to previously published protocols [29] with the following antibodies: polyclonal antibody NT12 (NT11) to Aβ (courtesy of P. Paganetti, Basel, Switzerland) [19], mouse monoclonal antibody W0-2 specific to human Aβ [28] (courtesy of K. Beyreuther, Heidelberg, Germany), mouse monoclonal antibody 6E10 specific to hAPP/Aβ (Signet Pathology Systems, Inc., Dedham, Massachusetts), monolconal antibodies specific to Aβx-40 (JRF/cAβ40/10) and Aβx-42 (JRF/cAβ42/26) [47], monoclonal antibody specific to rodent/mouse Aβ that does not cross-react with human Aβ (JRFrAβ1-15/2) [47], polyclonal antibody A4CT to the C-terminal 100 amino acids of hAPP (courtesy of K. Beyreuther), mouse monoclonal antibody 56C6 to neprilysin (CD10; Novocastra Laboratories, Newcastle upon Tyne, UK), polyclonal affinity-purified antibody IDE-1 to IDE protein (courtesy of D. Selkoe, Boston, USA), polyclonal antibody to synaptophysin (Dako, Glostrup, Denmark), mouse monoclonal antibody AT8 which recognizes hyperphosphorylated tau (Innogenetics, Heiden, Germany), rat monoclonal antibody to CD11b (Mac-1; Serotec, Oxford, UK), polyclonal antibody to Iba1 [48] (courtesy of Y. Imai, Tokyo, Japan) and polyclonal antibody to GFAP (Dako). Some sections were double-stained with NT12 and Congo red. Additional sections were stained histochemically for acetylcholinesterase [31] and Holmes silver staining.

**Assessment of APP and Aβ in graft and host by western blot.** Under deep inhalation anesthesia, engrafted mice were killed by decapitation. Brains were removed and sectioned on a vibratome (400 m thick slices) in ice-cold PBS. Slices were transferred onto a glass slide on ice. With the aid of a dissecting microscope and a Stoelting micropunch device (Stoelting, Wood Dale, Illinois), micropunches were taken from the graft. For comparison, micropunches were also taken from normal APP23 and B6 mice. Punches had a diameter of 0.74 mm and thus consisted of 172 g wet weight tissue [49].

To determine hAPP expression, punched samples were diluted in 30 l of homogenization buffer (50 mM Tris, pH 8; 150 mM NaCl; 5 mM EDTA; protease inhibitor cocktail (Roche Diagnostic, Mannheim, Germany) and 90 l sample buffer (0.48 M Bistris; 0.21 M Bicine; 1.33% w/v SDS; 20% w/v sucrose; 3.33% v/v 2-mercaptoethanol; 0.0053% w/v bromophenol blue). Subsequently, samples were Dounce-homogenized, sonicated and subjected to 10% Bicine/Tris 8M Urea SDS–PAGE [50]. Proteins were transferred onto a PVDF membrane, and hAPP was detected using monoclonal mouse 6E10 antibody. The secondary antibody was horseradish peroxidase-conjugated goat anti-mouse IgG (Chemicon, Temecula, California). Bands were visualized using SuperSignal (Pierce, Rockford, Illinois) and developed onto Kodak X-OMAT AR film (Rochester, New York).

To analyze Aβ levels, tissues of two micropunches were combined, and human Aβ was immunoprecipitated with antibody 6E10 and protein G Sepharose (Sigma, St. Louis, Missouri). Subsequent SDS–PAGE and blotting was done as described above. Synthetic Aβ1-40 and 1-42 (Bachem, Bubendorf, Switzerland) were used as controls. Different exposures of the films were digitized, and band density measurements for Aβ40 were made using NIH Image 1.61 (NIH, Bethesda, Maryland). Only bands within the linear range of the film were analyzed.

**ELISA to measure soluble extracellular Aβ in engrafted brain regions.** Neocortex, hippocampus, striatum and thalamus of 6 month-old male pre-depositing APP23 mice ( *n*= 8) were dissected on ice. Tissue from four mice was pooled and homogenized in 50 mM Tris (pH 8), 150 mM NaCl and 5 mM EDTA and protease inhibitor cocktail (Roche Diagnostic). The homogenate was centrifuged at 107,000 *g*for 1 h at 4 °C, and human Aβx-40 and Aβx-42 levels were determined in the supernatant by previously described sandwich ELISAs [47]. In brief, Aβ was captured with carboxy-terminal monoclonal antibodies that recognize exclusively either Aβx-40 (JRF/cAβ40/10) or Aβx-42 (JRF/cAβ42/26) and detected with horseradish peroxidase-conjugated JRF/Aβtot/17, which recognizes the amino-terminal 16 residues of human Aβ. All measurements were done in two or more replica wells. ELISA results reported are the mean of the two pooled tissue samples (ng Aβ per g wet weight), based on standard curves using synthetic Aβ1-40 and Aβ1-42 peptide standards (American Peptide, Sunnyvale, California).

**Serum titers of Aβ antibodies.** At various time points after grafting (30–510 d), retro-orbital blood samples were collected from selected engrafted mice by using heparin-coated capillary tubes. Samples were centrifuged, and the sera were immediately frozen on dry ice. Antibody titers were assessed by ELISA. Serial dilutions of sera were made onto microtiter plates coated with Aβ1-40 (50 ng/ml, Bachem). Detection was through alkaline phosphatase–conjugated

rabbit anti-mouse IgG (Calbiochem, San Diego, California) and 4-nitrophenol phosphate disodium salt hexahydrate (Fluka). Titers were defined as dilution yielding 50% of the maximal signal.

## References


1. Hardy, J. & Selkoe, D. J. The amyloid hypothesis of Alzheimer's disease: progress and problems on the road to therapeutics. *Science* **297**, 353-6 (2002).

2. Selkoe, D. J. Alzheimer's disease: genes, proteins, and therapy. *Physiol Rev* **81**, 741-66 (2001).

3. Geula, C. et al. Aging renders the brain vulnerable to amyloid β-protein neurotoxicity. *Nat Med* **4**, 827-31 (1998).

4. Kane, M. D. et al. Evidence for seeding of β-amyloid by intracerebral infusion of Alzheimer brain extracts in β-amyloid precursor protein-transgenic mice. *J Neurosci* **20**, 3606-11 (2000).

5. Martin, L. J., Pardo, C. A., Cork, L. C. & Price, D. L. Synaptic pathology and glial responses to neuronal injury precede the formation of senile plaques and amyloid deposits in the aging cerebral cortex. *Am J Pathol* **145**, 1358-81 (1994).

6. Hartmann, T. et al. Distinct sites of intracellular production for Alzheimer's disease Aβ40/42 amyloid peptides. *Nat Med* **3**, 1016-20 (1997).

7. Gouras, G. K. et al. Intraneuronal Aβ42 accumulation in human brain. *Am J Pathol* **156**, 15-20 (2000).

8. Walsh, D. M., Tseng, B. P., Rydel, R. E., Podlisny, M. B. & Selkoe, D. J. The oligomerization of amyloid β-protein begins intracellularly in cells derived from human brain. *Biochemistry* **39**, 10831-9 (2000).

9. Bayer, T. A. et al. Key factors in Alzheimer's disease: β-amyloid precursor protein processing, metabolism and intraneuronal transport. *Brain Pathol* **11**, 1-11 (2001).

10. Wirths, O. et al. Intraneuronal Aβ accumulation precedes plaque formation in β-amyloid precursor protein and presenilin-1 double-transgenic mice. *Neurosci Lett* **306**, 116-20 (2001).

11. D'Andrea, M. R., Nagele, R. G., Wang, H. Y., Peterson, P. A. & Lee, D. H. Evidence that neurones accumulating amyloid can undergo lysis to form amyloid plaques in Alzheimer's disease. *Histopathology* **38**, 120-34 (2001).

12. Brandner, S. et al. Normal host prion protein necessary for scrapie-induced neurotoxicity. *Nature* **379**, 339-43 (1996).

13. Richards, S. J. et al. Transplants of mouse trisomy 16 hippocampus provide a model of Alzheimer's disease neuropathology. *Embo J* **10**, 297-303 (1991).

14. Holtzman, D. M. et al. Mouse model of neurodegeneration: atrophy of basal forebrain cholinergic neurons in trisomy 16 transplants. *Proc Natl Acad Sci U S A* **89**, 1383-7 (1992).

15. Mantione, J. R. et al. Human neurons that constitutively secrete Aβ do not induce Alzheimer's disease pathology following transplantation and long-term survival in the rodent brain. *Brain Res* **671**, 333-7 (1995).

16. Bayer, T. A., Fossgreen, A., Czech, C., Beyreuther, K. & Wiestler, O. D. Plaque formation in brain transplants exposed to human β-amyloid precursor protein 695. *Acta Neuropathol (Berl)* **92**, 130-7 (1996).

17. Hsiao, K. et al. Correlative memory deficits, Aβ elevation, and amyloid plaques in transgenic mice. *Science* **274**, 99-102 (1996).

18. Games, D. et al. Alzheimer-type neuropathology in transgenic mice overexpressing V717F β-amyloid precursor protein. *Nature* **373**, 523-7 (1995).

19. Sturchler-Pierrat, C. et al. Two amyloid precursor protein transgenic mouse models with Alzheimer disease-like pathology. *Proc Natl Acad Sci U S A* **94**, 13287-92 (1997).

20. Brandner, S. et al. Normal host prion protein (PrPC) is required for scrapie spread within the central nervous system. *Proc Natl Acad Sci U S A* **93**, 13148-51 (1996).

21. Schenk, D. et al. Immunization with amyloid-β attenuates Alzheimer-disease-like pathology in the PDAPP mouse. *Nature* **400**, 173-7 (1999).

22. Pfeifer, M. et al. Cerebral hemorrhage after passive anti-Aβ immunotherapy. *Science* **298**, 1379 (2002).

23. Calhoun, M. E. et al. Neuron loss in APP transgenic mice. *Nature* **395**, 755-6 (1998).

24. Qiu, W. Q. et al. Insulin-degrading enzyme regulates extracellular levels of amyloid β-protein by degradation. *J Biol Chem* **273**, 32730-8 (1998).

25. Iwata, N. et al. Identification of the major Aβ1-42-degrading catabolic pathway in brain parenchyma: suppression leads to biochemical and pathological deposition. *Nat Med* **6**, 143-50 (2000).

26. Clinton, R. J., Jr. & Ebner, F. F. Time course of neocortical graft innervation by AChE-positive fibers. *J Comp Neurol* **277**, 557-77 (1988).

27. Lazarov, O., Lee, M., Peterson, D. A. & Sisodia, S. S. Evidence that synaptically released β-amyloid accumulates as extracellular deposits in the hippocampus of transgenic mice. *J Neurosci* **22**, 9785-93 (2002).

28. Wirths, O. et al. Intraneuronal APP/Aβ trafficking and plaque formation in β-amyloid precursor protein and presenilin-1 transgenic mice. *Brain Pathol* **12**, 275-86 (2002).

29. Stalder, M. et al. Association of microglia with amyloid plaques in brains of APP23 transgenic mice. *Am J Pathol* **154**, 1673-84 (1999).

30. Phinney, A. L. et al. Cerebral amyloid induces aberrant axonal sprouting and ectopic terminal formation in amyloid precursor protein transgenic mice. *J Neurosci* **19**, 8552-9 (1999).

31. Boncristiano, S. et al. Cholinergic changes in the APP23 transgenic mouse model of cerebral amyloidosis. *J Neurosci* **22**, 3234-43 (2002).

32. Bondolfi, L. et al. Amyloid-associated neuron loss and gliogenesis in the neocortex of amyloid precursor protein transgenic mice. *J Neurosci* **22**, 515-22 (2002).

33. Weller, R. O. Pathology of cerebrospinal fluid and interstitial fluid of the CNS: significance for Alzheimer disease, prion disorders and multiple sclerosis. *J Neuropathol Exp Neurol* **57**, 885-94 (1998).

34. Shibata, M. et al. Clearance of Alzheimer's amyloid-β(1-40) peptide from brain by LDL receptor-related protein-1 at the blood-brain barrier. *J Clin Invest* **106**, 1489-99 (2000).

35. DeMattos, R. B., Bales, K. R., Cummins, D. J., Paul, S. M. & Holtzman, D. M. Brain to plasma amyloid-β efflux: a measure of brai104 amyloid burden in a mouse model of Alzheimer's disease. *Science* **295**, 2264-7 (2002).

36. Calhoun, M. E. et al. Neuronal overexpression of mutant amyloid precursor protein results in prominent deposition of cerebrovascular amyloid. *Proc Natl Acad Sci U S A* **96**, 14088-93 (1999).

37. Selkoe, D. J. Alzheimer's disease is a synaptic failure. *Science* **298**, 789-91 (2002).

38. Bi, X., Gall, C. M., Zhou, J. & Lynch, G. Uptake and pathogenic effects of amyloid β peptide 1-42 are enhanced by integrin antagonists and blocked by NMDA receptor antagonists. *Neuroscience* **112**, 827-40 (2002).

39. Nagele, R. G., D'Andrea, M. R., Anderson, W. J. & Wang, H. Y. Intracellular accumulation of β-amyloid(1-42) in neurons is facilitated by the alpha 7 nicotinic acetylcholine receptor in Alzheimer's disease. *Neuroscience* **110**, 199-211 (2002).

40. Gates, M. A., Laywell, E. D., Fillmore, H. & Steindler, D. A. Astrocytes and extracellular matrix following intracerebral transplantation of embryonic ventral mesencephalon or lateral ganglionic eminence. *Neuroscience* **74**, 579-97 (1996).

41. Sykova, E., Roitbak, T., Mazel, T., Simonova, Z. & Harvey, A. R. Astrocytes, oligodendroglia, extracellular space volume and geometry in rat fetal brain grafts. *Neuroscience* **91**, 783-98 (1999).

42. Snow, A. D. et al. An important role of heparan sulfate proteoglycan (Perlecan) in a model system for the deposition and persistence of fibrillar A β-amyloid in rat brain. *Neuron* **12**, 219-34 (1994).

43. Wild-Bode, C. et al. Intracellular generation and accumulation of amyloid β-peptide terminating at amino acid 42. *J Biol Chem* **272**, 16085-8 (1997).

44. Urbanc, B. et al. Neurotoxic effects of thioflavin S-positive amyloid deposits in transgenic mice and Alzheimer's disease. *Proc Natl Acad Sci U S A* **99**, 13990-5 (2002).

45. Wong, T. P., Debeir, T., Duff, K. & Cuello, A. C. Reorganization of cholinergic terminals in the cerebral cortex and hippocampus in transgenic mice carrying mutated presenilin-1 and amyloid precursor protein transgenes. *J Neurosci* **19**, 2706-16 (1999).

46. Frautschy, S. A. et al. Microglial response to amyloid plaques in APPsw transgenic mice. *Am J Pathol* **152**, 307-17 (1998).

47. Mathews, P. M. et al. Calpain activity regulates the cell surface distribution of amyloid precursor protein. Inhibition of calpains enhances endosomal generation of β-cleaved C-terminal APP fragments. *J Biol Chem* **277**, 36415-24 (2002).

48. Ohsawa, K., Imai, Y., Kanazawa, H., Sasaki, Y. & Kohsaka, S. Involvement of Iba1 in membrane ruffling and phagocytosis of macrophages/microglia. *J Cell Sci* **113**, 3073-84 (2000).

49. Palkovits, M. Punch sampling biopsy technique. *Methods Enzymol* **103**, 368-76 (1983).

50. Wiltfang, J. et al. Improved electrophoretic separation and immunoblotting of β-amyloid (Aβ) peptides 1-40, 1-42, and 1-43. *Electrophoresis* **18**, 527-32 (1997).

# Conclusions

The objective of this thesis has been to gain new insights into the mechanisms that are involved in the development of CAA and CAA-associated pathology using a transgenic mouse approach. We have shown that the APP23 and APPDutch mice presented herein develop cerebrovascular amyloid deposits and associated pathology similar to those seen in AD and HCHWA-D. Thus, understanding the mechanisms leading to CAA formation in these transgenic mice will as well greatly improve our knowledge about the pathomechanisms that are involved in the development of CAA in humans.

A major finding of our studies is that Aβ in the vasculature of transgenic APP23 and APPDutch mice, due to the neuron-specific promoter used, is of neuronal origin. This finding strongly supports the hypothesis that also in humans neurons are likely to be the primary source of the vascular Aβ deposits observed. Besides neurons, other cell types have been shown to produce Aβ, and although they may contribute as an additional source of Aβ to the vascular amyloid, they do not seem to be necessarily involved in CAA formation. Further support of the idea that neuron-derived Aβ is sufficient to cause CAA is provided by the finding that CAA in transgenic mice shows striking similarities to human CAA. It mainly affects arteries and arterioles and the anatomical distribution of the Aβ deposits is comparable between transgenic mice and humans.

A second important observation of our work is that secreted soluble Aβ can be transported extracellularly before it accumulates as insoluble amyloid fibrils and therewith can cause pathological changes distant to its site of production. This observation is based on the occurrence of CAA-associated pathology such as SMC degeneration and intracerebral hemorrhage in APP23 and APPDutch mice, and on the presence of amyloid-associated neurodegeneration in wild-type grafts of APP23 hosts in the grafting experiments. Interestingly, the toxicity to both SMCs and neurons seems to be caused by extracellular amyloid deposits since we did not observe any internalization of transgene-derived Aβ by these cells. Degeneration of SMCs is likely to be driven by purely mechanical displacement by the amyloid within the vessel wall.

The third major finding is that the ratio of Aβ40:42 is an important determinant in the formation of parenchymal versus vascular amyloid. We show that steady-state levels of Aβ40 and Aβ42 in amyloid pre-depositing mice may determine the deposition pattern of the amyloid in depositing mice, with a high Aβ40:42 ratio leading preferentially to vascular amyloid deposition and a low Aβ40:42 ratio causing mainly parenchymal amyloidosis. In fact, both amyloid pre-depositing

and depositing APPDutch mice show a significant higher Aβ40:42 ratio when compared to APPwt mice that predominately develop parenchymal amyloid. The view that different levels of Aβ40 and Aβ42 seem to be able to drive amyloid pathology in different compartments is strengthened by the finding that parenchymal amyloid formation can be initiated in APPDutch mice by increasing Aβ42 levels as demonstrated to occur in APPDutch/PS45 double-transgenic mice. Like in APPDutch mice, parenchymal plaque formation in HCHWA-D is likely to be limited by the absence of Aβ42-driven parenchymal amyloid seeding. A thinking that is all the more imaginable as *in vitro* AβDutch42 has been shown to be even more fibrillogenic than Aβwt42. The finding that different levels of Aβ40 and Aβ42 are able to drive amyloid pathology either to the vasculature or the parenchyma has implications for the development of therapeutic strategies. Therapeutic compounds that aim at reducing parenchymal amyloid by clearing the more fibrillogenic Aβ42 might decrease the Aβ40:42 ratio and thus may potentiate CAA formation.

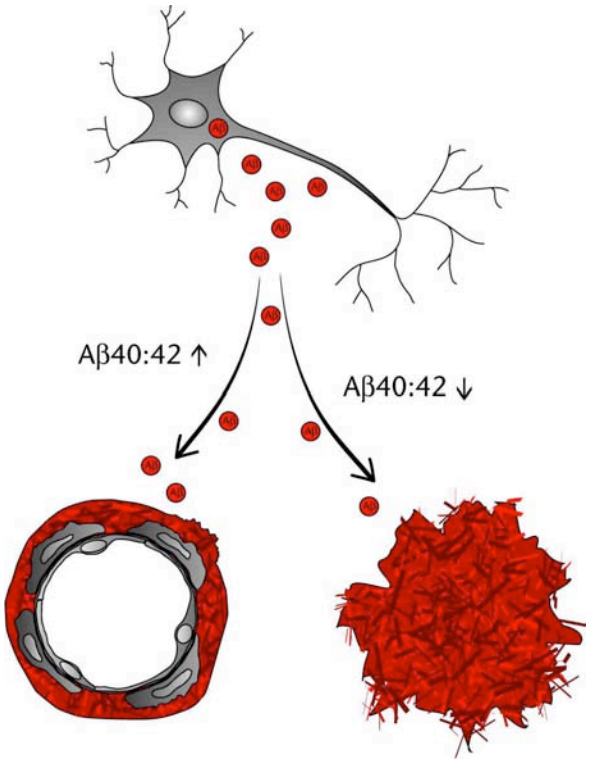


Schematic drawing illustrating a possible mechanism for vascular versus parenchymal amyloid formation.

# Curriculum Vitae and Bibliography

## Martin Christian Herzig

### Personal particulars


| | |
|---|---|
| Current Address: | Dammerkirchstrasse 74<br>4056 Basel<br>Switzerland<br>Phone: +41 76 564 74 70 |
| Business Address: | Institute of Pathology<br>Neuropathology<br>University of Basel<br>Schönbeinstrasse 40<br>4031 Basel<br>Switzerland<br>Phone: +41 61 265 37 96<br>E-mail: Martin.Herzig@unibas.ch |
| Date of Birth: | December 15, 1972 |
| Place of Birth: | Basel, Switzerland |
| Citizenship: | Swiss |


### Education

| | |
|---|---|
| 1999 - present | PhD Student in the group of Prof. Mathias Jucker<br>Institute of Pathology, University of Basel, Switzerland |
| 1999 | Diploma Thesis in Neurobiology: "Expression and function of the LIM homeodomain protein Apterous during embryonic brain development of Drosophila" (Herzig et al., 2001) in the group of Prof. Heinrich Reichert<br>Institute of Zoology, University of Basel, Switzerland |
| 1992 - 1999 | Studies in Biology<br>University of Basel, Switzerland |
| 1991 | High School Diploma: Graduation in economics<br>Muttenz, Switzerland |
| 1979 - 1991 | Schools in Switzerland |

# Bibliography

## Peer Reviewed Journal Papers

**Herzig MC**, Winkler DT, Burgermeister P, Pfeifer M, Kohler E, Schmidt SD, Danner S, Abramowski D, Stürchler-Pierrat C, Bürki K, van Duinen SG, Maat-Schieman MLC, Staufenbiel M, Mathews PM, Jucker M (2004) Neuron-derived Aβ is targeted to the vasculature in a mouse model of hereditary cerebral hemorrhage with amyloidosis-Dutch type. Nat Neurosci (*in press*)

Meyer-Luehmann M, Stalder M, **Herzig MC**, Kaeser SA, Kohler E, Pfeifer M, Boncristiano S, Mathews PM, Mercken M, Abramowski D, Staufenbiel M, Jucker M (2003) Extracellular amyloid formation and associated pathology in neural grafts. Nat Neurosci 6:370-377

Probst A, **Herzig MC**, Mistel C, Ipsen S, Tolnay M (2001) Perisomatic granules (non-plaque dystrophic dendrites) of hippocampal CA1 neurons in Alzheimer's disease and Pick's disease: a lesion distinct from granovacuolar degeneration. Acta Neuropathol (Berl) 102:636-644

Winkler DT*, Bondolfi L*, **Herzig MC***, Jann L, Calhoun ME, Wiederhold KH, Tolnay M, Staufenbiel M, Jucker M (2001) Spontaneous hemorrhagic stroke in a mouse model of cerebral amyloid angiopathy. J Neurosci 21:1619-1627

***contributed equally to this work**

**Herzig MC**, Thor S, Thomas JB, Reichert H, Hirth F (2001) Expression and function of the LIM homeodomain protein Apterous during embryonic brain development of Drosophila. Dev Genes Evol 211:545-554

## Book chapters

**Herzig MC**, Winkler DT, Walker LC, Jucker M (2001) Transgenic mouse models of cerebral amyloid angiopathy. Adv Exp Med Biol 487:123-128.

Jucker M, Calhoun ME, Phinney AL, Stalder M, Bondolfi L, Winkler DT, **Herzig MC**, Pfeifer M, Boncristiano S, Tolnay M, Probst A, Deller T, Abramowski D, Wiederhold KH, Sturchler-Pierrat C, Sommer B, Staufenbiel M (2001) Pathogenesis and mechanisms of cerebral amyloidosis in APP transgenic mice. Loss of function through gain of function; Research and perspectives in Alzheimer's disease; Springer Verlag Berlin Heidelberg New York; pp. 87-95

## Abstracts

**Herzig MC**, Burgermeister P, Schmidt SD, Kohler E, Pfeifer M, Winkler DT, Danner S, Abramowski D, Maat-Schieman MLC, Mathews PM, Staufenbiel M, Jucker M. The APP Dutch mutation targets neuronally produced Aβ to the vasculature. Program No 731.10. 2003 Abstract Viewer/Itinerary Planner. Washington, DC: Society for Neuroscience, 2003.

**Herzig MC**, Winkler DT, Pfeifer M, Burgermeister P, Schmidt SD, Mathews PM, Danner S, Abramowski D, Maat-Schieman MLC, Staufenbiel M, Jucker M. The APPDutch mutation is sufficient to target Aβ to the vasculature. Neurobiol Aging, 23 (1): 891 Suppl. 1 Jul-Aug 2002

Schmidt SD, Jiang Y, **Herzig MC**, Chishti MA, Duff KEK, Jucker M, Mercken M, Staufenbiel M, Westaway D, Nixon RA, Mathews PM. Murine Aβ co-deposition in transgenic mice: Analyses with species-specific antibodies and comparison of human and murine Aβ42 : Aβ40 ratios. Neurobiol Aging, 23 (1): 920 Suppl. 1 Jul-Aug 2002

Danner S, **Herzig MC**, Staufenbiel M, Wiederhold KH. Spacial relation of amyloid plaque associated neurodegenerative and inflammatory processes in APP23 transgenic mice analyzed by confocal microscopy. Neurobiol Aging, 23 (1): 905 Suppl. 1 Jul-Aug 2002

**Herzig MC**, Pfeifer M, Maat-Schieman MLC, Bondolfi L, Tolnay M, Abramowski D, Staufenbiel M, Jucker M, Winkler DT. Cerebral amyloid angiopathy causes hemorrhagic stroke in APP transgenic mice. Soc Neurosci Abstr, Vol 27, Program No 427.14, 2001

Jucker M, Calhoun ME, Phinney AL, Stalder M, Tolnay M, Wiederhold KH, Staufenbiel M, Winkler DT, Bondolfi L, Jann L, **Herzig MC**, Pfeifer M (2000) Cerebral amyloid angiopathy: What can we learn from transgenic mouse models? Alzheimer's reports 3: S28

Winkler DT, Bondolfi L, **Herzig MC**, Pfeifer M, Tolnay M, Wiederhold KH, Staufenbiel M, Jucker M (2000) Transgenic mouse models of cerebral amyloid angiopathy. Alzheimer's reports 3: S52

## Invited Presentations

**Herzig MC**. Transgenic mouse models of cerebral amyloidosis. 1st Symposium of the Hertie-Institute of Clinical Brain Research, Tübingen, 2003

During my PhD thesis, lectures and seminars of the following persons were taken: Markus Affolter, Silvia Arber, Yves-Alain Barde, Bernhard Bettler, Hans-R. Brenner, Pico Caroni, Mathias Jucker, Josef Kapfhammer, Andrew Matus, Adrian Merlo, Denis Monard, Andreas Monsch, Ulrich Müller, Cordula Nitsch, Uwe Otten, Alphonse Probst, Heinrich Reichert, Markus A. Rüegg, Nicole Schaeren-Wiemers, Erich Seifritz, Esther Stöckli and Markus Tolnay.